

BOSTON UNIVERSITY
GRADUATE SCHOOL OF ARTS AND SCIENCES

Dissertation

**FIRST PRINCIPLES AND EFFECTIVE THEORY APPROACHES TO
DYNAMICS OF COMPLEX NETWORKS**

by

NIMA DEHMAMY

B.A., Sharif University of Technology, 2006

M.A., Sharif University of Technology, 2008

Submitted in partial fulfillment of the
requirements for the degree of
Doctor of Philosophy

2016

Approved by

First Reader

H. Eugene Stanley, Ph.D.
William Fairfield Warren Distinguished Professor; Professor of Physics;
Professor of Chemistry; Professor of Biomedical Engineering;
Professor of Physiology ;

Second Reader

Pankaj Mehta, Ph.D.
Assistant Professor of Physics

To all those who compromised. My late aunt, my mom, my dad, my brother and sister, my former advisors, my collaborators, my friends and could-be-friends.

Acknowledgments

After my family, with their unwavering care and support, I am also greatly indebted to my advisors and professors who mentored me. Needless to mention, prof. Stanley, or Gene, as we like to call him, who took me in without hesitation at in my 4th year and supported all along till this day, teaching me all the professional skills needed for being a good academic and who remained patient with my unruliness the way a father would do. I also wish to thank my great collaborators, especially Irena Vodenska for also mentoring me and introducing me to the exciting problems and challenging world of systemic risk in finance and economy, Sergey Buldyrev and Shlomo Havlin for their deep insight and the expertise they bring into the projects, Navid Dianati, Asher Mullokandov, Tomislav Lipic for their collaboration and help, as well as everybody else in Gene's group

Another person who I greatly indebted to is my former advisor John Stachel who helped me a lot, along with Peter Bokulich, and made it possible for me to do my first real research project that led to my first paper. I'm also really thankful to Alejandra Castro for the research problem she proposed and her patience and kindness which led to our paper.

I won't be able to pay tribute to everyone I owe this to, so let me stop by thanking Boston University, along with other universities I greatly benefited from, most notably Harvard and MIT, and the Starbucks at Harvard Yard which is open till 1am and where I, arguably, spent most of my working hours.

FIRST PRINCIPLES AND EFFECTIVE THEORY APPROACHES IN COMPLEX NETWORKS

(Order No.)

NIMA DEHMAMY

Boston University Graduate School of Arts and Sciences, 2016

Major Professor: H. Eugene Stanley, Ph.D.

William Fairfield Warren Distinguished Professor; Professor of Physics;

Professor of Chemistry; Professor of Biomedical Engineering;

Professor of Physiology;

ABSTRACT

This dissertation concerns modeling two aspects of dynamics of complex networks: (1) response dynamics and (2) growth and formation.

A particularly challenging class of networks are ones in which both nodes and links are evolving over time – the most prominent example is a financial network. In the first part of the dissertation we present a model for the response dynamics in networks near a meta-stable point. We start with a Landau-Ginzburg approach and show that the most general lowest order Lagrangians for dynamical weighted networks can be used to derive conditions for stability under external shocks. Using a closely related model, which is easier to solve numerically, we propose a powerful and intuitive set of equations for response dynamics of financial networks. We find the stability conditions of the model and find two phases: “calm” phase, in which changes are sub-exponential and where the system moves to a new, close-by equilibrium; “frantic” phase, where changes are exponential, with negative blows resulting in crashes and positive ones leading to formation of “bubbles”. We empirically verify these claims by analyzing data from Eurozone crisis of 2009-2012 and stock markets. We show that the model correctly identifies the time-line of the Eurozone crisis, and in the

stock market data it correctly reproduces the auto-correlations and phases observed in the data.

The second half of the dissertation addresses the following question: Do networks that form due to local interactions (local in real space, or in an abstract parameter space) have characteristics different from networks formed of random or non-local interactions? Using interacting fields obeying Fokker-Planck equations we show that many network characteristics such as degree distribution, degree-degree correlation and clustering can either be derived analytically or there are analytical bounds on their behaviour. In particular, we derive recursive equations for all powers of the ensemble average of the adjacency matrix. We analyze a few real world networks and show that some networks that seem to form from local interactions indeed have characteristics almost identical to simulations based on our model, in contrast with many other networks.

Contents

1	Introduction	1
1.0.1	Some Definitions	2
1.1	Structure and Importance in Complex Networks	3
1.1.1	Communities	3
1.1.2	Centrality	5
1.2	Dynamics, Cascades and Response in Networks	6
1.3	Network Formation and Growth	7
1.4	Structure of Dissertation	8
2	Effective Theory Modeling of Networks	9
2.1	Landau-Ginzburg Modeling of Dynamics	11
2.2	Model Building and Notation	11
2.2.1	Possible Lagrangian Terms	12
2.2.2	Hamiltonian	13
2.3	Stability Analysis: A Simple Example	14
2.3.1	Bipartite Example with Similar Layer Sizes	14
2.4	Application to Financial Markets	15
2.5	Introduction to the Eurozone Crisis of 2009–2011	16
2.6	The GIIPS problem	19
2.7	Model and Notation	21
2.8	An Optimization Problem: Minimize Risk, Maximize Profit	21
2.8.1	Comment on Possible Lagrangian Terms	22
2.8.2	Time Derivative Terms In The Lagrangian	23

2.8.3	The Effect of Response times	24
2.9	Equations Of Motion	25
2.10	A Phenomenological Model for Financial Markets	26
2.10.1	Assumptions, simplifications and the GIIPS system	26
2.11	Notations and Definitions	27
2.11.1	The time evolution of GIIPS holdings and their price	27
2.12	Comparison of the Lagrangian and the Phenomenological Model	30
2.12.1	The Last Equation	31
2.13	The constants α, β	32
2.14	Effect Of Dissipation	32
2.14.1	Derivation with Explicit Response Times in the Lagrangian	33
2.15	Numerical Solutions	34
2.16	Application to European Sovereign Debt Crisis	34
2.16.1	Estimating values of $\gamma = \alpha\beta$	34
2.17	Simulations	37
2.18	Testing the Role of the Network	40
2.19	Shocking different banks	41
2.20	Systemic Risk and BankRank	42
2.21	Phase Diagram and Phase Transition	43
2.22	Other Values of α and β and the Phases	43
2.23	The phase Space	44
2.24	Robustness of the Ranking	47
2.25	BankRank and stability	48
2.26	Analytical results from the 1 Bank vs 1 Asset system	48
2.26.1	Validity of perturbation theory near the phase transition	52
2.27	Proof for $\gamma = 1$ using properties of the phase transition	53
2.28	Mean Field and Application to Stock Markets	57
2.28.1	About the Stock Market	57

2.28.2	Linear Response and the Stock market	58
2.29	Modeling Stock Market Dynamics using the Market Response model	59
2.29.1	Case 1: $\tau_A = 0$	60
2.29.2	Case 2: $\tau_E = 0$	61
2.29.3	Auto-correlations and Green's Function	63
2.30	Autocorrelation in Cumulative News Data	65
2.31	Fitting Bank Correlations	67
2.31.1	Instabilities in the Stock Market	68
3	Networks of Local Interactions	71
3.1	Introduction	71
3.2	General Properties of Networks of Local Interactions	72
3.2.1	The Network and its Adjacency Matrix	73
3.3	General potential derivations	74
3.3.1	Two-point Interactions and "Rendezvous Points"	75
3.4	Degree and Degree Distribution	77
3.4.1	Note on Analytical Solutions	78
3.5	Higher-Order Moments of the Network	78
3.5.1	Degree-Degree Correlation and Clustering	79
3.6	Examples: Network of interacting random walkers	79
3.6.1	General power-law example	81
3.6.2	Clustering	82
3.6.3	Explicit Analytical Bounds for Higher Network Moments of the Interacting Random Walkers	83
3.7	Diffusion in Spherically Symmetric Potential with Interactions	88
3.7.1	Degree Distribution in Radially Symmetric Cases	90
3.7.2	Establishments and Three-Point Interactions	91
3.8	Real Data Analysis	94

3.8.1	Co-authorship on arXiv.org: HEP Theory vs HEP Phenomenology .	95
3.8.2	Gowalla Geotagging Social Network	95
3.8.3	Protein-Protein interactions	96
3.9	Discussion	97
3.10	Cities: Businesses as “Rendezvous Point” for Interactions over Cities	98
3.10.1	Cellphone data from Shanghai	99
4	Concluding Remarks	106
	Appendices	108
A	Lagrangian and Hamiltonian in Response Dynamics of Networks	109
A.0.2	Equations of motion	109
A.1	Hamiltonian and Stability Analysis	110
A.1.1	Scaling and Simplifications	110
A.1.2	Hamiltonian	111
A.1.3	Potential and Its Minima	112
A.2	Equations of Motion	113
A.2.1	Implications and conservation laws of the variational method for fi- nancial networks	113
A.3	Generalized Langevin and logistic equations	114
A.3.1	Friction terms and variation	114
A.4	Dynamics	115
A.4.1	General non-linear Langevin-type action	116
A.5	Initial conditions for simulations	117
A.6	Initial conditions after the shock	117
A.7	Estimating $\gamma = \alpha\beta$	119
A.8	Continuous Time Dynamics	120
A.8.1	Derivation in continuous time limit for the phenomenological model	121

A.9 Time-dependent Mass	122
A.10 Green's Function	123
A.11 More General Field-theory Networks	125
A.11.1 Solution for Harmonic Potential with Strong Friction	125
A.11.2 Mapping to Curved Space	125
A.12 Analytical results	127
A.12.1 Adjacency Matrix and Partition Function	127
A.13 Analytical Results	130
A.13.1 Degree Function	131
A.14 Eurocrisis exposure data	133
Bibliography	138
Curriculum Vitae	144

List of Tables

2.1	Total amount of exposure of the banks in our data set to the sovereign debt of the GIIPS countries	20
2.2	Notation	28
A.1	GIIPS debt data used in the analysis. All numbers are in million Euros. Our data is based on two sources: 1) The EBA 2011 stress test data, which only includes exposure of European banks and funds (these are the ones where the “Code Name” is of the form CC123); 2) A list of top 50 global banks, insurance companies and funds with largest exposures to GIIPS debt by end of 2011 provided by S. Battiston et al. (These have a name as their “Code Name”), which was consolidated by us.	137

List of Figures

- 1.1 The network of interactions of characters in Victor Hugo’s “Les Miserables” generated using Gephi graph visualization software. The thickness (i.e. the weight) of the edges is proportional to the number of times they interact in the story and the size of the nodes is proportional to the total number of interactions they have with other nodes. The colors indicate “communities” or modules or cliques, as social scientists refer to them. These are groups of nodes which have strong connections among each themselves. There exist many, inequivalent definitions for a community inside a network. 6
- 2.1 To lowest order a financial network can be thought of as as a bipartite network of investors and funds they invest in. The thickness of the links is proportional to the amount of the investment of each investor in each fund. 9
- 2.2 (Left) A sketch of the network of banks vs assets. It is a directed, weighted bipartite graph. The thicknesses represent holding weights. Motion along the edges from banks to assets is described with the wighted adjacency matrix A , whose entries are $A_{i\mu}$, the number of bonds μ held by bank i , and the opposite direction, assets to banks, is described with A^T . (Right) $\sinh^{-1}(A)$ with A being the weighted adjacency matrix of the GIIPS holdings, (weighted by amount of banks’ holdings in GIIPS sovereign debt expressed in units of millions of Euros. The vertical axis denotes different banks (121 of them) and they are ordered in terms of their total exposures to GIIPS debt (higher exposure is at the bottom of the plot) Because holdings differ by orders of magnitude we have plotted $\sinh^{-1} A$ here. 20

2.3	Estimates of $\gamma = \alpha\beta$ over 4 months periods. Top: the shaded purple region is the error-bars based on the standard deviations and the solid lines are the averages of different γ calculated for each country. Bottom: Calculation of γ_μ for individual countries. The fact that the values for different countries are close to each other is a sign that our assumption of “herding” (i.e. same α and β for all GIIPS) is justified and that our model is applicable here. As can be seen, before the height of the crisis $0 < \gamma < 1$ and then it gradually grows. At the height of the crisis $1 < \gamma < 2$. After the crisis we see γ decrease again to $\gamma < 1$. Later we show that at $\gamma < 1$ the system rolls into a new equilibrium, but when $\gamma > 1$ the asset prices crash. Also note the time-line of bailouts: Greek bailout approved 2010/04 and 2010/09; Irish bailout 2010/10. This explains part of the movements in the lower plot. The following stock tickers were used for each country (only the top 4 holders of each GIIPS for which stock prices could be obtained from Yahoo Finance): Greece: NBG, EUROB.AT, TPEIR.AT, ATE.AT; Italy: ISP.MI, UCG.MI, BMPS.MI, BNP.PA; Portugal: BCP.LS, BPI.LS, SAN; Spain: BBVA, SAN; Ireland: BIR.F, AIB.MU, BEN	35
2.4	Shocking “Bank of America” with $\alpha = \beta = 0.6$. Left: plot of Asset prices over time. Greece incurs the greatest losses, falling to 75% of original value. Final prices are listed in the legend. Right: Equities of the 4 “most vulnerable banks” (2 of major Greek holders incur large losses and one Italian bank is predicted to fail due to the shock). IT043 is Banco Popolare, which has very small equity but large Italian debt holdings. The next two are Agricultural Bank of Greece and EFG Eurobank Ergasias, which are among top 4 Greek holders.	38

2.5	Simulation for larger values of α and β (values in legends are final price ratios $p_\mu(t_f)$). This time, in addition to Greek debt, Spanish and Portuguese debt show the next highest level of deterioration. The same four banks are the most vulnerable and this time two more of them fail. At $\alpha = \beta = 1.5$ the damages are much more severe than at $\alpha = \beta = 0.6$	38
2.6	Left: Top: BankRank (2.34): Ranking the banks in terms of the effect of their failure on the system. Top plot shows the ratio of final total GIIPS holdings in the system to the initial total GIIPS holdings. The BankRank tells us how much monetary damage the failing of one bank would cause. second plot on the left shows the Survival equity ratio E^*/\tilde{E} , third is the initial holdings and last is the initial equity, all sorted in terms of BankRank at $\alpha = \beta = 1.5$. As we see, none of these three variables correlates highly with BankRank. The ranking changes for different values of α and β . Right: Scatter plot of the holdings divided by maximum holding (Holdings/max) versus BankRank at four different values of $\alpha = \beta = [0.4, 0.6, 1, 1.5]$. As we see increasing $\alpha\beta$ decreases the correlation between BankRank and initial holdings. BankRank at $\gamma = \alpha\beta < 1$ is correlates well with the holdings and is anti-correlated with it. But BankRank at $\gamma = \alpha\beta > 1$ deviates significantly from the holdings. This means that in the unstable regime $\gamma > 1$ it is no longer true that only the largest holders have the highest systemic importance.	39
2.7	Randomizing which bank lends to which country, while keeping total debt constant for each country. The results differ dramatically from the real world data used in Fig. 2.4. In this example Portugal and Italy lose the most value, while Greece is the least vulnerable. Other random realizations yield different results.	41
2.8	Shocking different banks at $\alpha = \beta = 0.6$. The final prices turn out very similar.	41

2.9	Contrarian regimes: top, both $\alpha, \beta < 0$. Here many banks fail, even for relatively small α, β . The losses are devastating. Our model suggests that such a regime should be avoided. The bottom two plots show the two points $\alpha = \pm\beta, \beta = \pm 10$. The two results are almost identical. They also show that no appreciable amount of profit or loss is generated in these regimes, thus making them rather unfavorable for investors most of the time, but because of their safeness could be a contingency plan (buyout of bad assets by central banks is one such contrarian behavior).	45
2.10	Left: Phase diagram of the GIIPS sovereign debt data, using the sum of the final price ratios as the order parameter. We can see a clear change in the phase diagram from the red phase, where the average final price is high to the blue phase, where it drops to zero. The drop to the blue phase is more sudden in the $\alpha < 0, \beta < 0$ quadrant than the first quadrant. Right: The time it takes for the system to reach the new equilibrium phase. This relaxation time significantly increases around the transition region, which supports the idea that a phase transition (apparently second order) could be happening in the first and third quadrants. The dashed white line shows the curve $\gamma = \alpha\beta = 1$. It fits the red banks of long relaxation time very well. This may suggest that $\gamma = 1$ is a critical value which separates two phases of the system.	46
2.11	BankRank for different values of α and β . After the phase transition to the unstable region (e.g. $\alpha = \beta = 1.5$) the rankings change significantly.	47
2.12	Top 10 banks whose failure causes the most damage to the price of each country's sovereign bond.	47

2.13	Numerical solutions to the differential equations in a 1 bank vs 1 asset system.	
	The upper plots show a “stable” regime, where after the shock none of the variables decays to zero or blows up, but rather asymptotes to a new set of values. The lower plots are in the “unstable” regime where positive or negative shocks either result in collapse or blowing up or collapsing of some variables.	49
2.14	Phase diagram of the 1 bank vs 1 asset system, responding to sudden rise in E . Black denotes regions where $\partial_t E = A\partial_t p$ was very large at late times, and light orange where it was close to zero. This is only plotting the $\alpha, \beta > 0$ quadrant (left is a log-log plot, right is the regular linear scale diagram). The overlay are two fit functions for the phase transition curve. While $\alpha\beta = 1$ is not a very good fit for large β and small α , it fits fairly well for large α 's and we analytically prove this below.	49
2.15	Convolution of the daily change in cumulative news sentiments with itself. It exhibits strong seven day and 3.5 day patterns, which suggest that the trend of increase and decrease in the cumulative sentiment repeats itself weekly and has a more or less fixed weekly pattern. Red curve is the fit and blue triangles, connected by dashed lines, are the actual Sentiment change convolutions. .	66

2.16	Auto-correlations of stock returns $\partial_t p$ for a number of banks. The horizontal axis shows the number of days of lag δt in the auto-correlation $\int \partial_t p(t) \partial_t(t + \delta t) dt$. Left: The mean, with one standard deviation error bars, of the auto-correlations of stocks of 10 banks which showed the most largest negative auto-correlation for a lag of 1 days. The stocks consisted of: UBI.MI, HBANP, 0005.HK, SDA, PHNX.L, ALBKY, PXQ.MU, MBFJF, NHLD, ZIONW. UBI, Huntington Hldng, HSBC, Sadia S.A., Phoenix Grp, Alpha Bank, Phoenix Sat TV, Mitsubishi UFJ, National Hldg, Zions Bancorp.. Right: 10 bank stocks with the most positive value of auto-correlations after one day: KBC.L, WBC.AX, DUA, HBA-PG, DTT, ANZ.AX, ERH, HBC, CSCR, DVHL. The solid curve is a fit using a damped harmonic oscillator, which would be consistent with what our model predicts the return on stock prices to do.	68
2.17	The value of frequency squared ω^2 for 5 important large banks. The top shows the mean (green) and the standard deviation (width of the purple band) across the 5 banks. The top shows the mean (green) and the standard deviation (width of the purple band) across the 5 banks. Bottom shows ω^2 for individual banks.	69
2.18	Stock price behavior before and after the 2007-2008 crisis. the vertical axis is ω^2 and the horizontal axis is the return $\partial_t p$. the lower half denotes the unstable part. the lower right shows “bubbles” and exponential growth, while the lower left represents “crash” and exponential decay of stock price. . . .	70
3.1	Two isotropic randm walker interacting through a space and time-dependent interaction function $\Gamma(x, t)$	80
3.2	The spatial degree function $k(r, t, T)$ and RP distribution function $\Gamma(x, t)$ for various exponents in 2 spatial dimensions. The models are characterized by $k_{\max} = k_{\max}(T - t)$ taken here to be linear: $k_{\max}(s) \propto s$	81

3.3	Right: Random walker in a strong harmonic potential. The walker very quickly drift toward the center of the potential. After that, since the potential is flatter there, they have a more stochastic behavior. People’s daily commute toward the center of a city may also approximately be modeled through a similar process. Left: The background potential U affects the dynamics of each random walker. But on top of this background potential, the random walker may interact with each other. As in the previous section, to lowest order this interaction will be through the “Rendezvous Point” distribution Γ similar to the distribution of businesses over the city in which people may see each other and interact.	88
3.4	Three-point interaction of stochastic agents. If one of the agents is condensed to $\langle\phi\rangle$ this interaction will define a natural background, space-dependent interaction $\Gamma \propto \langle\phi\rangle$	92
3.5	Co-authorship network of High Energy Phenomenology. The left column zooms into the high degree tail. BA denotes a Barabasi-Albert simulations. As we see the high degree tail fits very well with the BA. Right shows the full network’s moments. As we see the lower degree part of the network fits very well with simulations from our model.	101
3.6	Co-authorship network of High Energy Phenomenology vs High Energy Theory. As we see they have different patterns of local clustering and degree-degree correlation. HEPPh is consistent with our model while HET is not.	102
3.7	Gowalla vs C. Elegans PPI and simulations from our model. The online platform Gowalla, which is <i>not</i> formed from local interactions and is highly non-local due to the fact that anyone can find anyone else in the online system, behaves very differently from the rest. Note the descending trend in the local clustering and degree-degree correlation.	102

3.8	Top row: Simulations with power-law degree distributions using our model in 2D space. Degree distributions of graphs generated for power-law distributions with $\gamma = 1, 2, 3$. In the left column the dashed lines represent $k^{-\gamma}$ for $\gamma = 1, 2, 3$. Second row: Human Protein-Protein Interaction (HS PPI) network compared to a simulation with power-law $P(k) \sim k^{-\gamma}$ with $\gamma = 2$ and Barabasi-Albert (BA) model with minimum degree $m = 9$ chosen to endow it with a density similar to the PPI network, and which gives it non-zero clustering. The very high degree part of the HS PPI behaves similar to the BA model in the clustering, but for most of the network the local clustering and the degree-degree distribution is closer to a $\gamma = 1$ simulation of our model. Bottom row: PPI of the worm <i>C. Elegans</i> . It's degree-degree correlation fits very well with a $\gamma = 1$ simulation of our model, but it has higher clustering than our model.	103
3.9	Paris and Shanghai night light satellite pictures (left) and radial distributions (right). The dashed lines in the plots on the right are "Rendezvous Point" distributions Γ which our model would predict would result in power-law degree distributions with exponents $\gamma = 1$ and 2.	104
3.10	Shanghai cell phone call network against the BA model and our model's simulations.	105

List of Abbreviations

	Greece, Italy, Ireland, Portugal and Spain.
GIIPS	Five of the troubled European countries during the Eurozone crisis
RP	Rendezvous Point

Chapter 1

Introduction

In this dissertation we will discuss some aspects of modeling dynamics and physics of “complex networks” [1]. A network is an “effective” description of a system comprised of entities (e.g. particles, people, objects, etc.) which we will refer to as “nodes”, “agents”, or “vertices” and will pictorially depict them as vertices in a graph. A network tries to capture the essence of the relations or interactions among these vertices. It’s an “effective” description in the sense that we neglect many of the complications about relations among nodes and replace that with one number.

A useful way to quantify many networks is to think of the “Adjacency Matrix”, i.e. A matrix A whose elements A_{ij} quantify the relation of node i and node j . The nonzero matrix elements A_{ij} are called “links” or “edges”. The adjacency matrix is said to be “unweighted” if it only has Boolean values 0 and 1, and “weighted” if its elements are not restricted to 0 and 1. Aside from the adjacency matrix, in some real world situations the agents (nodes) themselves may also carry some “attributes”. For instance, in a lending network of banks to banks, the adjacency matrix is a weighted an asymmetric matrix, but the banks, which constitute the nodes in the network, also have attributes such as “assets” or “capital” which quantifies the total money they have available and which will play a role in tackling many problems related to this network.

The most common type of network is an unweighted, undirected network, which can be understood as a simple graph, with no directions on the edges. The adjacency matrix of such networks is a symmetric binary matrix. The diagonal elements of the adjacency matrix may be nonzero if there are “self-loops”, i.e. only if a node has a relation to itself.

Such self-loops, are for example useful in describing self-reinforcing or self-inhibitory effects of density of chemicals involved in biological pathways such as the autoregulatory feedback loops in the circadian rhythm pathways in mammalian cells [2].

Examples of some real-world for which an effective description in terms of networks is reasonable include power grids, friendship networks, online social networks such as friendship on Facebook, network of followers on Twitter, financial markets and networks of economic transactions among companies.

1.0.1 Some Definitions

The adjacency matrix is the basic building block of a network. It captures direct interactions of two agents. In a way a network is the simplest way to quantify interactions, as it does not capture any 3-way interactions directly. To clarify this more, consider one popular class of networks, namely the “correlation-based” networks. These networks have an adjacency matrix that is constructed by manipulating Pearson correlation of signals from agents. For example one can look at the price of a stock i as a function of time $p_i(t)$ (also known as a financial “time series”) and calculate the correlation of this with the price of another stock

$$A_{ij} \sim \langle p_i p_j \rangle \equiv \frac{1}{T} \int_0^T dt \tilde{p}_i(t) \tilde{p}_j(t), \quad \tilde{p}(t) \equiv \frac{p(t) - \langle p(t) \rangle}{\sigma_p}$$

Such correlation-based networks will capture two-point functions, i.e. correlations of two p_i ’s here, but if the underlying dynamics contains three point interactions $p_i p_j p_k$ this network will never capture non-trivial 3-point or 4-point interactions that cannot be reduced to two-point functions.

Going back to the network, all network quantities that do not deal with nodes and only deal with their connections can be constructed from the adjacency matrix A_{ij} . One of the simplest and lowest order quantities for each node that is derived from A_{ij} is the “degree” of the node k_i

$$k_i \equiv \sum_j A_{ij}$$

Now we can define the first, lowest order statistics about the network, namely the “degree distribution” $P(k)$ which is the distribution of all the degrees in a network. In the later chapters we will introduce higher order “moments” of the network which are related to statistics of higher powers of the adjacency matrix, i.e. $[A^n]_{ij}$. Clearly, in order to exactly quantify the properties of a network one needs to look at statistics of as many powers n as needed. Since by definition complex networks are complex, in order to study how well a model describes a network there is no trivial way of matching nodes inside a model with nodes in a real-world complex network, especially given the fact that almost always the real data has a high level of noise. Therefore the only meaningful comparisons that may be done between a model and a real complex network are statistical comparisons and these need to be done on at least a few moments of the network to ensure the networks derived from a model match with the real data. A thorough introduction to the elementary properties and statistics of some real world networks can be found in [1].

1.1 Structure and Importance in Complex Networks

One class of problems that can be tackled in the network description of a system is whether there exist large scale structures such as communities within complex network.

1.1.1 Communities

There are many different, inequivalent ways one can define communities in a network. A simple method is to look for “cliques”, coined appropriately by social scientists. Cliques are comprised of nodes that have more connections with the nodes within the clique than the nodes outside of it. Though cliques may be useful in many social contexts, they are not the only communities one may be interested in. Often times the network is playing a role in transferring information or resources from one node to another. For instance in a bank-to-bank lending network the links in the network signify the flow of money between banks. In such scenarios a type of community one may be interested in is one which captures where money that starts out from one bank is most likely to go. If we denote the money of bank

i at time step t by $m_i(t)$ and assume that the lending network adjacency matrix element A_{ij} captures how this money flows from bank j to bank i , we have

$$\delta_t m_i(t) \equiv m_i(t+1) - m_i(t) = f_i(t) \sum A_{ij} m_j(t), \quad (1.1)$$

where f_i may be for instance related to the decision making of the banks on what fraction of the money they borrow from others they are ready to lend to others. If we wish to find out how the lending network “clusters” together, i.e. what the internal community structure looks like, we need a community detection method that follows the diffusion of money in the network. One can think of this flow of money as a diffusion or Markov process happening on the network. If $f_i = 1$ solving (1.1) simply yields an exponential function of the matrix

$$m_i(t) \sim [\exp[tA] \cdot m(0)]_i$$

If one chooses $f_i = 1/k_i$ then we will have a random-walk through the degree-normalized adjacency matrix. We won’t go into the details of this any further, but the take-home message is that the communities that are important for flow processes on the network are related to the spectrum of either the adjacency matrix or a modified matrix such as the degree-normalized adjacency matrix or the a more general $f_i A_{ij}$. This is because the eigenvalues of the matrix defining the flow are proportional to the life-time of their corresponding eigenvectors. Therefore starting the flow from a part of the network that mostly contributes to a certain eigenvector with a large eigenvalue would mean that the flow would remain distributed among the main components of that eigenvector for a long time. In this sense, these eigenvectors quantify flow communities which are important in problems concerning flows. Such methods of community detection are known as “Spectral clustering” methods and were studied by Newman et al [3, 4] and many other [5, 6].

Routing on the Internet is also a type of flow and there are other simpler quantities that can be derived from eigenvectors which we will briefly discuss below.

1.1.2 Centrality

Another aspect of relations in a network that is useful in many contexts is the notion of “centrality”. Centrality, in a broad sense, is a way to assign importance to nodes in the network. Depending on what aspect of the interactions are important to us, we may choose different centrality measures to be examined in a network. The simplest type of centrality is the “degree centrality” which basically means ranking nodes based on their degree. Another type of centrality which measures how much a node acts as a bridge between other nodes is the “betweenness centrality” which ranks the nodes based on how many of the paths connecting all other nodes needs to go through a particular node. For example, a node that isn’t strongly connected to a lot of nodes, and thus does not belong to a clique, may be the bridge connecting two communities to each other. Such nodes, sometimes called “weak ties” in social science, actually play an important role in social systems and they have a high betweenness centrality as any path from the community on one side of it to the community on the other side has to go through this node.

Another class of centrality measures which are again related to problems where we care about flows, as discussed above, are “eigenvector centrality” measures and various measures derived from them. In the most basic setting in a network with a single connected component, a flow process that happens through the adjacency matrix and which is redistributing resources put at different nodes will, after a long time, distribute the resources based on the largest eigenvalue eigenvector of the adjacency matrix. The reason behind this is easily seen if one expands the initial distribution vector $m_i(0)$ of resources on nodes in terms of eigenvectors of A , call them ϕ_i^λ . At each step the flow happens by acting with A_{ij} on the vector $m_i(t)$. Each time this happens the eigenvectors in m_i are enhanced by a factor of their eigenvalue λ . Therefore after many successive time-steps the largest eigenvalue eigenvector $\phi_i^{\lambda_{max}}$ is enhanced more than any other.

The flow process described is agnostic to flows that return to the initial node and treats them as any other flow. In some problems, such as routing requests on the Internet, or ranking importance websites based on the number of times other websites link to them

one might wish to ignore self-routing and do a smarter type of ranking. Derived centrality measures such as the Katz centrality and Google PageRank, which are modified versions of the eigenvector centrality, try to tackle such problems and introduce smarter rankings. The details of their definition as well as a more thorough discussion of centrality in general can be found in [1].

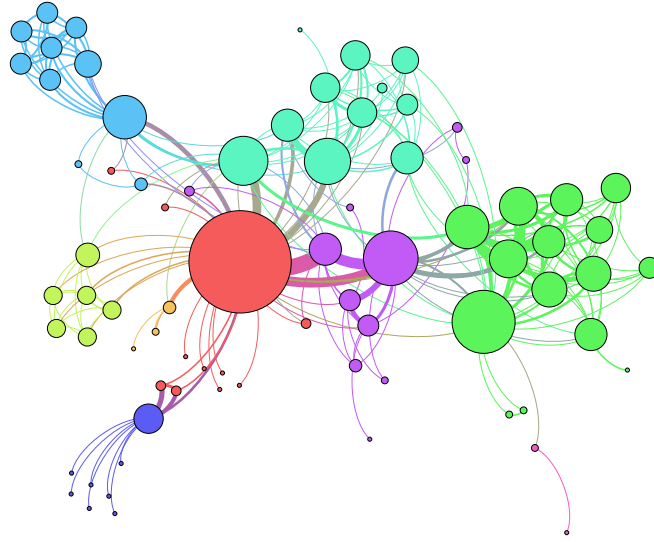


Figure 1.1: The network of interactions of characters in Victor Hugo’s “Les Misérables” generated using Gephi graph visualization software. The thickness (i.e. the weight) of the edges is proportional to the number of times they interact in the story and the size of the nodes is proportional to the total number of interactions they have with other nodes. The colors indicate “communities” or modules or cliques, as social scientists refer to them. These are groups of nodes which have strong connections among each themselves. There exist many, inequivalent definitions for a community inside a network.

1.2 Dynamics, Cascades and Response in Networks

Some of these networks are dynamic. Friendship networks may evolve in time, networks of investors and assets constantly change, and economic relations vary over time. Many financial crises are a result of cascades of losses propagating through a financial network. Modeling the response of networks is crucial for avoiding such crises.

Unfortunately, the centrality measures and spectral community detection methods discussed above all assume the network connections remain the same throughout the flow process and that they are not dynamical. Therefore, these methods cannot be applied to highly dynamical networks such as a stock market. The relevant questions about centrality in this context are very different. For example one can talk about how much loss the bankruptcy of one node in a financial market network can induce on the whole market, but this question cannot be answered using any static network-based centrality or flow measure discussed above. The goal of the second chapter of this dissertation is to start from the beginning and build a theory for quantifying the “effective theory” dynamics that one might expect from highly dynamical networks such as financial networks, and then introduce dynamical measures of importance of nodes based on what the dynamics would predict their failure would mean for the system.

1.3 Network Formation and Growth

Many networks, such as co-authorship networks, friendship networks and other social networks grow and evolve in time. The mechanisms underlying their growth are diverse. The third chapter of this dissertation concerns formation of such networks. We will focus on a subset of network growth mechanisms, namely the ones that involve local interactions in some parameter space. There exist many network models for formation of “random networks”, i.e. networks in which new nodes have global knowledge about all nodes in the system and can decide to connect to some existing nodes based on some growth protocol. One popular class of such models is the preferential attachment model, in which a new node preferentially attaches to nodes with higher number of connections. The goal of the third chapter is to examine whether having a network emerge from interactions that were local in nature, meaning they happened due to proximity or point-like interaction of agents inside some space and based on some physical dynamics that the nodes had in that space, will have quantitative effects on the structure of the network. Our claim here is that, in short, yes. Such networks have very specific structures observable in various network moments.

1.4 Structure of Dissertation

The dissertation consists of two main chapters, and a concluding chapter. The first main chapter is on using “effective theory” methods, such as Landau-Ginzburg models and other phenomenological methods, for modeling response of a network to shocks and classifying the phases of such systems. We apply these models to financial networks and identify stable and unstable phases of the system. The second main chapter concerns networks forming from local interactions. We propose a method that uses local stochastic field theory for constructing networks and find the characteristics of such networks. The results are very general and applicable for a variety of interaction mechanisms. We compare our findings with some real-world networks and find good agreement with some.

Chapter 2

Effective Theory Modeling of Networks

Many networks are dynamic. A friendship network, for instance, evolves over time because people make new acquaintances. In such networks, problems of interest usually concern the formation and deletion of links between the nodes and the nodes themselves do not have any attributes. But in many other networks, such as financial networks and power grids, the nodes have attributes that evolve in time.

Consider, for example a financial market. As sketched in Fig. 2.1, to lowest order one

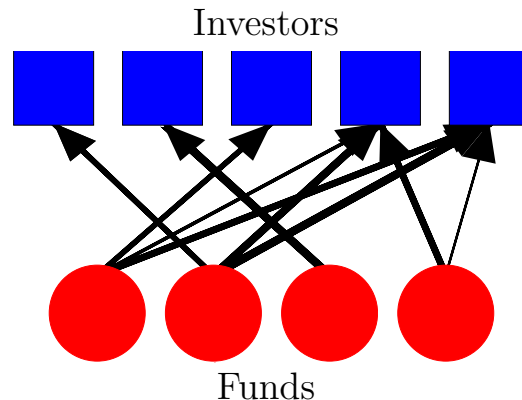


Figure 2.1: To lowest order a financial network can be thought of as as a bipartite network of investors and funds they invest in. The thickness of the links is proportional to the amount of the investment of each investor in each fund.

can think of this network as a bipartite network with investors in one layer and the funds they invest in in the other layer. The key difference between this network and a friendship network, aside from the approximate bipartite structure, is the fact that each node has certain attributes that can change over time. The quantity of each fund that the investors owns is the weight of the link between the investors and the fund. But the unit price of the

fund is an attribute that is different for each fund and which changes over time. Similarly, the net worth or total money that each investor has is an attribute specific to each investor and it varies over time. Thus both the links and the nodes in this network have attributes that are dynamic. There are also many single layer financial networks. Inter-bank lending networks [7], where each bank is lending money or investing in another bank. Thus each bank is both the investor and the fund in these networks.

Dynamical networks such as the ones described above are generally classified as “temporal networks” [8–10].

There also exist numerous methods for the case where the dynamics is only happening at the level of node attributes, while the network connections remain static. Some notable elegant methods involve the use of the network Laplacian as an operator that defines a Markov process for flow redistribution on the network. A good review with concrete examples for bipartite networks is [11]. This approach, however, does not tackle the case where the links are also evolving in time.

Lagrangian models are another alternative which provide a natural language for describing the evolution of a weighted network, both the node attributes and the links. Lagrangian control has been employed extensively in robotics for controlling a system of coupled degrees of freedom (see [12] and references therein). Lagrangian dynamics is essentially a linear optimization method in which the dynamics is optimizing the global objective function defined by the Lagrangian. In economic systems the agents are also trying to optimize their situation by, for instance, maximizing profit while minimizing risk at the same time, given the constraints that they are subject to. Thus it is just natural to use Lagrangians to describe evolution of economic and financial networks. Lagrangians are employed in finance for many decision-making problems and market evolutions because of this reason [13, 14].

Extending these ideas to a complex network of financial ties, or similar networks, and going beyond the limited scope of other works described above is the purpose of this chapter. In this chapter we show how simple familiar methods of effective model building such as Landau-Ginzburg theories can yield powerful results concerning how a random network may

respond to external noise, shocks or driving forces.

2.1 Landau-Ginzburg Modeling of Dynamics

Here we build a general Lagrangian for a dynamical network. The dynamics may be both in the weight of the links and in the functions assigned as attributes to nodes. This type of modeling works best for first order approximation of the response of a dynamical system near a saddle point or a local stable or meta-stable equilibrium point.

We will examine the properties of the Landau-Ginzburg type Lagrangians for describing response dynamics of networks. Both the links and the attributes we assign to nodes will change over time.

2.2 Model Building and Notation

Assume that we have N nodes. To each one we will assign one continuous number as their “attribute”. We denote this attribute for node i at time t by $\phi_i(t)$ and denote the vector of all ϕ_i ’s by Φ . Our weighted “adjacency matrix” is a matrix describing the connections between nodes and it will be a general $N \times N$ matrix of real or complex values. We will denote it by A .

We will first work with real Φ and A , but generalization to complex values will be straightforward. We wish to write down possible Lagrangians for how such a network may react to changes from a saddle-point solution of its dynamics. Thus, essentially we are building a Landau-Ginzburg model of response in networks. This will be essentially the same as regular Landau-Ginzburg with Φ being the dynamic field, except that now there is an additional set of degrees of freedom in the links A . In Landau-Ginzburg theories, generally we start around an equilibrium and therefore the first order expansion terms go to zero. However here, because the system is more complicated here with time-dependent $A(t)$ we cannot be sure that at a local saddle-point all first order derivatives are zero. Basically this is to say that there must exist some order parameters Ψ which, if the system is written in terms of them, the Landau-Ginzburg model would have no first order $\Psi^T \partial_t \Psi$

type term in it. But our initial choice Φ may not have this property¹. Therefore we will also keep track of possible first-order Lagrangian terms.

2.2.1 Possible Lagrangian Terms

Let's start by writing the simplest scalar terms that can be formed from Φ and A . We do not wish to go beyond two time derivatives for now. The simplest models with nontrivial dynamics will have a single time derivative, but we wish to go up to two time derivatives because that is what generally variations around a local minimum will contain.

Note that A is not necessarily symmetric. Let's denote the symmetric (Hermitian for complex values) and anti-symmetric (anti-Hermitian) part of it by:

$$A_+ \equiv \frac{1}{2}(A + A^T), \quad A_- \equiv \frac{1}{2}(A - A^T).$$

The only lowest order scalars that can be formed are $\Phi^T A \Phi$ and its derivatives. Thus, to lowest order, a Landau-Ginzburg Lagrangian for this system would look like:

$$\begin{aligned} \mathcal{L} = & a \partial_t \Phi^T A \partial_t \Phi + q_1 \partial_t \Phi^T \partial_t A \Phi + q_2 \partial_t \Phi^T \partial_t A^T \Phi \\ & + b_1 \Phi^T A \partial_t \Phi + b_2 \Phi^T A^T \partial_t \Phi + c \Phi^T A \Phi \\ = & a \partial_t \Phi^T A_+ \partial_t \Phi + q_+ \Phi^T \partial_t A_+ \partial_t \Phi + q_- \Phi^T \partial_t A_- \partial_t \Phi \\ & + b_+ \Phi^T A_+ \partial_t \Phi + b_- \Phi^T A_- \partial_t \Phi + c \Phi^T A_+ \Phi \end{aligned} \tag{2.1}$$

Although this is a quadratic Lagrangian in terms of Φ , the full Lagrangian is not quadratic because A is also a dynamic variable.

¹note that in networks we prefer not to take a linear combinations of Φ as an order parameter because it mixes different nodes.

2.2.2 Hamiltonian

Let's first group terms together.

$$\begin{aligned}
B_{\pm} &\equiv q_{\pm} \partial_t A_{\pm} + b_{\pm} A_{\pm} \\
B &\equiv B_+ + B_- \\
bA &\equiv b_+ A_+ + b_- A_- \\
\mathcal{L} &= a \partial_t \Phi^T A_+ \partial_t \Phi + \Phi^T B \partial_t \Phi + c \Phi^T A_+ \Phi
\end{aligned} \tag{2.2}$$

The conjugate momenta are:

$$\begin{aligned}
P \equiv \pi_{\Phi} &= \frac{\partial \mathcal{L}}{\partial \partial_t \Phi^T} = 2a A_+ \partial_t \Phi + B^T \Phi \\
\pi_{A_{\pm}} &= \frac{\partial \mathcal{L}}{\partial \partial_t A_{\pm}} = q_{\pm} \partial_t (\Phi) \Phi^T \\
&= \frac{q_{\pm}}{4a} A_+^{-1} (\pi_{\Phi} - B^T \Phi) \Phi^T
\end{aligned} \tag{2.3}$$

Now, recall that the Hamilton equations for a variable x and its conjugate p are:

$$\partial_t p = -\frac{\partial H}{\partial q}, \quad \partial_t q = \frac{\partial H}{\partial p}$$

But $\partial_t \Phi$ appears in both π_{Φ} and $\pi_{A_{\pm}}$. Therefore, doing the usual Legendre transform $\mathcal{H} = \vec{p} \cdot \partial_t \vec{x} - \mathcal{L}$ with all three variables Φ, A_{\pm} will fail to satisfy the $\partial_t q$ Hamilton's equation for the obvious reason that $\partial_t \Phi$ appears in two terms of the Legendre transformation. We will show the general reason in appendix A. The issue is that A_{\pm} only appears to first order in the Lagrangian and is coupled to Φ . Therefore we will only do one Legendre transform and only write the Hamiltonian in terms of the π_{Φ} and not $\pi_{A_{\pm}}$. This will ensure that Hamilton's equations will be satisfied.

The Hamiltonian becomes (assuming $|A_+| \neq 0$):

$$\begin{aligned}
\mathcal{H}(P, \Phi, A_{\pm}, \partial_t A_{\pm}) &= \partial_t \Phi^T \pi_{\Phi} - \mathcal{L} \\
&= a \partial_t \Phi^T A_+ \partial_t \Phi - c \Phi^T A_+ \Phi
\end{aligned}$$

$$\begin{aligned}
&= \frac{1}{4a}(P^T - \Phi^T B)A_+^{-1}(P - B^T \Phi) - c\Phi^T A_+ \Phi \\
&= \frac{1}{4a}P^T A_+^{-1}P - \frac{1}{2a}P^T A_+^{-1}B^T \Phi + \frac{1}{4a}\Phi^T B A_+^{-1}B^T \Phi - c\Phi^T A_+ \Phi
\end{aligned} \tag{2.4}$$

The terms without P are the potential terms. We wish to understand their behavior. The potential energy terms are therefore:

$$\mathcal{V} = \Phi^T V \Phi, \quad V \equiv \frac{1}{4a}B A_+^{-1}B^T - cA_+$$

2.3 Stability Analysis: A Simple Example

Here we want to understand what the saddle points of the above Hamiltonian are. We will assume that there are extra dissipative terms in the equation of motion which kill all momenta. We want to see if the system admits stable or unstable equilibria. That is we wish to solve:

$$\frac{\partial \mathcal{V}}{\partial \Phi^T} = V \Phi = 0$$

The necessary condition for this to have solutions for $\Phi^T \Phi \neq 0$ is to have $|V| = 0$.

When the quadratic $\Phi^T V \Phi$ potential has a minimum for Φ , that is when generally $|V| > 0$, we should be able to find stable equilibria for Φ and A . The potential will be unstable when $|V| < 0$. Therefore we expect a smooth second order phase transition to occur where $|V| = 0$. Let's examine under what circumstances this happens in a solvable case.

2.3.1 Bipartite Example with Similar Layer Sizes

Assume:

$$A_+ = \begin{pmatrix} 0 & M \\ M & 0 \end{pmatrix}, \quad A_+ = \begin{pmatrix} 0 & M \\ -M & 0 \end{pmatrix}$$

This is characteristic of a bipartite, unidirectional network. Also assume that $|M| \neq 0$ (i.e. it's a square matrix and invertible). This will have the property that:

$$A_+^{-1}A_- = \begin{pmatrix} -1 & 0 \\ 0 & 1 \end{pmatrix}, \Rightarrow A_-A_+^{-1}A_- = -A_+$$

Let's first see if there may be solutions where all movements seize in A and $\partial_t A = 0$. This Leads to:

$$\begin{aligned} B_{\pm} &\rightarrow bA \\ V &\rightarrow \frac{1}{4a} (b_+^2 A_+ + b_-^2 A_- A_+^{-1} A_-) - cA_+ \\ &= \frac{1}{4a} (b_+^2 A_+ - b_-^2 A_+) - cA_+ \end{aligned} \tag{2.5}$$

Where the b_+b_- terms cancel from $A_- + A_-^T = 0$. When $|A_+| \neq 0$ the only way to have a saddle point for the potential is to have:

$$b_+^2 - b_-^2 - 4ac = 0$$

We will discuss below how by rescaling the degrees of freedom some of the coefficients can be absorbed into Φ, A , but let us make use of one such freedoms and scale $b_1 \rightarrow 1$. This makes $b_{\pm} = (1 \pm b_2)/2$. Plugging into the equation above we have:

$$b_2 = ac$$

Which, when $c = 0$ gives $b = 0$.

2.4 Application to Financial Markets

Financial markets have investors on one side and assets on the other. This natural bipartite structure and their dynamical nature makes our model a good candidate for describing their response to shocks.

The abstract exposition of the previous section can indeed be made more concrete and

be applied to specific problems in financial networks. We will take a phenomenological approach below and will tackle a concrete problem, namely the fragility of the network of financial institutions who lent money to sovereign governments in Europe. Below we will describe the problem of the Eurozone crisis of 2009 to 2011. It has all the complications of a financial network where all elements have dynamics. In addition, the exact approach from above proves to be hard to simulate numerically and we resort to a simplified version for the actual computations. After describing the economic details of the problem and existing literature, we will argue how this problem can be understood as an optimization problem with response times, akin to many systems encountered in physics. We will then move on to numerical solutions of the equations. The model also allows for rigorous investigation of stability conditions for this network and we both derive these conditions analytically and support the results through numerical simulations.

2.5 Introduction to the Eurozone Crisis of 2009–2011

Financial networks are dynamic. To assess their systemic importance to the world-wide economic network and avert losses we need models that take the time variations of the links and nodes into account. Using the methodology of classical mechanics and Laplacian determinism we develop a model that can predict the response of the financial network to a shock. We also propose a way of measuring the systemic importance of the banks, which we call BankRank. Using European Bank Authority 2011 stress test exposure data, we apply our model to the bipartite network connecting the largest institutional debt holders of the troubled European countries (Greece, Italy, Portugal, Spain, and Ireland). From simulating our model we can determine whether an network is in a “stable” state in which shocks do not cause major losses, or an “unstable” state in which devastating damages occur. Fitting the parameters of the model, which play the role of physical coupling constants, to Eurozone crisis data shows that before the Eurozone crisis the system was mostly in a “stable” regime, and that during the crisis it transitioned into an “unstable” regime. The numerical solutions produced by our model match closely the actual time-line of events of the crisis. We also find

that, while the largest holders are usually more important, in the unstable regime smaller holders also exhibit systemic importance. Our model also proves useful for determining the vulnerability of banks and assets to shocks. This suggests that our model may be a useful tool for simulating the response dynamics of shared portfolio networks.

Recent financial crises have motivated the scientific community to seek new interdisciplinary approaches to modeling the dynamics of global economic systems. Many of the existing economic models assume a mean-field approach, and although they do include noise and fluctuations, the detailed structure of the economic network is generally not taken into account. Over the past decade there has been heightened interest in analyzing the “pathways of financial contagion.” The seminal papers were by Allen and Gale [15, 16] and these were followed by many other studies [17–22]. Economists have recently become aware that econometrics has traditionally paid insufficient attention to two factors: (i) the structure of economic networks and (ii) their dynamics. Studies indicate that a more thorough approach to the examination of economic systems must necessarily take network structure into consideration [23–30].

One example of this approach is the work of Battiston et al. [31]. They study the 2008 banking crisis and use network analysis to develop a measure of bank importance. By defining a dynamic centrality measurement called DebtRank that measures interbank lending relationships and their importance in propagating network distress, they show that the banks that must be rescued if a crash is to be avoided (those that are “too big too fail”) are the ones that are more “central” in terms of their DebtRank.

Another recent event that has motivated and provided the focus for our study reported here is the 2011 European Sovereign Debt Crisis. It began in 2010 when the yield on the Greek sovereign debt started to diverge from the sovereign debt yield of other European countries, and this led to a Greek government bailout [32]. The nature of the sovereign debt crisis and resulting network behavior that we analyze here differs somewhat from that of the US banking crisis. Here we focus on the funds that several Eurozone countries—Greece, Italy, Ireland, Portugal, and Spain (GIIPS)—had borrowed from the banking system

through the issuing of bonds. When these governments faced fiscal difficulties, the banks holding their sovereign debt faced a dilemma: should they divest some of their holdings at reduced values or should they wait out the crisis. The bank/sovereign-debt network that we analyze in this study is a bilayer network. Although DebtRank has also been used to study bipartite networks, e.g., to describe the lending relationships between banks and firms in Japan [33], it does not take into account that link weights exhibit a dynamic behavior.

Huang et al. [34] and Caccioli et al. [35] analyzed a similar problem, that of cascading failure in a bipartite network of banks vs assets in which risk propagates among banks through overlapping portfolios (see also Ref. [36]). Although network connections in real-world financial systems, e.g., interbank lending networks or stock markets, are dynamic, neither of the above models [34,35] take this into account. Other models by Hałaj and Kok [37], which use simulated networks similar to real systems, or by Battiston et al. [38] allow the nodes to be dynamic but not the links (see, however, Ref. [39], in which dynamic behavior occurs when a financial network attempts to optimize “risk adjusted” assets [40]). Our approach differs from both of these because by introducing only two parameters which play the role of coupling constants in physics we can enable all network variables to be dynamic. Our model is related to Caccioli et al. [35] and Battiston et al. [31] but differs in that we allow both nodes and links to be dynamic.

We use a time-slice of the GIIPS sovereign debt holders network from the end of 2011 to focus on a simplified version of the network structure and use it to set the initial conditions for our model. We start by proposing, solely on phenomenological grounds, a set of dynamical equations. Based on our analysis we observe that:

1. When we model how a system responds to an individual bank experiencing a shock, our analysis is in accordance with real-world results, e.g., in our simulations Greek debt is clearly the most vulnerable.
2. The dynamics arising from our model produces different end states for the system depending on the values of the parameters.

In order to determine which banks play a systemically dominant role in this bipartite network, we adjust the equity of each bank until it goes bankrupt and then quantify the impact (the BankRank) of the bank’s failure on the system. We simulate the dynamics for different parameter values and observe that the system exhibits at least two distinctive phases, one in which a new equilibrium is reached without much damage and one in which the monetary damage is quite significant, even devastating.

2.6 The GIIPS problem

Governments borrow money by issuing sovereign (national) bonds that trade in a bond market (which is similar to a stock market²).

Our GIIPS data are from the 137 banks, investment funds, and insurance companies that were the top holders in the GIIPS sovereign bond-holder network in 2011. (Hereafter we will use “banks” to refer to all these financial institutions.) Table 2.1 shows the percentages of the sovereign bonds issued by each GIIPS country owned by these banks. Since our model requires knowing the equity of each bank, we reduce our dataset to the 121 banks whose equity value was obtainable. By the end of 2011, two important Greek banks—the National Bank of Greece and Piraeus Bank—had negative equities. Because our model only considers banks that can execute trades based on positive capital, we also had to eliminate these two banks from our analysis. Figure 2.2 shows the weighted adjacency matrix of this network.³

When a country defaults on sovereign debt (or stops paying interest as it comes due) the consequences are usually grave. To prevent cascading sovereign defaults, the European Union, the European Central Bank (ECB), and the International Monetary Fund jointly

²The entity that issues a bond (e.g., the government in case of sovereign bond) promises to pay interest. Governments also promise to return the face value of the loan at the “maturity” date. Bonds, unlike stocks, have maturities and interest payments. A detailed description of some of these bond characteristics can be found in Ref. [41]. As is the case with stocks, the value of these sovereign bonds increases when countries are doing well, and supply and demand ultimately determine the value of the bonds. If, however, the country becomes troubled and the market perceives that the government will not be able to pay back the debt, the price of the bond can crash, which was the case of Greece.

³The intensity of the color is proportional to $\text{Arcsinh}(A)$ for better visibility. For large $A_{i\mu}$, $\text{arcsinh}(A) \approx \log(2A)$.

Table 2.1: Total amount of exposure of the banks in our data set to the sovereign debt of the GIIPS countries

	Greece	Italy	Portugal	Spain	Ireland
Total (bnEu)	96.90	420.55	48.93	333.46	32.60
% in Banks	35.37	25.62	38.04	48.12	36.39

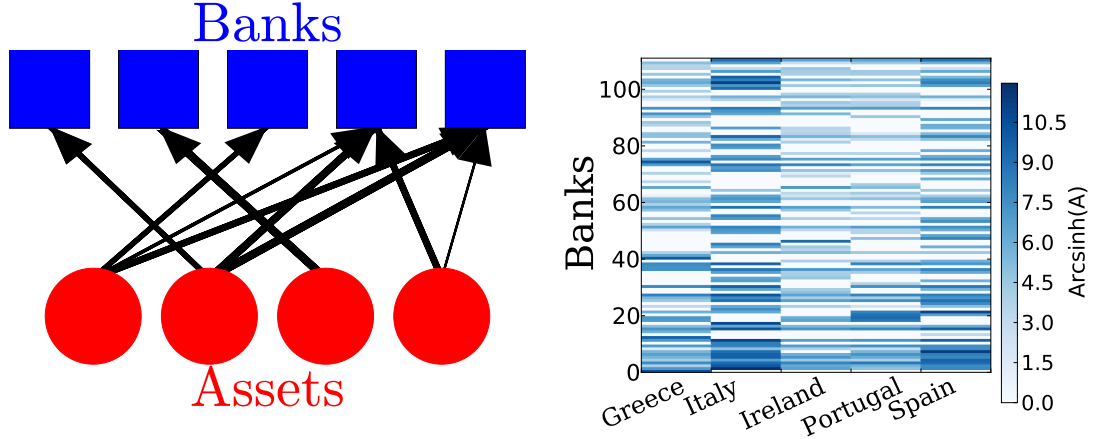


Figure 2.2: (Left) A sketch of the network of banks vs assets. It is a directed, weighted bipartite graph. The thicknesses represent holding weights. Motion along the edges from banks to assets is described with the weighted adjacency matrix A , whose entries are $A_{i\mu}$, the number of bonds μ held by bank i , and the opposite direction, assets to banks, is described with A^T . (Right) $\sinh^{-1}(A)$ with A being the weighted adjacency matrix of the GIIPS holdings, (weighted by amount of banks' holdings in GIIPS sovereign debt expressed in units of millions of Euros. The vertical axis denotes different banks (121 of them) and they are ordered in terms of their total exposures to GIIPS debt (higher exposure is at the bottom of the plot) Because holdings differ by orders of magnitude we have plotted $\sinh^{-1} A$ here.

established financial programs to provide funding to troubled European countries. Funding was conditional on implementing austerity measures and stabilizing the financial system in order to promote growth and increase productivity. We use our sovereign debt data as the initial condition for a model of cascading distress propagating through a bipartite bank network in which banks only affect each other through shared portfolios. In order to develop a framework for analyzing these problems that goes beyond simply determining how distress propagates through the links, we construct a model in which dynamic change affects both the weights of links and the attributes of nodes. Figure 2.2 shows the weighted adjacency matrix of this network in log format.

2.7 Model and Notation

The system that we study is a bipartite network as shown in Fig. 2.2. On one side we have the GIIPS sovereign bonds, which we call “assets,” and on the other we have the “banks” that own the GIIPS bonds. The nodes on the “asset” side are labeled using Greek indices μ, ν, \dots . To each asset μ we assign a “price,” $p_\mu(t)$ at time t . The “bank” nodes are labeled using Roman indices i, j, \dots . Each bank node has an “equity” $E_i(t)$, a time t , and an initial value of asset μ . Each bank in the network can have differing amounts of holdings in each of the asset types. The amount of asset (e.g. number of bonds) μ that bank i holds is denoted by $A_{i\mu}(t)$, which is essentially an entry of the weighted adjacency matrix A of the network. In our model we begin with a set of phenomenological equations describing how each of the variables $E_i(t)$, $A_{i\mu}(t)$, and $p_\mu(t)$ evolve over time. A key feature of our model is that the weights of links $A_{i\mu}$ are time-dependent, and this introduces dynamics into our network.

2.8 An Optimization Problem: Minimize Risk, Maximize Profit

In a market the investors and the traders are optimizing between averting losses and maximizing their profit. A Lagrangian approach is a simple approach to such optimization problems.

2.8.1 Comment on Possible Lagrangian Terms

We know that our equations may have dissipation, but let us first try to find the most general non-dissipative dynamical model for a system like ours, subject to certain assumptions about simplicity. We do not have information about long term behavior of the system and the global forces driving it to the (near) equilibrium state it may be in presently. Thus we will not say much about the potential energy terms $V(E, A, p)$. We wish to find the response dynamics of this system and will assume that we are sitting near equilibrium where the conservative forces are small, $F = -\nabla V \approx 0$, and the potential is extremely flat, i.e. second derivatives like $\partial_A \partial_p V$ are much smaller than parameters like α and β . So we will basically neglect the potential energy terms and focus on terms with time derivatives.

Since we are interested in the dynamics of propagation of a shock in this system, we are mostly interested in terms which define an interaction through the links in the network. Thus terms like $E^T E$ or $p^T p$ or their time derivatives are not interesting because they don't define such interactions. Neither is the trace term $\text{Tr}[A^T A]$ because it does not involve the node attributes E and p at all. Terms like $E^T A A^T E$ partly satisfy our criteria, but they do not give rise to propagation from banks' E to GIIPS holdings' p . Plus, we want to examine the simplest possible model. obviously it is possible to have arbitrary powers of each of the variables E, A, p , but we will restrict ourselves to the lowest order of them which would give rise to an interaction between the banks' equity E and the asset prices p . The possible interaction terms can only be the following, and their time derivatives:

$$E^T A p, \quad E^T A A^T A p, \quad E^T A (A^T A)^n p$$

with arbitrary power n . But since we want the simplest possible case, we are left with the lowest order interaction, which is only:

$$E^T A p$$

This will result in a great simplification. Since we dismissed the potential energy term,

we only need to deal with various time derivatives of this term. Following physical intuition, we will only consider terms with up to two time derivatives, and not higher than that.

2.8.2 Time Derivative Terms In The Lagrangian

Let's first try to quantify “exposure” to loss (i.e. risk) or profit. The net worth or “equity”, E_i , of the investor i , is changing over time. The investors wish to increase their net worth, so they wish to have $\partial_t E_i > 0$. From the perspective of the response of the market, though, $\partial_t E_i$ is only relevant if it is “coupled” to the market. Agent i couples to the market through its assets $\sum_\mu A_{i\mu} p_\mu = (Ap)_i$. Therefore the term relevant for the market response is the scalar

$$\sum_{i,\mu} \partial_t E_i A_{i\mu} p_\mu = \partial_t E^T Ap.$$

But an important part of the equity of the investors is their “assets” in the market, $(Ap)_i$. Thus the investors also wish to make profit in the market, meaning positive $(\partial_t A) \cdot p$ or $A \cdot \partial_t p$. Similarly, the assets are only relevant if they are coupled to the equity, E_i because the assets of agent i are only relevant if the net worth E_i is significant. Thus the relevant terms for the response of the system are the scalars $E^T (\partial_t A) p$ and $E^T A \partial_t p$.

Depending on the situation, these three terms may not all be positive, or negative. The investors will optimize a linear combination of the three terms

$$L_1 \equiv \gamma_1 \partial_t E^T Ap + \gamma_2 E^T \partial_t Ap + \gamma_3 E^T A \partial_t p \quad (2.6)$$

In principle each investor may have a different strategy and the three parameters $\gamma_{1,2,3}$ could be different for each investor. We will, however, assume that for the market sector in consideration the response results from a so-called “herding effect” in which all parties react collectively to a change, meaning that the coupling constants are similar for all investors.

Since adding a term which is a complete time derivative like $-\gamma_2 \partial_t (E^T Ap)$ would not change the equations of motion, we can get rid of one term, say the second term, and just keep two terms. Since the units of our Lagrangian do not matter, we may absorb one of the

two constants, say γ_3 (if it's nonzero) as an overall coefficient of the Lagrangian. Thus we are only left with a single and only work with $\gamma \equiv -\gamma_1/\gamma_3$, where the minus sign is just for consistency with equations from the main text. In conclusion, the Lagrangian terms with a single time derivative look like:

$$L_1 \equiv \gamma \partial_t E^T A p - E^T A \partial_t p$$

2.8.3 The Effect of Response times

In a real system no reaction happens instantaneously and there is a “response time” associated with every reaction. This, for instance, could mean that the decision of investor i to react to a change at time t will appear as a change in her/his portfolio (i.e. connections $A_{i\mu}$) at a later time. This could heuristically be shown by replacing, say

$$E^T(t)A(t)\partial_t p(t) \rightarrow E^T(t)A(t+\tau)\partial_t p(t) \approx E^T(t)A(t)\partial_t p(t) + \tau E^T(t)\partial_t A(t)\partial_t p(t). \quad (2.7)$$

Thus the effect of these response times can be understood through higher order derivative terms. We will first discuss the general case below and derive the equations of motion for this system. After that we will first introduce a phenomenological model with equations similar to the ones below, but more suited for numerical simulations. In the end, we show how putting response times similar to (2.7) yields almost exactly the structure of the phenomenological equations.

2.8.3.1 Two Time Derivatives

We may have three terms again⁴:

$$L_2 \equiv a \partial_t E^T \partial_t A p + b \partial_t E^T A \partial_t p + c E^T \partial_t A \partial_t p \quad (2.8)$$

⁴we may of course have both derivatives on a single variable, but that is going to result in the same equations of motion as having them on different variables.

Now that we have already scaled the Lagrangian to absorb γ_3 we cannot absorb any of a, b or c in that manner. However, since we have one extra time derivative in L_2 , and we set $\gamma_3 \rightarrow 1$ in L_γ , a, b and c will have units of time. one of them can be absorbed by rescaling t , but for now we will keep all three.

This is it. We basically wrote down all possible terms we could have in a Lagrangian (subject to the constraints we chose for simplicity) and we ended up with only 5 Lagrangian terms. From these we get only 3 free coefficients and one time unit (one of a, b or c). One of these coefficients, γ , is dimensionless and should therefore be the main coupling of the theory and states of the system definitely have to be a function of γ . The other two coefficients are in L_2 and have dimensions of time. They will determine the time scales or the “time lags” in the model. As we can see, these very simple assumptions led to exactly the same number of time lags that we knew should be there intuitively. Our model was slightly simpler than this, but still very close to this. The only mismatch is that we get one coupling γ here, while in our model we had two, namely, α and β . But below we will argue that that is because in the model we assumed coupling to the “rest of the world” and that coupling provides the missing degree of freedom.

2.9 Equations Of Motion

Let’s derive the equations of motion from the action

$$S = \int dt L = \int dt (L_\gamma + L_2)$$

Again, we are assuming that the potential energy is constant and very flat in the region we are investigating. Variations with respect to p and E yield⁵

$$\delta_p S : \quad 0 = (-a + b + c) \partial_t E^T \partial_t A + b \partial_t^2 E^T A + c E^T \partial_t^2 A$$

⁵The variations and Euler-Lagrange equations are defined as:

$$\delta_{x(t)} S \equiv \partial_t \frac{\partial L}{\partial(\partial_t x(t))} - \frac{\partial L}{\partial x(t)}$$

where we assume not to have higher than first time derivative $\partial_t x$ in the action

$$-(\gamma + 1)\partial_t E^T A - E^T \partial_t A \quad (2.9)$$

$$\begin{aligned} \delta_E S : \quad 0 &= (a + b - c)\partial_t A \partial_t p + b A \partial_t^2 p + a \partial_t^2 A p \\ &+ (\gamma + 1)A \partial_t p + \gamma \partial_t A p \end{aligned} \quad (2.10)$$

$$\begin{aligned} \delta_A S : \quad 0 &= (a - b + c)\partial_t E \partial_t p^T + a \partial_t^2 E p^T + c E \partial_t^2 p^T \\ &+ \gamma \partial_t E p^T - E \partial_t p^T \end{aligned} \quad (2.11)$$

Where in the last equation, there is no dot product and the combination $E p^T$ is a matrix of the same form as A^T . These are the most general form of the equations.

2.10 A Phenomenological Model for Financial Markets

2.10.1 Assumptions, simplifications and the GIIPS system

The key assumptions that differentiate our model from other banking system or dynamic network models are:

1. The banks do not *exclusively* trade with each other. They may trade with an external entity, which may be the ECB or other, smaller investors.⁶
2. When there is no change in equity, price, or bond holdings, nothing happens and there is no intrinsic dynamic activity in our financial network.
3. The model describes the short time response of the system and disregards slow, long-term driving forces of the market.
4. We assume the agents in the system will copy each others actions, producing the so-called “herding effect.” This is why we assume the “coupling constants” (the free parameters) are the same for all agents.

⁶This is appropriate in the case of GIIPS sovereign debt because, in addition to the ECB (which buys some of the bonds if there is a need to stabilize the system), a large number of investors hold GIIPS sovereign debt. This is important to keep in mind because in most problems associated with banking or financial networks agents are assumed to be trading with each other.

2.11 Notations and Definitions

The equity E_i of a bank is defined as

$$E_i = \sum_{\mu} A_{i\mu} p_{\mu} + C_i - L_i.$$

Here p_{μ} is the “price ratio” of asset μ , which is the price of asset μ at time t divided by its price at $t = 0$. Hence $p_{\mu}(t = 0) = 1$. C_i is the bank’s cash, and L_i is bank’s liability. These parameters evolve in time. Bank i will fail if its equity goes to zero,

$$if : \quad E_i = 0 \quad \rightarrow \quad \text{Bank } i \text{ fails.}$$

We assume that the liabilities are independent of the part of the market we are considering and are constant. For convenience we define

$$c_i \equiv C_i - L_i.$$

Two other dependent variables that we use are the “bank asset value” $V_i \equiv \sum_{\mu} A_{i\mu} p_{\mu}$ and the total GIIPS sovereign bonds on the market $A_{\mu} \equiv \sum_i A_{i\mu}$.

2.11.1 The time evolution of GIIPS holdings and their price

For changes in equity we have

$$\delta E_i = \sum_{\mu} ((\delta A_{i\mu}) p_{\mu} + A_{i\mu} \delta p_{\mu}) + \delta c_i.$$

Here we assume that the cash minus liability changes according to the amount of money earned through the sale of GIIPS holdings,

$$\delta c_i = - \sum_{\mu} (\delta A_{i\mu}) p_{\mu} + \delta S_i(t),$$

Table 2.2: Notation

symbol	denotes
$A_{i\mu}(t)$	Holdings of bank i in asset μ at time t
$p_\mu(t)$	Normalized price of asset μ at time t ($p_\mu(0) = 1$)
$E_i(t)$	Equity of bank i at time t .
α	“Inverse market depth” factor of price to a sale.
β	Banks’ “Panic” factor.

where the minus sign indicates that a sale means $\delta A_{i\mu} < 0$ and this should add positive cash to the equity of bank i . $\delta S_i(t)$ is the cash made from transactions outside of the network of $A_{i\mu}$. The first term in δc_i cancels one term in δE_i and we get (all at time t)

$$\delta E_i = \sum_{\mu} A_{i\mu} \delta p_{\mu} + \delta S_i(t). \quad (2.12)$$

In the secondary market for the bonds (where issued bonds are traded in a manner similar to stocks) the prices are primarily determined by supply and demand. We use a simple model for the pricing that should hold as a first-order approximation. We assume the price changes to be

$$\delta p_{\mu}(t + \tau_A) = \alpha \frac{\delta A_{\mu}(t)}{A_{\mu}(t)} p_{\mu}(t), \quad (2.13)$$

Where coupling constant α is the market sensitivity, or in other words the “inverse of the market depth,” i.e. the fraction of sales ($\delta A/A$) required to reduce the price by one unit ($\delta p/p$) is equal to $1/\alpha$. We are assuming that the market is “liquid” meaning that any amount of assets can be sold or bought without a problem. We have defined $\delta p_{\mu}(t) \equiv p_{\mu}(t) - p_{\mu}(t - \delta t)$ is the change in price from the previous step, $\delta A_{\mu}(t) = A_{\mu}(t) - A_{\mu}(t - \delta t)$ the net trading (number of purchases minus sales) of asset μ , and τ_A the “response time of the market.” We choose the same “inverse market depth” for all GIIPS holdings μ , assuming that they belong to the same class of assets. We then define how the GIIPS holdings are sold or bought, i.e., we define $\delta A_{i\mu}$.

We assume that if a bank’s equity shrinks it will start selling GIIPS holdings in order to continue meeting its liability obligations, and that if a bank’s equity shrinks because of

asset value deterioration it will sell a fraction of its entire portfolio to ensure meeting those obligations. A bank thus determines what fraction of its equity has been lost in the previous step and sells according to

$$\delta A_{i\mu}(t + \tau_B) = \beta \frac{\delta E_i(t)}{E_i(t)} A_{i\mu}(t), \quad (2.14)$$

where τ_B is the “response time of the banks,” and β is the second coupling constant of our model, which we call the “panic factor.” The larger the panic factor, the larger will be the portion of GIIPS assets traded by the banks. Here we assume that banks purchase using the same protocol as when selling and sell the same fraction of all their GIIPS assets. The above equations can be converted to differential equations by simply replacing $\delta F \rightarrow dF/dt$. If we assume that the time lags are small, we can expand the equations with τ_A, τ_B to first-order and get

$$\frac{dF(t + \tau)}{dt} \approx \frac{d}{dt} \left(F(t) + \tau \frac{dF}{dt} \right)$$

For brevity, we define $\partial_t \equiv \frac{d}{dt}$. The three equations become:

$$(\tau_B \partial_t^2 + \partial_t) A_{i\mu}(t) = \beta \frac{\partial_t E_i(t)}{E_i(t)} A_{i\mu}(t) \quad (2.15)$$

$$(\tau_A \partial_t^2 + \partial_t) p_\mu(t) = \alpha \frac{\partial_t A_\mu(t)}{A_\mu(t)} p_\mu(t) \quad (2.16)$$

$$\partial_t E_i(t) = \sum_\mu A_{i\mu}(t) \partial_t p_\mu(t) + f_i(t). \quad (2.17)$$

where $f_i = dS_i/dt$ has the meaning of external force. where τ_B is the time-scale in which Banks respond to the change, and τ_A is the time-scale of market’s response.⁷ All essential variables of our model are summarized in Table 2.2.

⁷Without a time lag, these equations would be primarily constraint equations relating the first-order time derivatives of E, p, A to each other. Note however that in simulating this dynamic system the order in which we update the variables matters because most of the nontrivial dynamic behavior follows from this time lag between updates.

2.12 Comparison of the Lagrangian and the Phenomenological Model

Save for the equation (2.17) which is the result of an extra constraint on how the cash c_i changes in time, the first two equations are actually closely related to (2.10) and (2.9). This can be seen as follows. Consider the case in (2.10) and (2.9) where

$$a = c \equiv \tau, \quad b = 0$$

The first two equations become:

$$\delta_p S : \quad E^T (\tau \partial_t^2 A - \partial_t A) = (\gamma + 1) \partial_t E^T A \quad (2.18)$$

$$\delta_E S : \quad \left(\frac{\tau}{\gamma} \partial_t^2 A + \partial_t A \right) p = -\frac{\gamma + 1}{\gamma} A \partial_t p \quad (2.19)$$

To compare these equations with our original equations, let us approximate the second order terms $\partial_t^2 A$ on the right as Taylor expansions of first order terms:

$$\begin{aligned} E^T (\tau \partial_t^2 A - \partial_t A) &\approx -E^T \partial_t A (t - \tau) \\ \left(\frac{\tau}{\gamma} \partial_t^2 A + \partial_t A \right) p &\approx \partial_t A \left(t + \frac{\tau}{\gamma} \right) p \end{aligned} \quad (2.20)$$

Thus, it is approximately as if we have:

$$\delta_p S : \quad E^T(t) \partial_t A(t - \tau) = -(\gamma + 1) \partial_t E^T(t) A(t) \quad (2.21)$$

$$\delta_E S : \quad A(t) \partial_t p(t) = -\frac{\gamma}{\gamma + 1} \partial_t A \left(t + \frac{\tau}{\gamma} \right) p(t) \quad (2.22)$$

This does not have the exact same time lags as our original model, but it is very close to that. As we see, the coefficients $a = c = \tau$ did not modify the coupling coefficient once we wrote the equations in the time lagged format and the only coupling that matters is the dimensionless constant γ . As for more general choices of a, b and c , it is not hard to see based on the same analogy that they can be interpreted as different time lag structures in the equations and it may even be possible to generate time lags precisely like our original model.

The key point here is that, once we absorb the second order time derivatives as time-lags, no matter what the lags are, the terms on both sides will superficially have just a single time derivative, though with time lags. This and the structure of the equations (2.9) and (2.10) ensure that once all time lags have been absorbed, the coefficient of the equation is a function of γ only and it can only have the form that appears in equations (2.18) and (2.19).

2.12.1 The Last Equation

The equation $\partial_t E = A\partial_t p$ was not discussed above and in fact it is not related to the equations of motion or the Lagrangian discussed above. The origin of this equation come from the assumption that we made about “cash” and “liabilities” back in equation

$$\delta c_i = - \sum_{\mu} (\delta A_{i\mu}) p_{\mu}.$$

This assumption about how cash changes with trading, while assuming the liabilities stay fixed are “constraints” put on the system by hand. Therefore $\partial_t E = A\partial_t p$ is a constraint equation and should be treated as such in the Lagrangian formulation. To include it, we have to introduce a set of Lagrange multipliers (which in reality are representing a quantity that couples to the cash in the system, though we are not quite sure what the real world interpretation of this Lagrange multiplier is) C_i which have no explicit dynamics and add the following term to the Lagrangian

$$L_C \equiv C^T (\partial_t E - A\partial_t p)$$

The full Lagrangian is then $L_2 + L_{\gamma} + L_C$ and the equation of motion for C only imposes the constraints $\partial_t E = A\partial_t p$.

2.13 The constants α, β

If we now compare (2.18) and (2.19) with (A.25) and (A.26) we see that we should have

$$\alpha = \frac{-\gamma}{\gamma + 1}, \quad \beta = -(\gamma + 1) \quad (2.23)$$

and $\alpha\beta = \gamma$. However, as we see, this Lagrangian approach only allows for one free coupling, γ , instead of two. We will argue below how dissipation can give us the other degree of freedom we need. But before that, it would be instructive to know what the phase space of our discrete time model would have looked like, had we worked with the “non-dissipative” part of the dynamics only, meaning that we only had one coupling γ like our derivation here.

2.14 Effect Of Dissipation

The most natural thing to expect of the “rest of the world” is to generate a drift in the change of prices in a certain way. One simple way to implement this is to put a term proportional to $\partial_t p$ in equation (2.19). To make the indices work, we have to add a term like $\lambda A \partial_t p$, where λ is like a mean-field approximation of the effect of the rest of the world on this market. The sign of λ determines whether the drift is lowering or increasing the prices. One way to keep these equations consistent is to have:

$$\gamma \partial_t (Ap) + A \partial_t p - \lambda A \partial_t p = 0 \quad (2.24)$$

$$-\gamma \partial_t E^T A - \partial_t (E^T A) + \lambda \partial_t E^T A = 0 \quad (2.25)$$

$$\gamma p \partial_t E^T - \partial_t p E^T = 0 \quad (2.26)$$

Comparing to (2.18) and (2.19) this yields:

$$\alpha = \frac{\gamma}{\lambda - \gamma - 1}, \quad \beta = \lambda - \gamma - 1 \quad (2.27)$$

To quantify how much this deviates from the “closed market” case we rewrite (2.27) as:

$$\beta = \frac{-1}{\alpha + 1}(1 - \lambda) \quad (2.28)$$

It would be instructive to know what the phase space looks like in terms of the new set of parameters: γ , which is the relative importance of $\partial_t E^T A p$ and $E^T A \partial_t p$ in the dynamic behavior, and λ , which quantifies “dissipation drift” caused by the rest of the world.

The above analysis suggests that γ and λ are natural couplings that can be used to describe the system.

2.14.1 Derivation with Explicit Response Times in the Lagrangian

$$\begin{aligned} L &= -E^T(t)A(t)\partial_t p(t + \tau_2) + \gamma \partial_t E^T(t)A(t + \tau_1)\partial_t p(t) \\ &= \gamma (\tau_1 \partial_t E^T \partial_t A p + \partial_t E^T A p) \\ &\quad + \tau_2 (\partial_t E^T A \partial_t p + E^T \partial_t A \partial_t p) - E^T A \partial_t p \\ &\quad + (-cA\partial_t p - f + \partial_t E) \lambda_c + O(\tau_i^2) \end{aligned} \quad (2.29)$$

Where λ_c is a Lagrange multiplier that enforces the last equation (2.17).

Two of the equations of motion become

$$\delta_p S : \quad E^T(t)\partial_t A(t - \tau_2) = -(\gamma + 1)\partial_t E^T\left(t - \frac{\tau_2}{\gamma + 1}\right)A(t) + O(u^2) \quad (2.30)$$

$$\delta_E S : \quad A(t)\partial_t p\left(t + \frac{\tau_2}{\gamma + 1}\right) = -\frac{\gamma}{\gamma + 1}\partial_t A(t + \tau_1)p(t) + O(u^2) \quad (2.31)$$

Where $u \in \{\partial_t p, \partial_t A, \partial_t E\}$. These equations again have a somewhat different response time appearance than the phenomenological model, but have otherwise a structure very similar to (2.15) and (2.16). And if we add dissipative term as we discussed before we can have independent couplings α and β .

Now we turn to applying the phenomenological version of the model to the Eurozone crisis. After that we will explore the phase space of that model.

2.15 Numerical Solutions

In our simulations we use these differential equations and choose $\tau_A = \tau_B = 1$. One of them can always be chosen as a time unit and set to one, but setting them equal is an assumption and may not be true in reality. Our analysis showed that the choice of $\tau_{A,B}$ does not affect the stability of the system and that the stability only depends on α , β and the shock. The $f_i(t)$, which are changes in the equity from what banks own outside of this network, can be thought of as external noise or driving force. We use $f_i(t)$ to shock the banks and make them go bankrupt. We shock a single bank, say bank i , at a time by setting $f_i(t) = sE_i\delta(t)$, which instantaneously reduces the equity of bank i by a fraction s , and $f_j = 0$ for all other $j \neq i$.⁸ Plugging $f_i(t)$ into Eq. (2.15) and integrating yields

$$\partial_t A_{i\mu}(0) = \beta A_{i\mu}(0) \ln(1 + s). \quad (2.32)$$

And we set $\partial_t A_{j\mu}(0) = 0$ for $j \neq i$. This and $E_i(0) \rightarrow (1 + s)E_i(0)$ are the initial conditions resulting from $f_i(t)$ which we start with. In addition, we require $E, A, p \geq 0$ during the simulations. In our simulations we select $s = -0.1$. We also find that⁹ the exact value of s does not affect the final state of the system.

2.16 Application to European Sovereign Debt Crisis

We apply our model to the GIIPS data mentioned above. Before looking at the simulations of Eqs. (2.15)–(2.17), we estimate the values of our parameters in the case of the GIIPS sovereign debt crisis.

2.16.1 Estimating values of $\gamma = \alpha\beta$

We use approximate versions of Eqs. (2.15)–(2.17) to estimate the product of parameters α and β . The distribution of the assets is roughly log-normal, so a small number of banks hold a significant portion of each GIIPS country's debt. Thus using only the equity of the

⁸Here $\delta(t)$ is the Dirac delta or impulse function.

⁹except near the stability limit, where a strong shock can push the system into the unstable regime,

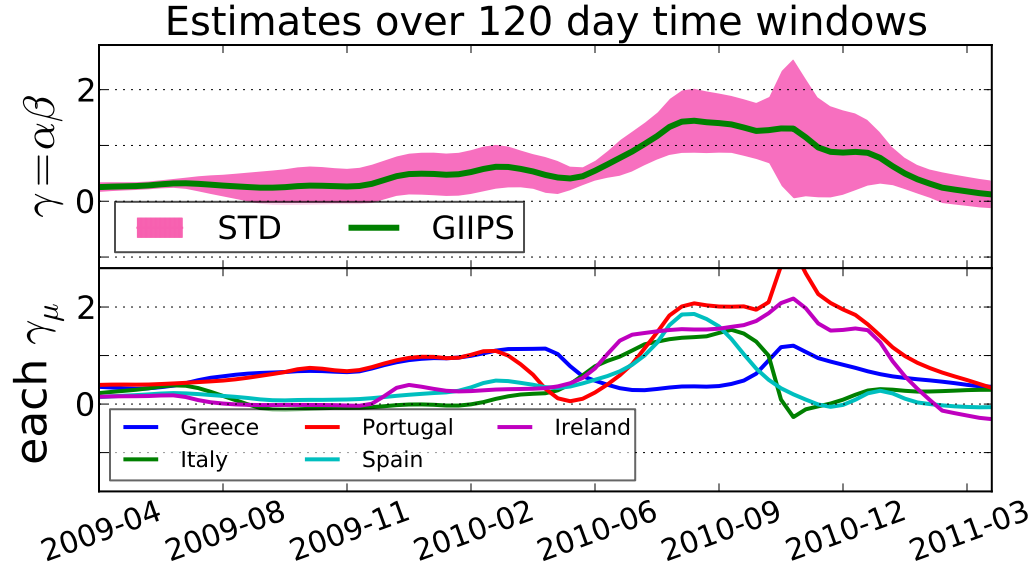


Figure 2.3: Estimates of $\gamma = \alpha\beta$ over 4 months periods. Top: the shaded purple region is the error-bars based on the standard deviations and the solid lines are the averages of different γ calculated for each country. Bottom: Calculation of γ_μ for individual countries. The fact that the values for different countries are close to each other is a sign that our assumption of “herding” (i.e. same α and β for all GIIPS) is justified and that our model is applicable here. As can be seen, before the height of the crisis $0 < |\gamma| < 1$ and then it gradually grows. At the height of the crisis $1 < \gamma < 2$. After the crisis we see γ decrease again to $\gamma < 1$. Later we show that at $\gamma < 1$ the system rolls into a new equilibrium, but when $\gamma > 1$ the asset prices crash. Also note the time-line of bailouts: Greek bailout approved 2010/04 and 2010/09; Irish bailout 2010/10. This explains part of the movements in the lower plot. The following stock tickers were used for each country (only the top 4 holders of each GIIPS for which stock prices could be obtained from Yahoo Finance): Greece: NBG, EUROB.AT, TPEIR.AT, ATE.AT; Italy: ISP.MI, UCG.MI, BMPS.MI, BNP.PA; Portugal: BCP.LS, BPI.LS, SAN; Spain: BBVA, SAN; Ireland: BIR.F, AIB.MU, BEN

dominant holders for each country μ will give us a good estimate of γ . Let us denote the set of dominant holders by “Dom”. In our estimates we use the top 2, 3 or 4 holders for each country¹⁰. We estimate that the response times τ_A, τ_B are at most on the order of several days. Thus we will calculate $\gamma = \alpha\beta$ over a period of four months to allow the system to reach its new final state. Thus Eq. (2.14) allows us to write

$$\frac{\delta A_\mu}{A_\mu} \approx \beta \sum_{i \in \text{Dom}} \frac{\delta E_i}{E_i} \frac{A_{i\mu}}{A_\mu}$$

Where the $A_{i\mu}/A_\mu$ factor makes sure that we have a weighted average of log returns $\delta E_i/E_i$ based on how large their holdings are¹¹. Using this approximation we can relate the first two equations¹²,

$$\frac{\delta p_\mu}{p_\mu} \approx \alpha \frac{\delta A_\mu}{A_\mu} \approx \alpha\beta \sum_{i \in \text{Dom}} \frac{\delta E_i}{E_i} \frac{A_{i\mu}}{A_\mu}.$$

Thus we can approximate γ as

$$\gamma \approx \frac{\delta p_\mu / p_\mu}{\sum_{i \in \text{Dom}} \frac{A_{i\mu}}{A_\mu} \delta E_i / E_i}. \quad (2.33)$$

We evaluate γ for each country μ . If the values are similar for different μ values it may indicate that the “herding effect” is a factor. This both supports our model and suggests that it is applicable to this problem. We evaluate γ for the time period between early 2009, when the crisis was just beginning, and early 2011, when most government bailouts had either been paid or scheduled.

We use the “adjusted close” value for the stock prices, which accounts for changes in the number of outstanding shares to a degree. Thus the movements in stock prices may be

¹⁰These handful of holders hold 45% of Greek, 41% of Italian, 48% of Irish, 29% of Portuguese and 31% of Spanish debt in our data.

¹¹Also, for $A_\mu = \sum_{i \in \text{Dom}} A_{i\mu}$ we will only use the dominant holders “Dom.”

¹²The equity of the banks is mostly comprised of the shareholders’ equity, or common stocks. These banks usually have multiple stock tickers, but there is generally one or two main stock tickers where most of the equity is. We can use the movements in these main stocks to estimate $\delta E_i/E_i$. For this approximation we use the following formula:

$$\frac{\delta E_i}{E_i} = \frac{E_i(t_f) - E_i(t_i)}{(E_i(t_f) + E_i(t_i))/2}$$

where $E_i(t_i)$ is the stock price at the beginning of the period and $E_i(t_f)$ is at the end of it.

used as a proxy for the changes in the equity of banks. Many of the major movements (or slope changes) in each country's γ values seem to coincide with bailout payment dates (See Fig. 2.3 caption).

Figure 2.3 shows the average γ values during this period with standard deviation error-bars. The bottom of the figure shows the individual values of γ obtained using each country.

Figure 2.3 shows that before the crisis $0 < |\gamma| < 1$, but at the height of the crisis $\gamma > 1$. More detailed analysis of our model reveals that $\gamma > 1$ is an unstable phase in which a negative shock to the equity of any bank will cause most asset prices to fall dramatically to nearly zero. Similarly, a positive shock will cause the formation of bubbles. When $0 < \gamma < 1$, on the other hand, after a shock the system smoothly transitions into a new equilibrium and, although some banks may fail, no asset prices will fall to zero.

2.17 Simulations

We find that when values of α and β are small, e.g., $|\alpha\beta| < 1$, shocking any of the banks in the network will result in the same final state (see Fig. 2.8), i.e. the final state does not depend on which bank is shocked. It only depends on α and β . This state is a new stable equilibrium. If we shock the system a second time the prices do not change significantly, i.e., less than 0.1%). Figure 2.4 shows a sample of the time evolution of the asset prices and the equity of the banks that incurred the largest losses.

Figure 2.4 shows results that seem in line with what actually happened during the European debt crisis, although the damage shown for Ireland is less than what actually occurred. In this figure, bailouts are disregarded. Three of the four most vulnerable banks (MVB) shown in Figs. 2.4 and 2.5 are holders of Greek debt. In this simulation, Greek debt is the asset that loses the most value. Note that the loss prediction produced by the model is based solely on the network of banks holding GIIPS sovereign debt and provides information about the economies of these countries, with Greece experiencing the largest loss, followed by Portugal (real-world data indicates that Ireland's loss was as severe as Portugal's).

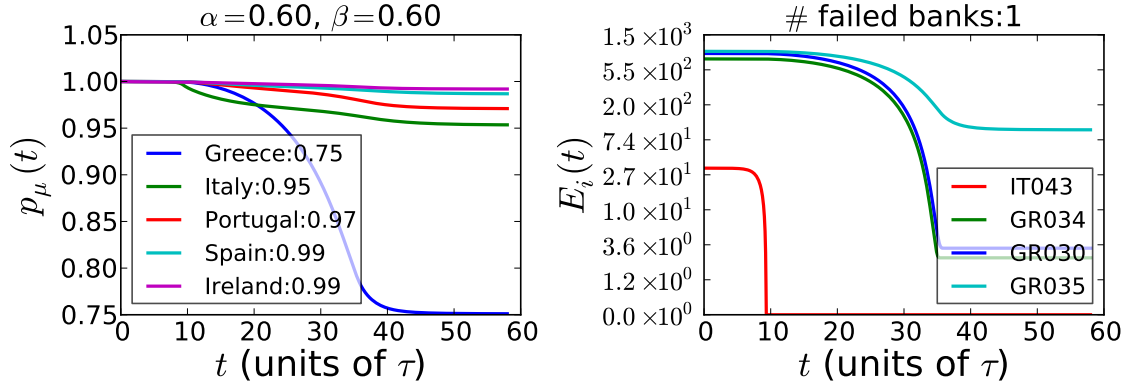


Figure 2.4: Shocking “Bank of America” with $\alpha = \beta = 0.6$. Left: plot of Asset prices over time. Greece incurs the greatest losses, falling to 75% of original value. Final prices are listed in the legend. Right: Equities of the 4 “most vulnerable banks” (2 of major Greek holders incur large losses and one Italian bank is predicted to fail due to the shock). IT043 is Banco Popolare, which has very small equity but large Italian debt holdings. The next two are Agricultural Bank of Greece and EFG Eurobank Ergasias, which are among top 4 Greek holders.

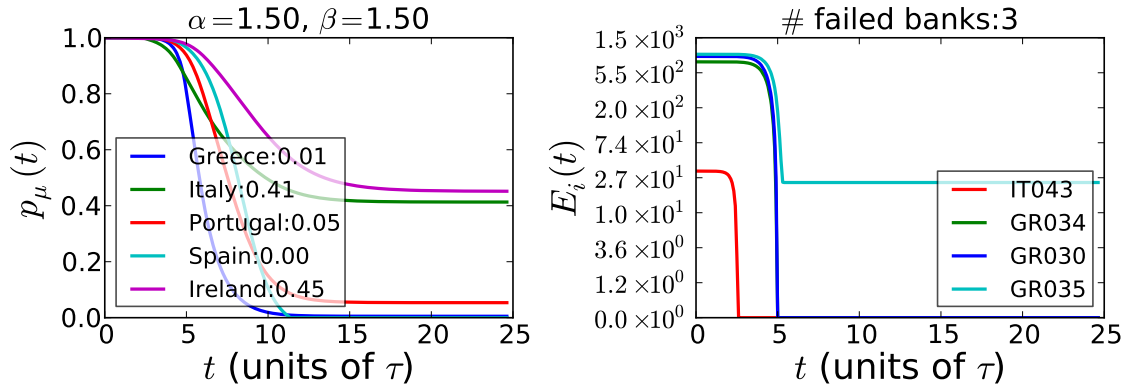


Figure 2.5: Simulation for larger values of α and β (values in legends are final price ratios $p_\mu(t_f)$). This time, in addition to Greek debt, Spanish and Portuguese debt show the next highest level of deterioration. The same four banks are the most vulnerable and this time two more of them fail. At $\alpha = \beta = 1.5$ the damages are much more severe than at $\alpha = \beta = 0.6$.

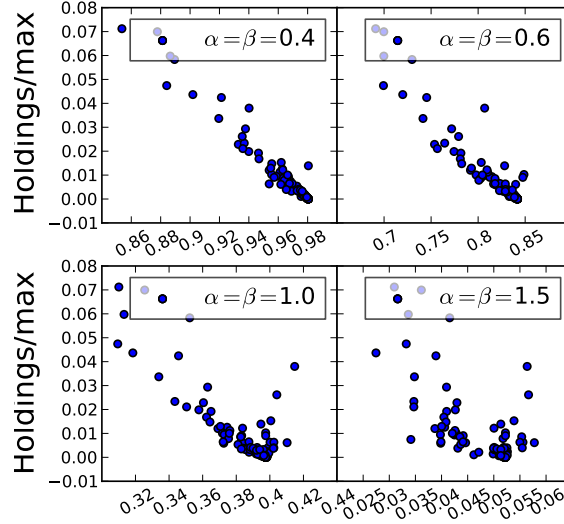
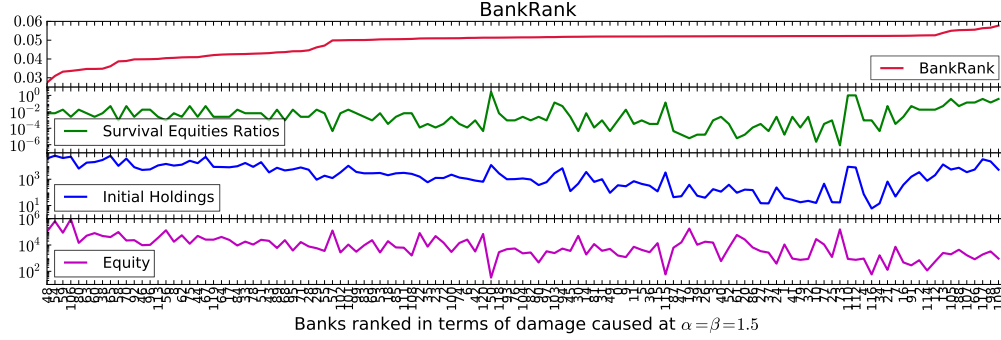


Figure 2.6: Left: Top: BankRank (2.34): Ranking the banks in terms of the effect of their failure on the system. Top plot shows the ratio of final total GIIPS holdings in the system to the initial total GIIPS holdings. The BankRank tells us how much monetary damage the failing of one bank would cause. second plot on the left shows the Survival equity ratio E^*/\tilde{E} , third is the initial holdings and last is the initial equity, all sorted in terms of BankRank at $\alpha = \beta = 1.5$. As we see, none of these three variables correlates highly with BankRank. The ranking changes for different values of α and β . Right: Scatter plot of the holdings divided by maximum holding (Holdings/max) versus BankRank at four different values of $\alpha = \beta = [0.4, 0.6, 1, 1.5]$. As we see increasing $\alpha\beta$ decreases the correlation between BankRank and initial holdings. BankRank at $\gamma = \alpha\beta < 1$ is correlated well with the holdings and is anti-correlated with it. But BankRank at $\gamma = \alpha\beta > 1$ deviates significantly from the holdings. This means that in the unstable regime $\gamma > 1$ it is no longer true that only the largest holders have the highest systemic importance.

Note that the new equilibrium depends on α and β . From the real world data in Fig. 2.3 we see that before the onset of the crisis $\alpha\beta < 1$ and thus the response of the system to a shock is to move to a new equilibrium not far from the initial conditions (similar to Fig. 2.4). At the height of the crisis, however, when $\gamma = \alpha\beta \approx 2$, even a small shock can have a devastating effect and precipitate a crisis (as in Fig. 2.5). Although many banks incur significant losses when α and β values are at their highest, the same four banks fail.

In the SI we show the effects of rewiring the banks who lend to each country, meaning we take $A_{i\mu}$ and take random permutations of index i so that the equities of banks connected to each country changes randomly. Interestingly, such a rewiring changes the damages suffered by GIIPS bonds entirely, meaning that Greece will no longer be the most vulnerable. This shows that in our model, while the quantitative behavior of the system only depends on α and β , the final prices and equities depend strongly on the network structure.

2.18 Testing the Role of the Network

Our goal is to determine how much of the above behavior is caused by the network structure and how much by the value of the outstanding debts. To examine the dependence of the results on network structure, i.e., to determine which banks hold which country's debt and how much bank equities matter, we randomize the network and redo our analysis. We do not change the value of the total GIIPS sovereign debt held by the banks. We only rewire the links in the network, changing the amount of debt held by each bank and the countries to which each bank lends money.

Figure 2.7 shows an example of this randomization and how dramatically it changes the end result, and it demonstrates two important features of the model: (i) system dynamics are strongly affected by network structure, i.e., knowing such global variables as the equity and exposure of individual banks is not sufficient, and (ii) real-world data seems to indicate that it was the structure of the network of lenders to Greece that caused Greek sovereign bonds to become the most vulnerable. This suggests that our model may be useful as a stress testing tool for banking networks, or any network of investors with shared portfolios.

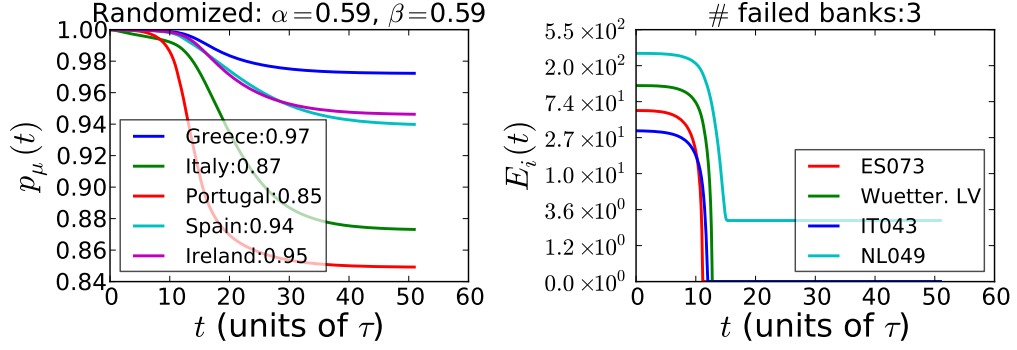


Figure 2.7: Randomizing which bank lends to which country, while keeping total debt constant for each country. The results differ dramatically from the real world data used in Fig. 2.4. In this example Portugal and Italy lose the most value, while Greece is the least vulnerable. Other random realizations yield different results.

2.19 Shocking different banks

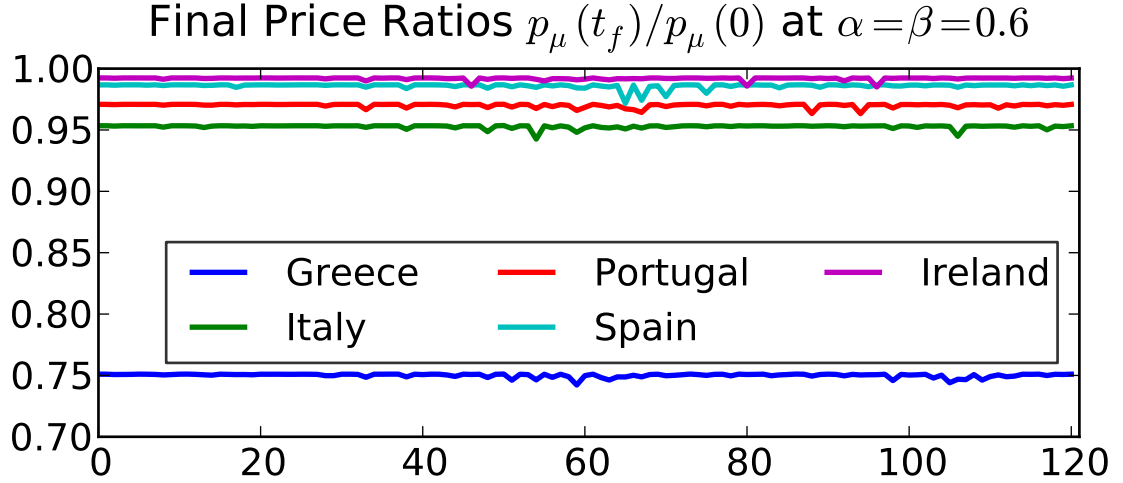


Figure 2.8: Shocking different banks at $\alpha = \beta = 0.6$. The final prices turn out very similar.

Fig. 2.8 shows the final prices found from shocking different banks. They are all almost identical. However, the small variation and the variations in the $A_{i\mu}(t_f)$ can be used to construct BankRank and find that different banks have different amounts of influence.

2.20 Systemic Risk and BankRank

We find that a bank can cause a large amount of systemic damage when its equity level is at the bare minimum necessary to survive a shock. Banks with very low equity fail rapidly, no longer trade, and thus no longer transmit damage to the system. Failing banks with enough equity to survive for a significant period of time, on the other hand, continue to transmit damage into the system and thus cause more damage than extremely weak banks. Based on this observation we rank the banks using a “survival equity ratio”, i.e., the fraction of actual equity a bank needs in order to survive once a shock enters the system through other banks. The total damage done to the system varies significantly from bank to bank. To rank the systemic importance of each bank we measure the effect their failure has on the system. Since normally no banks other than the four mentioned above fail, we modify the data slightly. The steps we take are as follows:

1. We increase the equity of the four failing banks to $\tilde{E}_i(0) = \sum_{\mu} A_{i\mu}(0)p_{\mu}(0)$ to keep them from failing and significantly damaging the system, and $\tilde{E}_i = E_i$ for non-failing banks. Doing so makes the system resilient to shocks when $\gamma = \alpha\beta < 1$, and the drop in prices falls below 1% (the system has reached a stable phase). But in the unstable regime where $\gamma > 1$ the system does still incur significant losses.
2. To assess the systemic importance of bank i , we run separate simulations with initial conditions changed to $\tilde{E}_i(0)$ until we find the value of E_i^* such that for $\tilde{E}_i > E_i^*$ the bank doesn't fail, and for $\tilde{E}_i < E_i^*$ it fails. We call this E_i^*/E_i the “survival equity ratio”. Note that for any i the shock is done to the same bank j ($i \neq j$), selected from the largest banks in the system. Also, note that the behavior of the system practically doesn't depend on j .
3. We calculate the total GIIPS holdings $\sum_k (A \cdot p)_k$ left in the system.

We define “BankRank” of bank i to be the ratio of the final holdings to initial holdings when $\tilde{E}_i = E_i^*$. BankRank of i is equal to the amount of monetary damage the system

would take if bank i fails:

$$\text{BankRank of } i : R^i = \frac{\sum_j (A \cdot p)_j(t_f)}{\sum_j (A \cdot p)_j(0)} \bigg|_{\tilde{E}_i = E_i^*}. \quad (2.34)$$

The smaller the value of R_i , the greater the systemic importance of bank i .

Fig. 2.6 on the left shows the BankRank in the unstable regime at $\alpha = \beta = 1.5$ and how it compares to the initial holdings, minimum ratio of equity required for survival E_i^*/E_i , and initial equities. We observe some correlation between BankRank and each of these variables. The best correlations are between BankRank and initial holdings. On the right of Fig. 2.6 we show the correlations of the initial holdings with BankRank. In the stable regime where $\alpha\beta < 1$ the holdings correlate well with BankRank, while in the unstable regime $\alpha\beta > 1$ the correlation becomes much weaker. Thus while in the stable regime holding almost completely determine the systemic importance of a bank, in the unstable regime this is no longer the case and many small holders will have high systemic importance.

One can also rank the banks in terms of their stability from their “survival equity ratio,” E_i^*/E_i . This ratio can serve as a stress-test for individual banks. The smaller the ratio, the more stable is the bank.

2.21 Phase Diagram and Phase Transition

Now we do a systematic numerical analysis of different phases of this phenomenological model. We identify to phases and what appears to be a second order phase transition between them. We then modify the equations (2.15)–(2.17) and analytically derive the condition for the phase transition.

2.22 Other Values of α and β and the Phases

The examples we plotted above were all from the $\alpha, \beta > 0$ quadrant. This is what one normally expects from this system: $\beta > 0$ means if a bank incurs a loss, they try to make up for it by making money from selling GIIPS holdings; $\alpha > 0$ means if there is selling

pressure (more supply than demand) the prices will go down. There are, however, cases where the opposite happens. “Contrarian” agents in a market are those who, for example, buy more GIIPS holdings when they incur losses, hoping to recover some of their losses by reducing the average cost of investment. The market may also sometimes behave in a contrarian fashion, when there is an anticipation of good news that overcomes the selling pressure, or when other investors outside our network (such as smaller investors or the ECB) are actually exerting a buying pressure. Plots of those cases can be found in the SI in Fig. 2.9, where in general the numerical solutions in the contrarian regime lead to the following conclusions:

1. In the third quadrant $\alpha < 0, \beta < 0$, where both investors and market are contrarian, losses are devastating. Many more banks fail for a small negative value for both α and β and the asset prices quickly plummet down to zero.
2. The second and fourth quadrant where $\gamma = \alpha\beta < 0$ are almost identical. No banks fail in these regimes, but also the amount of money lost or generated during the trading is negligible. This makes these regimes (either the investors or the market is contrarian, but not both) good for preventing failures, but they are very undesirable for profit making.

2.23 The phase Space

Fig. 2.10 shows an example of the average final prices and relaxation time for the system for various values of α and β . It seems the system has two prominent phases: One in which a new equilibrium is reached without a significant depreciation in all of the GIIPS holdings (upper left and lower right quadrants), and one where all GIIPS holdings become worthless (above dashed line in the upper right quadrant and all of lower left quadrant). In the third quadrant the transition is much more abrupt than in the first quadrant. In both quadrants in the transition region the relaxation time becomes very large, which means that the forces driving the dynamics become very weak. Both the smoothness and the relaxation time

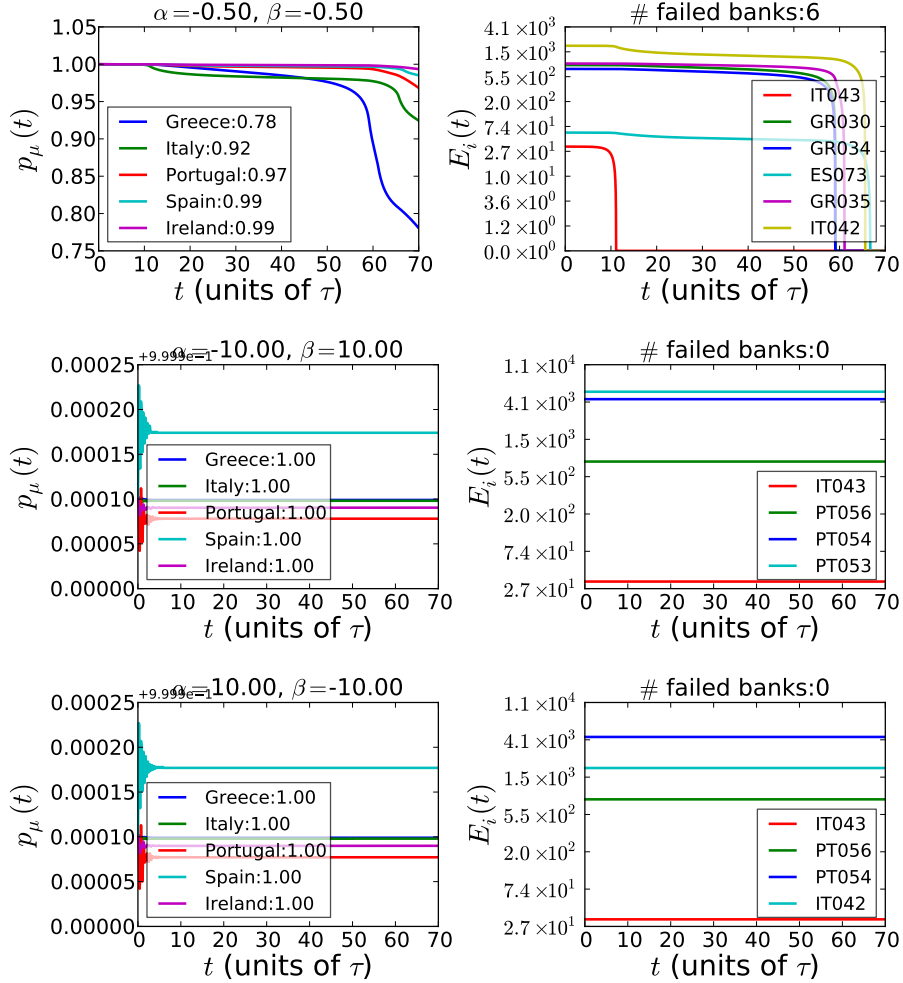


Figure 2.9: Contrarian regimes: top, both $\alpha, \beta < 0$. Here many banks fail, even for relatively small α, β . The losses are devastating. Our model suggests that such a regime should be avoided. The bottom two plots show the two points $\alpha = \pm\beta, \beta = \pm 10$. The two results are almost identical. They also show that no appreciable amount of profit or loss is generated in these regimes, thus making them rather unfavorable for investors most of the time, but because of their safeness could be a contingency plan (buyout of bad assets by central banks is one such contrarian behavior).

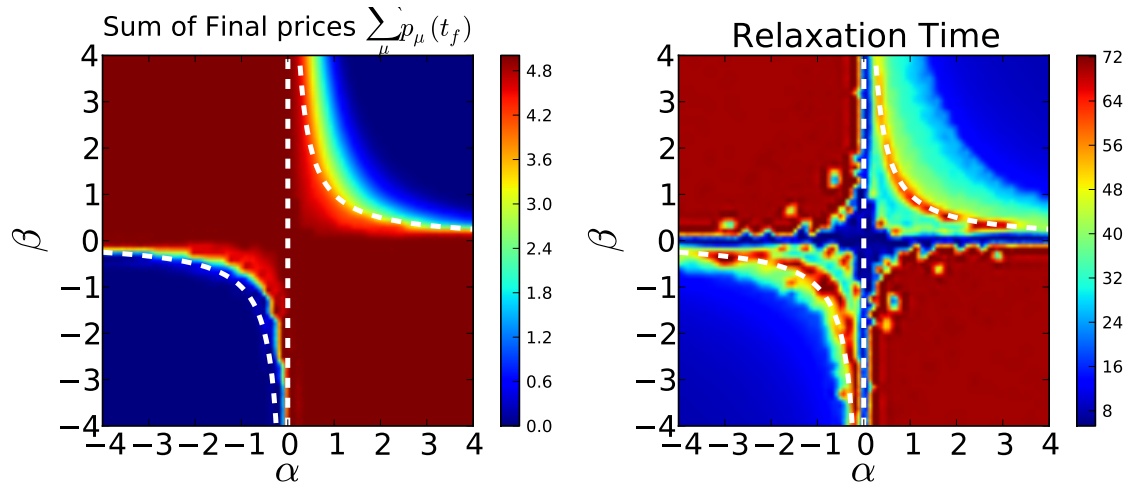


Figure 2.10: Left: Phase diagram of the GIIPS sovereign debt data, using the sum of the final price ratios as the order parameter. We can see a clear change in the phase diagram from the red phase, where the average final price is high to the blue phase, where it drops to zero. The drop to the blue phase is more sudden in the $\alpha < 0, \beta < 0$ quadrant than the first quadrant. Right: The time it takes for the system to reach the new equilibrium phase. This relaxation time significantly increases around the transition region, which supports the idea that a phase transition (apparently second order) could be happening in the first and third quadrants. The dashed white line shows the curve $\gamma = \alpha\beta = 1$. It fits the red banks of long relaxation time very well. This may suggest that $\gamma = 1$ is a critical value which separates two phases of the system.

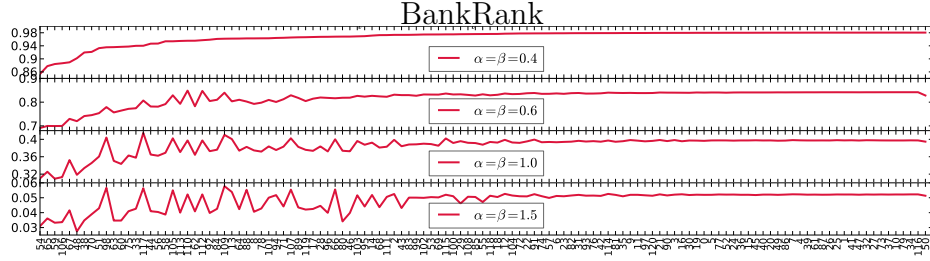


Figure 2.11: BankRank for different values of α and β . After the phase transition to the unstable region (e.g. $\alpha = \beta = 1.5$) the rankings change significantly.

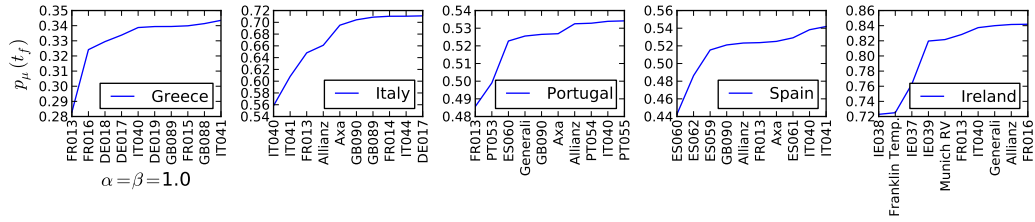


Figure 2.12: Top 10 banks whose failure causes the most damage to the price of each country's sovereign bond.

growth seem to be signalling the existence of a second order phase transition. The phase transition in the first quadrant seems to be described well by:

$$\gamma = \alpha\beta = 1.$$

But this result is not exact and below we derive a more precise form for this equation, which is:

$$\gamma = 1 + f_0, \quad (2.35)$$

where f_0 is the magnitude of the initial shock $f_i(t) = f_0\delta(t)$ for a fixed i that's being shocked. Analytical derivations of this are the subject of another paper which we are working on.

2.24 Robustness of the Ranking

Fig. 2.11 compares the BankRank for three different values of positive α and β . Some banks' BankRanks change slightly, but the overall results are similar.

Fig. 2.11 shows how the ranking changes as α and β increase. At small $\alpha\beta$ the ranking

has high degree of correlation with holdings, basically meaning that the larger the money a bank holds, the more important it is. For large $\alpha\beta$, however, this ranking changes significantly and some smaller players become much more important than before. Fig.2.12 shows the top 10 banks whose failure at $\alpha = \beta = 1$ causes the largest damage to each of the 5 GIIPS assets.

2.25 BankRank and stability

From examining the simulations more closely and from numerical analysis of the differential equations (2.16),(2.15) and (2.17) in networks of few nodes, presented below, we see that as expected the equations have either stable or unstable solutions. Stable ones are those where the initial shock is dampened quickly and the system goes to a new equilibrium, without any of the variables E, A, p either collapsing exponentially to zero or blowing up exponentially. Such behaviors in response to sudden rise or sudden fall in E in a 1 bank vs 1 asset system is shown in figure 2.13. A phase diagram using $\partial_t E$ of the 1 by 1 system is shown in figure 2.14.

2.26 Analytical results from the 1 Bank vs 1 Asset system

Here we present the analytical solution to the 1 by 1 model and derive the curve where the phase transition is happening in figure 2.14. At any time t the equations for a 1 by 1 system become

$$\begin{aligned}\frac{(\partial_t + \tau_B \partial_t^2)A}{A} &= \beta \frac{\partial_t E}{E} = \beta \frac{A \partial_t p}{E} \\ \frac{(\partial_t + \tau_A \partial_t^2)p}{p} &= \alpha \frac{\partial_t A}{A}\end{aligned}\tag{2.36}$$

Below we will try to find the condition for a phase transition in the solutions to these equations.

We can try to eliminate A and E . We first need to find the expression for $\partial_t^2 A/A$ first.

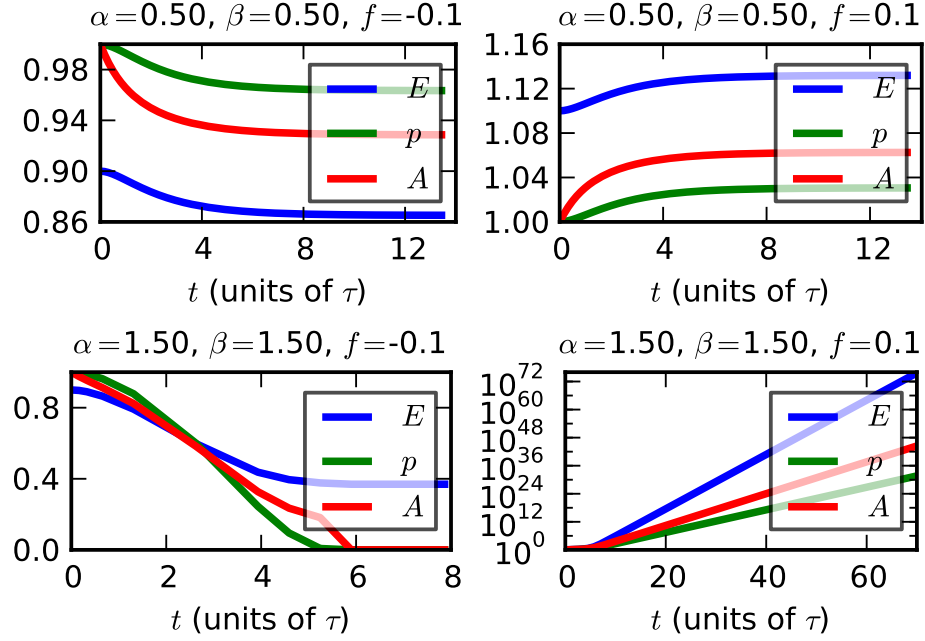


Figure 2.13: Numerical solutions to the differential equations in a 1 bank vs 1 asset system. The upper plots show a “stable” regime, where after the shock none of the variables decays to zero or blows up, but rather asymptotes to a new set of values. The lower plots are in the “unstable” regime where positive or negative shocks either result in collapse or blowing up or collapsing of some variables.

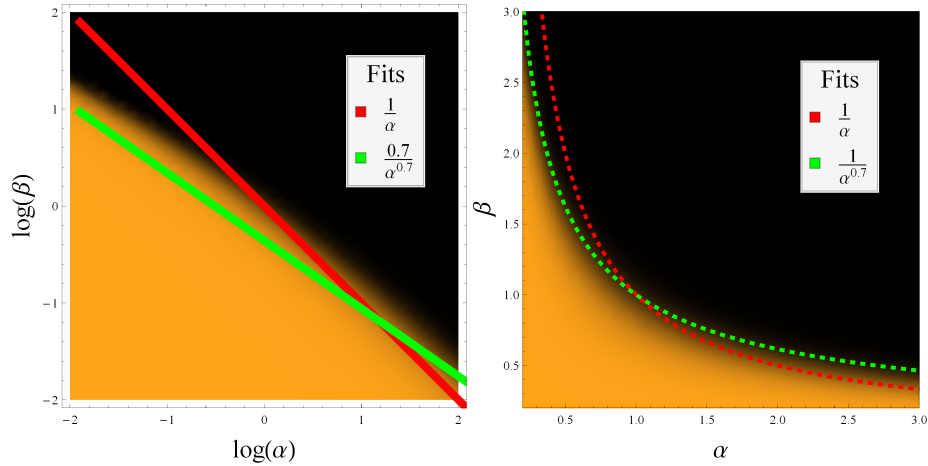


Figure 2.14: Phase diagram of the 1 bank vs 1 asset system, responding to sudden rise in E . Black denotes regions where $\partial_t E = A \partial_t p$ was very large at late times, and light orange where it was close to zero. This is only plotting the $\alpha, \beta > 0$ quadrant (left is a log-log plot, right is the regular linear scale diagram). The overlay are two fit functions for the phase transition curve. While $\alpha\beta = 1$ is not a very good fit for large β and small α , it fits fairly well for large α 's and we analytically prove this below.

Taking another derivative from the second equation yields

$$\frac{(\partial_t^2 + \tau_A \partial_t^3)p}{p} - \frac{(\partial_t + \tau_A \partial_t^2)p \partial_t p}{p^2} = \alpha \frac{\partial_t^2 A}{A} - \alpha \left(\frac{\partial_t A}{A} \right)^2 \quad (2.37)$$

combining this with the first equation results in:

$$\begin{aligned} \frac{(\partial_t + \tau_A \partial_t^2)p}{p} + \tau_B \frac{(\partial_t^2 + \tau_A \partial_t^3)p}{p} &= \gamma \frac{A \partial_t p}{E} + O((\partial_t p)^2) \\ \left[\tau_A \tau_B \partial_t^2 + (\tau_A + \tau_B) \partial_t + \left(1 - \gamma \frac{Ap}{E} \right) \right] \partial_t p &= O((\partial_t p)^2), \end{aligned} \quad (2.38)$$

where the nonlinear term is again quadratic in p (thus a generalized form of the Fisher equation) and looks like

$$\begin{aligned} O((\partial_t p)^2) &= \tau_B \frac{(1 + \tau_A \partial_t) \partial_t p \partial_t p}{p} \\ &\quad - \alpha \tau_B \frac{((1 + \tau_A \partial_t) \partial_t p)^2}{p} \end{aligned} \quad (2.39)$$

Below we will also show that in the stable regime the non-linearity in the frequency, namely the $\gamma Ap/E$ term, is of the order $O(\partial_t A \partial_t p)$ and thus remains small if we show that at small times the behavior of $\partial_t p$ in the stable regime is oscillating around zero.

This time the dynamics is richer and we have a damped oscillator with a driving force coupled to p and nonlinearities of type $\sim (\partial_t p)^2$. Taking the return $u \equiv \partial_t p$ as the fundamental variable, the nonlinearities are roughly of type $u^2 + a \partial_t u^2$. In short, the equations are

$$\begin{aligned} [\tau \partial_t^2 + \partial_t + \omega^2] u &= O(u^2, \partial_t u^2) \\ \frac{1}{\tau} &= \frac{1}{\tau_B} + \frac{1}{\tau_A}, \quad \omega^2 = \frac{1 - \gamma \frac{Ap}{E}}{\tau_B + \tau_A}, \\ p(t) &= \int^t u(t') dt' \end{aligned} \quad (2.40)$$

Although ω^2 depends on A, p and E , we can use an approximate time dependent exponential

ansatz $u \sim u_0 \exp[\lambda t]$. The solutions to λ are:

$$\lambda_{\pm} = \frac{-1 \pm \sqrt{1 - 4\tau\omega^2}}{2\tau}$$

When $\omega^2 > 0$ and $1 - 4\tau\omega^2 < 0$ there will be oscillatory solutions. For example when $\gamma \frac{Ap}{E} < -1$, which only happens for negative γ we have such oscillatory solutions. This is consistent with the simulations which showed the oscillatory behavior was in the $\alpha\beta < 0$ quadrants. For the stability, however we care about the real solutions.

When $\omega^2 < 0$, which happens when $\gamma \frac{Ap}{E} > 1$, we will have two real solutions with opposite signs. The presence of the positive root signals an instability because the solution diverges. For a delta function shock of magnitude f at $t = 0$ we found that:

$$E_0 \rightarrow E_0(1 + f)$$

Having initially scaled to $E_0 = A_0 = p_0 = 1$, the condition for existence of the positive root becomes:

$$t = 0 : \quad \gamma > \frac{E}{Ap} = (1 + f)$$

This dependence on the shock magnitude is normal, as a strong enough kick can kick a particle out of a local minimum. The shock can be arbitrarily small and therefore the absolute condition for stability is as we anticipated

$$\textbf{unstable at:} \quad \gamma > 1 \tag{2.41}$$

Now the question is, which solution does the system pick when it is shocked. The return $\partial_t p$ is

$$\partial_t p(t) = u(t) = u_+ e^{\lambda_+ t} + u_- e^{\lambda_- t}$$

Since at $t = 0$ the initial conditions dictated $\partial_t p(0) = 0$ we have

$$u_+ = -u_-$$

And therefore both solutions appear with equal strength. It follows that whenever one of the solutions (u_- in our case) is positive the solution diverges. When $f > 0$ a bubble forms and grows exponentially and when $f < 0$, because our variables are non-negative, the price just crashes to zero. This proves that the sufficient condition for stability is $\gamma < 1$. Also note that the nonlinear terms are all proportional to $\partial_t p$ and therefore at $t = 0$

$$O(u^2(0), \partial_t u^2(0)) = 0$$

and so the solution is exact at $t = 0$.

2.26.1 Validity of perturbation theory near the phase transition

For the above solution to be valid we must confirm that the corrections are small. We must find a small parameter that exists in the neglected terms which allows perturbative solutions to be viable. We had two sets of nonlinearities: (1) $O((\partial_t p)^2)$; (2) $\gamma A p/E$.

2.26.1.1 the non-linearity $O((\partial_t p)^2)$

First let us examine the nonlinear terms in $O((\partial_t p)^2)$. Note that the instability happens when the larger root λ_- becomes positive. Thus near the transition we have

$$\begin{aligned} 4\tau\omega^2 &\ll 1 \\ \lambda_+ &\approx -\frac{1}{\tau} + \omega^2 \\ \lambda_- &\approx -\omega^2 \end{aligned} \tag{2.42}$$

And so being close to the phase transition means $\lambda_- \ll 1/\tau$. The consequence of this is that for $O((\partial_t p)^2)$ we get (using the $u_+ = -u_-$ found above)

$$\begin{aligned} \tau_A \partial_t u &= \tau_A u_+ \left(\lambda_+ e^{\lambda_+ t} - \lambda_- e^{\lambda_- t} \right) \\ &\approx \tau_A u_+ \left(\lambda_+ e^{\lambda_+ t} - \lambda_- e^{\lambda_- t} \right) \\ O(u^2) &= \tau_B \frac{u(1 + \tau_A \partial_t)u}{p} \end{aligned}$$

$$\begin{aligned}
& -\alpha\tau_B \frac{((1+\tau_A\partial_t)u)^2}{p} \\
& \approx \tau_B \frac{u(1+\tau_A u_+(\lambda_+-\lambda_-))u}{p} \\
& -\alpha\tau_B \frac{((1+\tau_A\partial_t)u)^2}{p}
\end{aligned} \tag{2.43}$$

2.26.1.2 The non-linearity $\gamma Ap/E$

We wish to examine if the assumption that in the stable regime $\partial_t A, \partial_t p, \partial_E$ remain small is a consistent assumption, thus making perturbative expansion valid. Any term above non-linear in $\partial_t A, \partial_t p, \partial_E$ is thus higher order in this approximation. We wish to find the part of $\gamma Ap/E \partial_t p$ that is linear in the first time derivative. In the stable regime changes are slow and thus a short time after the shock we can expand the variables in Taylor series near $t = 0$. Again, we will rescale the variables at $t = 0$ to $E_0 = p_0 = A_0 = 1$. Using the (2.17) $\partial_t E = A \partial_t p$ we get

$$\begin{aligned}
\frac{A(t)p(t)}{E(t)} \partial_t p &= \frac{A_0 p_0 + t(\partial_t A_0 p_0 + A_0 \partial_t p_0)}{E_0 + t A_0 \partial_t p_0} \partial_t p \\
&\approx \frac{1}{E_0} (A_0 p_0 + t(\partial_t A_0 p_0)) \partial_t p \\
&= \partial_t p + O(\partial_t A_0 \partial_t p) \approx \partial_t p
\end{aligned} \tag{2.44}$$

Thus the assumption of smallness of the derivatives is consistent and we may use perturbation theory and safely discard the non-linear terms in finding the stability conditions. This way the stability condition is just having a positive ω^2 in (2.41). One can also check the stability by explicitly using the exponential ansatz found above as is given in what follows.

2.27 Proof for $\gamma = 1$ using properties of the phase transition

Since we have coupled second order equations, the solutions may be estimated using an exponential ansatz as follows. Equations (2.15) and (2.16) are second order and therefore

will naturally have two solutions for A and p . Also, since $\partial_t E = A\partial_t p$, E will also have two modes. Therefore the exponential ansatz must have at least two exponents. Thus for each of the three variables $X = E, p, A$ we have:

$$E \sim X_0 + X_1 \exp[w_{X1}t] + X_2 \exp[w_{X2}t]$$

In principle the exponents can be time-dependent, but we will first try and see if there are asymptotically exponential solutions. Thus we assume that they vary slowly with time. By choosing the units of E, p, A to be such that at $t = 0 + \epsilon$, $p = A = 1$ and the shocked equity is $E = 1 + f$, the boundary conditions that we had become:

$$A_0 = 1 - A_1 - A_2, \quad p_0 = 1 - p_1 - p_2, \quad E_0 = 1 + f - E_1 - E_2$$

and:

$$\begin{aligned} \partial_t E(0) &= 0 = w_{E1}E_1 + w_{E2}E_2 = 0 \\ &= A\partial_t p = w_{p1}p_1 + w_{p2}p_2 \\ \partial_t A(0) &= \frac{\beta}{\tau_B} \ln(1 + f) = w_{A1}A_1 + w_{A2}A_2 \end{aligned} \tag{2.45}$$

At the phase transition we expect the greater exponents, which we take to be w_{X2} , to become small relative to other time-scales in the problem, i.e. τ_A, τ_B , and change sign from negative (which would result in exponential decay) to positive (which results in divergence of E, p, A). This means that close to the phase transition:

$$|w_{X2}| \ll |w_{X1}|, \quad w_{X2} \ll \frac{1}{\tau_A} + \frac{1}{\tau_B}$$

From the initial conditions, this results in:

$$\begin{aligned} |E_1| &= \left| \frac{w_{E2}}{w_{E1}} E_2 \right| \ll |E_2|, & \Rightarrow E_0 &= 1 + f - \left(1 - \frac{w_{E2}}{w_{E1}} \right) E_2 \approx 1 + f - E_2 \\ |p_1| &\ll |p_2|, & \Rightarrow p_0 &\approx 1 - p_2 \end{aligned} \tag{2.46}$$

For A we have a little more details.

$$A_1 = \frac{\beta}{w_{A1}\tau_B} \ln(1+f) - \frac{w_{A2}}{w_{A1}} A_2 \approx \frac{\beta}{w_{A1}\tau_B} \ln(1+f)$$

Which for small shocks $f \ll 1$ reduces to:

$$A_1 \approx \frac{\beta}{w_{A1}\tau_B} f$$

Now back to the equations (2.15)-(2.17). First let us reexamine the third equation (2.17).

The effect of a delta function shock $f(t) = f_0\delta(t)$ is the above $\partial_t A$ and $E(+\epsilon) = (1+f_0)$.

Since $|w_{X2}| \ll |w_{X1}|$ and $w_{X1} < 0$ we can neglect $\exp[w_{X1}t]$. The last equation becomes:

$$\begin{aligned} \partial_t E &= w_{E2} E_2 (e^{w_{E2}t} - e^{w_{E1}t}) \approx w_{E2} E_2 e^{w_{E2}t} \\ &= A \partial_t p = (1 + A_1 (e^{w_{A1}t} - 1) + A_2 (e^{w_{A2}t} - 1)) w_{p2} p_2 (e^{w_{p2}t} - e^{w_{p1}t}) \\ &\approx \left(1 + \frac{\beta}{w_{A1}\tau_B} f + A_2 (w_{A2}t) \right) w_{p2} p_2 e^{w_{p2}t} \end{aligned} \tag{2.47}$$

For arbitrary t this relation can only hold if $w_{E2} = w_{p2}$. Thus we define:

$$w \equiv w_{E2} = w_{p2}$$

Let us also get an estimate for w_{A1} , the smaller exponent in A . We will go very close to the transition line where $w_{X2} \approx 0$. From Eq. (2.15) we have:

$$\frac{(\tau_B \partial_t + 1) \partial_t A}{A} = \beta \frac{\partial_t E}{E} \approx \beta \frac{w E_2 e^{wt}}{E} \approx 0$$

With an exponential ansatz the left hand side is:

$$(\tau_B w_A + 1) w_A = 0$$

The greater root is $w_{A2} = 0$ and the smaller root is $w_{A1} = 1/\tau_B$. Even away from the

transition line we approximately have:

$$w_{A1} + w_{A2} \approx \frac{1}{\tau_B}$$

Thus we can approximate the expression for A_1 to:

$$A_1 \approx \frac{\beta}{\tau_B} \ln(1 + f) \approx \beta f$$

This way Eq. (2.17) becomes

$$E_2 \approx (1 + \beta f + A_2 (w_{A2} t)) p_2 \approx (1 + \beta f) p_2 \quad (2.48)$$

Eq. (2.15) becomes

$$\frac{(\tau_B w_{A2} + 1) w_{A2} A_2 e^{w_{A2} t}}{1 + \beta f (e^{t/\tau_B} - 1) + A_2 w_{A2} t} \approx \beta \frac{w E_2 e^{wt}}{1 + f + E_2 w t} \quad (2.49)$$

Which again only holds if $w_{A2} = w$. Thus

$$w_{A2} = w_{E2} = w_{p2} = w$$

Again, note that the condition for being close to the transition point was:

$$w \ll \frac{1}{\tau_A} + \frac{1}{\tau_B}$$

Discarding higher than linear order terms in w and looking at times $t/\tau_B \gg 1$ yields:

$$\frac{A_2}{1 - \beta f} = \beta \frac{E_2}{1 + f} + O(w) \quad (2.50)$$

Performing the same procedure on Eq. (2.16) results in (since $w \ll \frac{1}{\tau_{A,B}}$)

$$\begin{aligned} \frac{(\tau_A w + 1) w p_2 e^{wt}}{1 + p_2 w t} &\approx \alpha \frac{w A_2 e^{wt}}{1 + \beta f (e^{t/\tau_B} - 1) + A_2 w_{A2} t} \\ p_2 &= \alpha \frac{A_2}{1 - \beta f} + O(w) = \alpha \beta \frac{E_2}{(1 + f)} + O(w) \end{aligned}$$

$$\approx \gamma \frac{1 + \beta f}{1 + f} p_2 + O(w) \quad (2.51)$$

And so, the condition for the phase transition becomes:

$$\gamma = \frac{1 + f}{1 - \beta f}$$

Now, taking the shock to zero $f \rightarrow 0$ results in a phase transition at:

$$\text{Phase Transition at: } \gamma = 1 \quad (2.52)$$

2.28 Mean Field and Application to Stock Markets

The most famous type of financial network is the stock market. Too lowest order the stock market has the same structure as the one we worked with above. The problem in analyzing the stock market is that, unlike the dataset we had for the Eurozone crisis, suitable data about the investors is very hard to come by. Thus we need to infer things like the investors' equities E_i or their portfolio $A_{i\mu}$ in an indirect way. The first step in doing such an inference could be to work with a “mean field” version of the models described above in which we assume the network is uniform and thus get rid of the indices i for instance. This way we can try to eliminate the two unknown investor variables E and A and work only with the stock prices, which is available publicly. This allows us to get a rough idea what the model predicts about the behavior of the prices and check the claims of the model empirically from stock market data.

Below we show that using extra mean field assumptions the equations of motion can be simplified further to yield an approximate equation for the movements in stock prices.

2.28.1 About the Stock Market

The question of what drives stock price movements is a fundamental one in the theory of financial markets, and one which has profound implications for forecasting and managing financial crises. We describe a model of stock market return dynamics based on investor

behavior which accurately describes the daily return responses observed in real-world markets. Our model is similar to one previously proposed by us for describing the response of banking asset networks to shocks. The model has natural "calm" regimes, where market movements are slow and losses and profits are small, and "frantic" regimes, in which returns are exponential and either bubbles form or crashes happen. As in real markets, these regimes are distinct and separated by a phase transition. We confirm this behavior by analyzing stock market data for a wide range of financial institutions across different time periods. Our model is micro-economic in nature and accounts for the network of investors in the market, provides systemic information about macro-economic behavior, and incorporates in a natural way both endogenous and exogenous factors which influence market behavior. In particular, we use this model to probe quantitatively the impact of external financial news on price dynamics, and develop a theoretical framework for testing the efficient market hypothesis. In addition to providing fundamental insight into the dynamics of prices, our model can identify parameters which serve as an early warning tool for detecting system-wide dynamics which lead to crashes.

2.28.2 Linear Response and the Stock market

The dynamics of process in the stock market is surely complicated. But we can still do a systematic analysis of the system by viewing it as a driven stochastic system. The easiest thing to check would be to what degree the prices of stocks behave like a perturbed linear system, obeying an equation of the type

$$[\Delta_t]\partial_t p(t) \approx F(t) \tag{2.53}$$

where Δ_t is a complicated, time-dependent differential operator and $F(t)$ is a general force term encoding everything that is happening *outside* the market (i.e. as economist would say, "exogenous" factors). $F(t)$ could depend on economic news or changes that force the prices to move. But we will assume that the lowest order effect of the investor behavior and thus the dynamics of the financial network is mostly captured by Δ_t . First we want to

know if assuming an operator that is approximately independent of p (thus working with the linear part of the equation) yields an equation that is consistent with real world stock market data. For this aim, let us first see what the model we worked with in the previous sections can say about the stock market and then see how we can check the behaviour in the stock market data.

2.29 Modeling Stock Market Dynamics using the Market Response model

We can think of a stock market as an approximately bipartite, weighted network, with investors on one side and the stocks they own on the other side. We propose to model the response dynamics of this system with the same model we used for the Eurozone crisis. Since we would also like to quantify the effect of exogenous factors such as news, we will slightly modify the equations. Similar to the GIIPS model, E_i represents the “equity” (net worth) of investor i , p_μ the value of each share of stock μ , and $A_{i\mu}$ the number of shares of stock μ that investor i owns. All of these variables are time-dependent. The general form of the equations with exogenous factors included would be

$$\begin{aligned}\frac{\delta A(t + \tau_A)}{A} &= \beta \left(\frac{\delta E(t + \tau_E)}{E} + S \right) \\ \frac{\delta p(t + \tau_p)}{p} &= \alpha \left(\frac{\delta A(t)}{A} + S \right) \\ \delta E(t) &= A \delta p(t)\end{aligned}\tag{2.54}$$

Where τ_x are response times. S here can represent any external force, such as the “sentiment” S_N towards the stock from the news (i.e. if there was more good news or bad news about it), or how often it occurred in the news O_N . We assume that it affects both the trading of the brokers (first equation) and the bidding on the prices. However, the psychological factors α and β could also be affected by the news and maybe they could even be the primary way through which news affects the prices:

$$\alpha = \alpha(O_N, S_N, \partial_t O_N, \partial_t S_N), \quad \beta = \beta(O_N, S_N, \partial_t O_N, \partial_t S_N)$$

For small τ_x the first two equations become second order equations in ∂_t . We want to get rid of E and find an effective equation for p .

2.29.1 Case 1: $\tau_A = 0$

First suppose that $\tau_A = 0$. The equity E is comprised of assets Ap plus some cash c :

$$E = Ap + c, \quad \partial_t c = \partial_t Ap$$

Let's also assume that $Ap \gg c$, i.e. most of the capital is in the form of these assets $E \approx Ap$.

$$\begin{aligned} \frac{\partial_t A}{A} &= \beta \frac{(\partial_t + \tau_E \partial_t^2) E}{E} + \beta S \\ \frac{(\partial_t + \tau_p \partial_t^2) p}{p} &= \alpha \frac{\partial_t A}{A} + \alpha S \\ \partial_t^2 E &= \partial_t A \partial_t p + A \partial_t^2 p \end{aligned} \tag{2.55}$$

Defining $\gamma = \alpha\beta$ we have:

$$\begin{aligned} \frac{(\partial_t + \tau_p \partial_t^2) p}{p} &= \gamma \frac{(\partial_t + \tau_E \partial_t^2) E}{E} + (\gamma + \alpha) S \\ &= \gamma \frac{A \partial_t p + \tau_E (\partial_t A \partial_t p + A \partial_t^2 p)}{Ap + c} + (\gamma + \alpha) S \\ &\approx \gamma \frac{\partial_t p + \tau_E ((\partial_t + \tau_p \partial_t^2) p \partial_t p / p + \partial_t^2 p)}{p} + (\gamma + \alpha) S \end{aligned} \tag{2.56}$$

Cleaning this equation up yields:

$$((1 - \gamma) \partial_t + (\tau_p - \gamma \tau_E) \partial_t^2) p - (\gamma + \alpha) S p = \gamma \tau_E (\partial_t + \tau_p \partial_t^2) p \partial_t \ln p \tag{2.57}$$

This equation includes an interesting non-linear term. But aside from that the linear part has the form:

$$\begin{aligned} [(1 - \gamma) + (\tau_p - \gamma\tau_E)\partial_t] \partial_t p &= (\gamma + \alpha)Sp + O((\partial_t p)^2) \\ O((\partial_t p)^2) &= \gamma\tau_E(\partial_t + \tau_p\partial_t^2)p\partial_t \ln p \end{aligned} \quad (2.58)$$

When the force term Sp with its coefficients are much smaller than the left hand side, the equation has phase transitions around $\gamma = 1$ and $\gamma = \tau_p/\tau_E$ where $\partial_t p$ will have goes from converging (stable damped) to diverging (bubble forming) solutions. The exponential solution in absence of S is:

$$\partial_t p \sim \exp \left[-\frac{1 - \gamma}{\tau_p - \gamma\tau_E} t \right]$$

2.29.2 Case 2: $\tau_E = 0$

First suppose that $\tau_E = 0$. Again, we will use $E \approx Ap$.

$$\begin{aligned} Eq_1 : \quad \frac{(\partial_t + \tau_A\partial_t^2)A}{A} &= \beta\frac{\partial_t E}{E} + \beta S = \beta\frac{A\partial_t p}{Ap} + \beta S \\ Eq_2 : \quad \frac{(\partial_t + \tau_p\partial_t^2)p}{p} &= \alpha\frac{\partial_t A}{A} + \alpha S \end{aligned} \quad (2.59)$$

Take $\alpha Eq_1 + Eq_2 + \tau_A\partial_t Eq_2$

$$\begin{aligned} & -\alpha\tau_A p\partial_t S + \frac{\alpha\tau_A(\partial_t A)^2}{A^2}p \\ & -(\alpha + \gamma)Sp - \frac{\tau_A u^2}{p} - \frac{\tau_A\tau_p u\partial_t u}{p} \\ & + [\tau_A\tau_p\partial_t^2 + (\tau_A + \tau_p)\partial_t + (1 - \gamma)]u = 0 \end{aligned} \quad (2.60)$$

Where $u = \partial_t p$. From Eq_2 we can also get rid of $\partial_t A/A$

$$+ \tau_A\tau_p\partial_t^2 u + (1 - \gamma - 2\tau_A S)u$$

$$\begin{aligned}
& + (\tau_A + \tau_p - 2\tau_A\tau_p S) \partial_t u \\
& = (-\alpha\tau_A S + \alpha + \gamma)Sp + \alpha\tau_A p \partial_t S \\
& + \frac{\tau_A}{\alpha p} ((\alpha - 1)u^2 + (\alpha - 2)\tau_p u \partial_t u - (\tau_p \partial_t u)^2)
\end{aligned} \tag{2.61}$$

In short, the equations are:

$$\begin{aligned}
& [\tau \partial_t^2 + \eta \partial_t + \omega^2] u = aSp + b(\partial_t S)p + O(u^2, \partial_t u^2) \\
& \frac{1}{\tau} = \frac{1}{\tau_A} + \frac{1}{\tau_p}, \quad \eta = 1 - 2\tau S, \quad \omega^2 = \frac{1 - \gamma - 2\tau_A S}{\tau_A + \tau_p}, \\
& a = \frac{\gamma + \alpha - \alpha\tau_A S}{\tau_A + \tau_p}, \quad b = \frac{\tau_A \alpha}{\tau_A + \tau_p}, \quad p(t) = \int^t u(t') dt' \\
& O(u^2, \partial_t u^2) = \frac{\tau_A ((\alpha - 1)u^2 + (\alpha - 2)\tau_p u \partial_t u - (\tau_p \partial_t u)^2)}{\alpha p(\tau_A + \tau_p)}
\end{aligned} \tag{2.62}$$

This time, we first need to find the expression for $\partial_t^2 A/A$ first:

$$\begin{aligned}
& \frac{(\partial_t + \tau_A \partial_t^2)A}{A} = \beta \frac{\partial_t E}{E} + \beta S = \beta \frac{A \partial_t p}{Ap} + \beta S \\
& \frac{(\partial_t^2 + \tau_p \partial_t^3)p}{p} - \frac{(\partial_t + \tau_p \partial_t^2)p \partial_t p}{p^2} = \alpha \frac{\partial_t^2 A}{A} - \alpha \left(\frac{\partial_t A}{A} \right)^2 + \alpha \partial_t S
\end{aligned} \tag{2.63}$$

$$\begin{aligned}
& \frac{(\partial_t + \tau_p \partial_t^2)p}{p} + \tau_A \frac{(\partial_t^2 + \tau_p \partial_t^3)p}{p} = \gamma \frac{\partial_t p}{p} + (\gamma + \alpha + \tau_A \alpha \partial_t)S + O((\partial_t p)^2) \\
& [\tau_p \tau_A \partial_t^2 + (\tau_p + \tau_A) \partial_t + (1 - \gamma)] \partial_t p = (\gamma + \alpha)Sp + \tau_A \alpha (\partial_t S)p + O((\partial_t p)^2)
\end{aligned} \tag{2.64}$$

Where the nonlinear term is again quadratic in p (thus a generalized form of the Fisher equation) and looks like:

$$O((\partial_t p)^2) = \tau_A \frac{(\partial_t + \tau_p \partial_t^2)p \partial_t p}{p} - \alpha \tau_A \frac{((\partial_t + \tau_p \partial_t^2)p)^2}{p} \tag{2.65}$$

This time the dynamics is richer and we have a damped oscillator with a driving force cou-

pled to p and nonlinearities of type $\sim (\partial_t p)^2$. Taking the return $u \equiv \partial_t p$ as the fundamental variable, the nonlinearities are roughly of type $u^2 + a\partial_t u^2$. But the thing to note is that the frequency depends on $(1 - \gamma)$ again. For $\gamma < 1$ it has the usual stable damped oscillator solutions, while $\gamma > 1$ will result in instabilities and divergent solutions. So interestingly, the phase transition at $\gamma = 1$ is still there and doesn't seem to be affected by the choice of time-lags.

In short, the equations are:

$$\begin{aligned} [\tau \partial_t^2 + \partial_t + \omega^2] u &= aSp + b(\partial_t S)p + O(u^2, \partial_t u^2) \\ \frac{1}{\tau} &= \frac{1}{\tau_A} + \frac{1}{\tau_p} \end{aligned} \quad (2.66)$$

$$\omega^2 = \frac{1 - \gamma}{\tau_A + \tau_p}, \quad a = \frac{\gamma + \alpha}{\tau_A + \tau_p}, \quad b = \frac{\tau_A \alpha}{\tau_A + \tau_p} \quad (2.67)$$

$$p(t) = \int_0^t u(t') dt' \quad (2.68)$$

The amazing point is that this equation has shocking resemblance to the empirical equation we found for the return based on the analysis we did using the Green's function. In addition, though, this equation tells us how this model expects the News Sentiments to enter, which is the rough two terms, one from S and one from $\partial_t S$, but both multiplied into p itself. We have not checked for this type of appearance yet. Also, γ and α may themselves be functions of S and occurrences O . Moreover, this equation provides a natural nonlinear term, which start becoming significant close to a phase transition to the “frantic” state and thus can be used to model the behavior near the transition.

2.29.3 Auto-correlations and Green's Function

How do we verify the claim that the stock market follows the stochastic equations with a random force as described in the section above? Clearly we cannot simulate or predict the stochastic fluctuations in the stock prices. But just as in Brownian motion, we can use Linear response. A version of the Kubo formula may apply here is the forces are sufficiently random and memory-less, i.e. correlations at different times decay faster than any other

time-scale in the system (random Gaussian noise)

$$\int dy F(y) F(t+y) \approx \sigma_F^2 \delta(t) \quad (2.69)$$

For the linear part of the equation we have

$$\begin{aligned} u(t) &\equiv \partial_t p(t) [\Delta_t] u(t) = F(t) \\ u(t) &= \int d\lambda G(t; \lambda) \mathcal{F}(\lambda). \end{aligned} \quad (2.70)$$

Here $G(t_f; t_i)$ is the Green's function for the linear part of the operator $[\Delta_t]$. if the process is memory-less, the Green's function is a “propagator” that may be used as above to propagate the state from t_i to t_f . In these memory-less settings we have a Markov process and we have

$$\int d\lambda G(t_i; \lambda) G(\lambda; t_f) \approx G(t_i; t_f) \quad (2.71)$$

If the forces approximately satisfy (2.69) within a time-window of interest we can use the usual linear response procedure and conclude

$$\int d\lambda u(\lambda) u(t - \lambda) = \int d\lambda dx dy G(\lambda; y) \mathcal{F}(y) G(t - \lambda; x) \mathcal{F}(x). \quad (2.72)$$

In the general case, this can't be simplified further. If, however, we have simpler case where the Linear operator Δ_t has approximately no explicit time dependence over a certain time window of interest, then the Green's function will only be a function of the time difference

$$\Delta_t \approx \Delta_{t+a} \quad \Rightarrow \quad G(t_i; t_f) \approx G(t_i + a; t_f + a) \approx G(t_f - t_i) \quad (2.73)$$

over such time windows, the auto-correlation above simplifies significantly and becomes the familiar expression for any quadratic field theory. Using (2.69) we have

$$\begin{aligned}
\int d\lambda u(\lambda)u(t-\lambda) &= \int d\lambda dx dy G(\lambda-y)\mathcal{F}(y)G(t-\lambda-x)\mathcal{F}(x) \\
&= \int d\lambda dx' dy' G(y')\mathcal{F}(\lambda-y')G(t-x')\mathcal{F}(x'-\lambda) \\
&= \int dy' dx' G(y')G(t-x') \int d\lambda \mathcal{F}(\lambda-y')\mathcal{F}(x'-\lambda) \\
&= \int dx' G(x')G(t-x') \\
&= G(t).
\end{aligned} \tag{2.74}$$

Thus the auto-correlations of the “return” $u(t) = \partial_t p(t)$ contains all the information about the linear and slowly varying part (this is to say, time-independent part) of the differential operator Δ_t . Some more discussion of this can be found in appendix A.10. Let us now examine this in real data.

2.30 Autocorrelation in Cumulative News Data

Let us first make a comment about the driving forces in the market. An important thing that investors look at are financial news. We want to briefly discuss whether the news data has some of the qualities that we expect from a random Gaussian F or if more care needs to be taken.

We had access to some compiled financial news through collaborators (owners of the website <http://newstream.ijs.si/>). The news, both occurrence and sentiments, exhibit peculiar patterns. For instance, take the occurrence weighted sentiment data and sum all the sentiments for all corporate entities and call it S_c :

$$S_c(t) = \sum_{i \in Ont} S_i(t)$$

Now we will perform some auto-correlation computations. First we compute the convolution

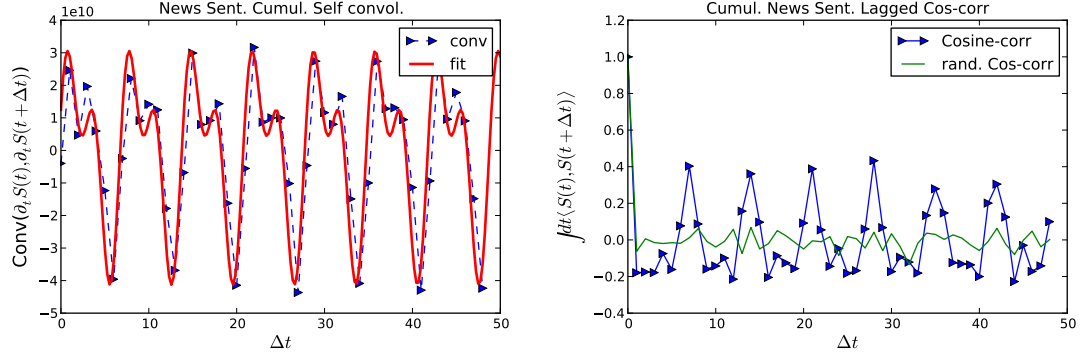


Figure 2.15: Convolution of the daily change in cumulative news sentiments with itself. It exhibits strong seven day and 3.5 day patterns, which suggest that the trend of increase and decrease in the cumulative sentiment repeats itself weekly and has a more or less fixed weekly pattern. Red curve is the fit and blue triangles, connected by dashed lines, are the actual Sentiment change convolutions.

of $S_c(t)$ with itself to get a sense of its lagged aut-correlation:

$$\text{Conv}(\partial_t S_c, \partial_t S_c) = \int dy \partial_t S_c(t) \partial_t S_c(t - y)$$

The result is shown in Fig. 2.15. As we can see there are very strong and clear 7-day patterns which persist. The fitted red curve includes the leading frequency terms ($\omega_0 = 2\pi/(7\text{days})$):

$$\text{fit} = 2.50 \times 10^{10} \left(\sin(\omega_0 t) + \frac{1}{2} [\sin(2\omega_0 t) + \cos(2\omega_0 t)] \right)$$

The above features in the cumulative news is because of the weekly cycle of business days. Although news about individual companies does not show such auto-correlation, we should be weary of this feature. In particular, since this will violate our assumption about decay of correlations in F beyond 7 days, we cannot trust auto-correlations in returns $u = \partial_t p$ as a proxy for Δ_t beyond a business week, i.e. 5 days.

2.31 Fitting Bank Correlations

We analyzed the stock prices for a number of bank stocks. Contrary to common wisdom, there do exist many persisting correlations between stock prices from one day to the next and they are well-known. However, there does not exist any conclusive theory about the reason why they exist and some argue that they are artifacts of non-synchronicity in trading [42]. There is no consensus on this matter yet. We argue here that from the point of view of stochastic processes the auto-correlation can contain information about the linear part of the dynamics as shown above. Especially if the pattern is consistent over various snapshots of the data then it must be taken seriously and the linear part of the dynamics plays an important role.

We analyzed many stocks and from the analysis of daily data (end of day prices only and not the movements within a day) it seems that the best fit for auto-correlations has a very familiar form, namely that of a damped harmonic oscillator whose frequency slowly changes over different months.

$$\text{fit : } \frac{\int dt \partial_t P(t + \Delta t) P(t)}{\int dt \partial_t P(t)^2} \approx \exp \left[-\frac{\Delta t}{2\tau} \right] \cos(\omega \Delta t)$$

This may arise if $\partial_t P$ satisfies a damped oscillator equation as follows:

$$\begin{aligned} (\tau \partial_t^2 + \partial_t + m) \partial_t P(t) &= F(t) \\ \partial_t P(t) &= \int dy \int \frac{dk}{2\pi} \frac{F(y) e^{ik(t-y)} \theta(t-y)}{(-\tau k^2 + ik + m)} \\ \text{Poles at: } k &= \frac{-i \pm \sqrt{4\tau m - 1}}{2\tau} \\ \omega &\equiv \frac{\sqrt{4\tau m - 1}}{2\tau} \\ \partial_t P(t) &= \int d\Delta t e^{-\Delta t/(2\tau)} \cos(\omega \Delta t) F(t - \Delta t) \end{aligned} \quad (2.75)$$

We computed the cosine correlation for a few of the corporate classes and found that τ and ω are within similar ranges. For the class of Banks, we found that while $\tau \approx 0.4$, ω

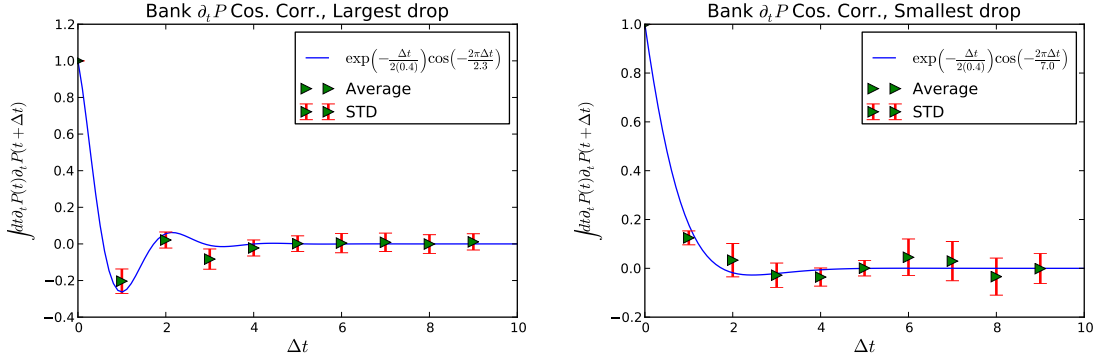


Figure 2.16: Auto-correlations of stock returns $\partial_t p$ for a number of banks. The horizontal axis shows the number of days of lag δt in the auto-correlation $\int \partial_t p(t) \partial_t p(t + \delta t) dt$. Left: The mean, with one standard deviation error bars, of the auto-correlations of stocks of 10 banks which showed the most largest negative auto-correlation for a lag of 1 days. The stocks consisted of: UBL.MI, HBANP, 0005.HK, SDA, PHNX.L, ALBKY, PXQ.MU, MBFJF, NHLD, ZIONW. UBI, Huntington Hldng, HSBC, Sadia S.A., Phoenix Grp, Alpha Bank, Phoenix Sat TV, Mitsubishi UFJ, National Hldg, Zions Bancorp.. Right: 10 bank stocks with the most positive value of auto-correlations after one day: KBC.L, WBC.AX, DUA, HBA-PG, DTT, ANZ.AX, ERH, HBC, CSCR, DVHI. The solid curve is a fit using a damped harmonic oscillator, which would be consistent with what our model predicts the return on stock prices to do.

varies significantly (units):

$$\tau \approx 0.4(\text{days}) \quad T = \frac{2\pi}{\omega} \in [2.3, 7.0](\text{days})$$

Figure 2.17 shows the frequency squared evaluated for 5 important U.S. banks. As we see, not only do the individual banks mostly have a positive and very slowly varying ω^2 , interrupted occasionally by important dips into $\omega^2 < 0$ which is the unstable phase, the 5 bank stocks also show a high degree of “herding”, i.e. similar values of ω^2 for all five banks with small standard deviations.

2.31.1 Instabilities in the Stock Market

Note that having a $\omega^2 < 0$ does not necessarily mean a crash. It only means that the the state is unstable and thus not sustainable. We can examine whether or not certain stocks were in a “crisis” state and were crashing, or that they were forming a “bubble”

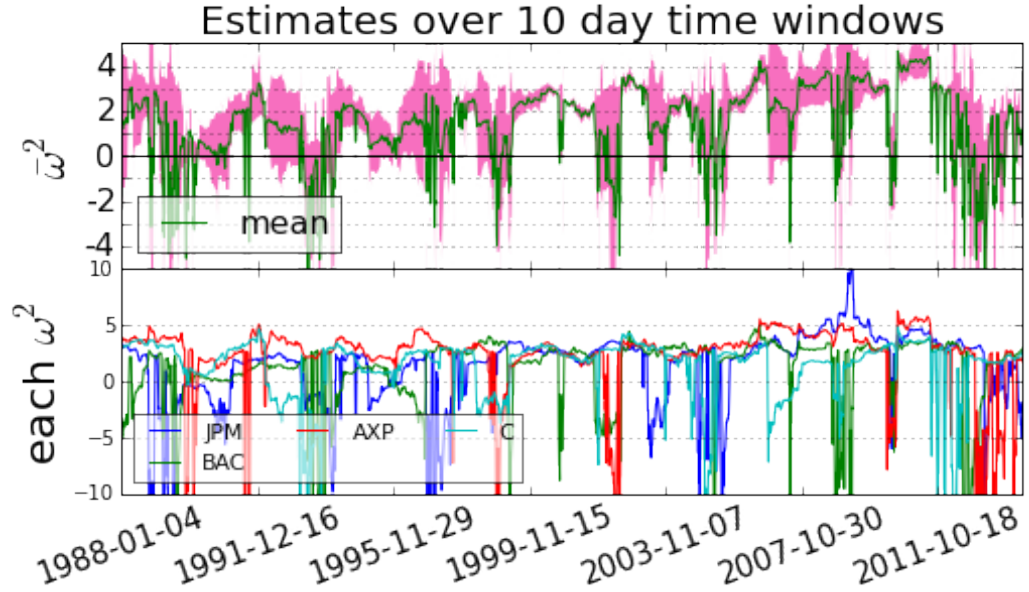


Figure 2.17: The value of frequency squared ω^2 for 5 important large banks. The top shows the mean (green) and the standard deviation (width of the purple band) across the 5 banks. The top shows the mean (green) and the standard deviation (width of the purple band) across the 5 banks. Bottom shows ω^2 for individual banks.

which is characterized by period of exponential gain in value. Figure 2.18 shows this for some important stocks during the crisis of 2007-2008. We can see that before the crisis the Citigroup (the red dots denoted by C) had periods of exponential drop during the crisis in the left plot (where both $\omega^2 < 0$ and $\partial_t p < 0$, i.e. the third quadrant). The right plot is from after the banking bailout. No other bank has such a prominent presence in the third quadrant as the Citigroup and, as we know, Citigroup was the only one that went bankrupt. As you can see Bank of America (BAC) had some exponential growth periods (where both $\omega^2 < 0$ and $\partial_t p > 0$, i.e. the fourth quadrant), recovering from the crisis.

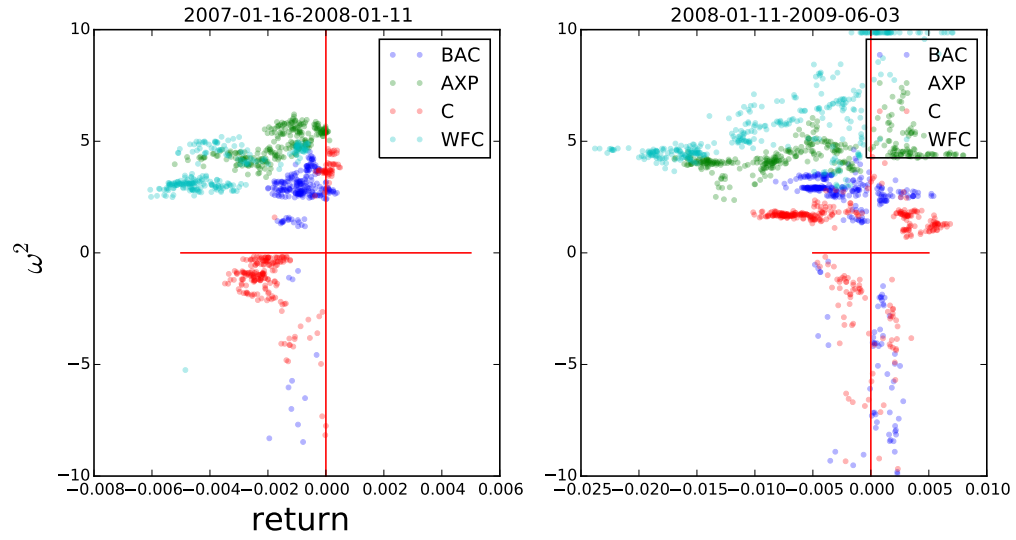


Figure 2.18: Stock price behavior before and after the 2007-2008 crisis. the vertical axis is ω^2 and the horizontal axis is the return $\partial_t p$. the lower half denotes the unstable part. the lower right shows “bubbles” and exponential growth, while the lower left represents “crash” and exponential decay of stock price.

Chapter 3

Networks of Local Interactions

Many networks form out of local interactions. Many friendships form from face-to-face encounters (locality in real space). Many collaborations are a result of similarity in the topic of research (locality in an abstract space). The Goal of this chapter is to lay the foundation for a general framework that could be used for modeling such “networks of local-interactions”.

Many physical interactions are local and we have powerful tools, especially in field theory, for modelling with local interactions.

3.1 Introduction

Network growth models generally disregard how proximity and dynamics of agents affect the probability of establishing links. In popular models such as Erdős-Rényi, Watts-Strogatz [43], or Barabási-Albert (BA) [44] the interactions among nodes do not depend on any physical or network “distance.” In some networks, such as social networks, the links are generally established only if nodes make contact, either through physical proximity or in the virtual world. It has been found that the probability of people contacting each other through phones fall with the distance and that it can be described by the so-called “gravity model” [45]. Some studies also suggest that physical proximity plays an important role in scientific collaborations [46].

Many real-world networks are either scale-free or at least have a fat-tailed degree distribution [47]. It has been shown that scale-free networks have very short average path lengths, $L \propto \log \log N$, for N nodes, and are therefore “ultra-small-world” [48]. In Watts-

Strogatz networks, the small world property is generated by randomly adding long range links to an otherwise locally clustered network. This may appear to suggest that locality is not conducive to the small-world property, much less to the scale-free property which implies even shorter average distances between nodes.

Contrary to this, as we show below, it is possible to generate scale-free networks based on locally interacting agents under natural circumstances. The model we propose is a geometric model, in that the agents reside on a metric space and interactions depend on metric distances. In this model, agents stochastically traverse the space and form connections only when they encounter each other at designated centers. The global characteristics of the network are then determined by the spatial distribution of these *rendezvous points* (RP). As such, it is naturally suited for describing contact networks of people over cities.

An important feature of our model is that it produces a relatively high clustering coefficient akin to those observed in some biological networks, including neuron firing correlations [49] and protein-protein interactions [47]. There do exist models capable of producing arbitrary degree distributions or relatively high clustering [50–53],

but BA-like models have very low clustering unless substantially modified [54].

The framework we introduce here is very general. The model may be solved for agents moving according to a variety of different stochastic processes. For any such process, given any desired degree distribution, we can analytically solve the spatial rendezvous point distribution that results in that degree distribution and vice versa. In this paper, we both derive the general results for arbitrary dynamics and solve and simulate a concrete example of friendship networks in cities modelled through random walkers in a harmonic potential.

We first outline the general idea and state the main results. We then compare this to data about cities and analyze cell phone data from Shanghai.

3.2 General Properties of Networks of Local Interactions

Fokker-Planck equations are essentially classical field theory equations for stochastic processes. The machinery of perturbative field theory is well suited for describing local interac-

tions among weakly interacting stochastic agents. Therefore, we will build our model using field theory. Consider Locally interacting agents¹ whose dynamics can be described using Fokker-Planck equations². Consider $N \gg 1$ agents. Denote the initial location in the n dimensional space of agent i by x_i . Then each agent i has assigned to it a probability density $\hat{\phi}_i(x, t)$ of being found in the infinitesimal vicinity of point x at time t . In general, without interactions among agents, the Fokker-Planck equation of the above process is linear, with possible source terms $J_i(x, t) = \delta(t - t_0)\delta^n(x - x_i)$

$$\mathcal{L}_{x,t}\phi_i(x, t) = J_i(x, t) \quad (3.1)$$

The probability of agents i, j, \dots interacting locally is conditioned upon them all being present at a point in space and thus, to first order, depends on the product of $\mathcal{V} \sim \phi_i \phi_j \dots$. Such local interactions modify the Fokker-Planck equation to

$$\mathcal{L}_{x,t}\phi_i(x, t) = J_i(x, t) - \frac{\delta \mathcal{V}}{\delta \phi_i} \quad (3.2)$$

3.2.1 The Network and its Adjacency Matrix

A network can be understood in terms of the connections between agents i and j . Since each agent i is defined through some stochastic dynamics captured by the operator $\mathcal{L}_{x,t}$, the probability distribution of agents i, j with $i \neq j$ are independent random variables and thus uncorrelated, unless there is an interaction \mathcal{V} that connects the two. Thus the correlation of the ensemble average of the locations of the agents, i.e. their probability distributions ϕ_i over all space would reduce to a simple product

$$\text{if: } \mathcal{V} = 0 \quad \Rightarrow \quad \langle \phi_i \phi_j \rangle = \langle \phi_i \rangle \langle \phi_j \rangle$$

and conversely if they are coupled through an interaction their probability distributions will be correlated. Thus we conclude that a natural candidate for the adjacency matrix A of a

¹We assume interactions are rare (weakly interacting) so that perturbation theory is applicable.

²Any other linear equation of motion works just as well

network of the interactions of such agents is the amount of correlation in their probability densities. With no interaction, ϕ_i and ϕ_j are independent and so the ensemble average, time averaged to time T , $\langle \rangle_T$, of their product would be $\langle \phi_i \phi_j \rangle_T = \langle \phi_i \rangle_T \langle \phi_j \rangle_T$. Thus we define

$$A_{ij}(T) \equiv \langle \phi_i \phi_j \rangle_T - \langle \phi_i \rangle_T \langle \phi_j \rangle_T \quad (3.3)$$

This A_{ij} measures the ensemble average of how correlated the two densities are, up to time T .

Since we assume that \mathcal{V} in Eq. (3.2) represents weak interactions, we can use perturbation theory to evaluate A_{ij} . Note that when dealing with N agents with $N \gg 1$ we can have a natural $1/N$ suppression in some correlation functions.

3.3 General potential derivations

We want the interaction potential to be finite, so that the whole system has finite energy or action. Since ϕ_i are probability distributions of the agents over space we have $\int d^d x \phi_i = 1$. Consider a simple case where we have a two-point interaction of the form

$$\mathcal{V} \sim \sum_{ij} \Gamma_{ij} \phi_i \phi_j$$

Now suppose an extreme case where the way agent i interacts with another agent j is independent of i, j and space-independent. In this case the total number of interactions of agent i with other agents is given by

$$\Gamma_{ij} \sim c, \quad \Rightarrow \quad \sum_j \Gamma_{ij} \sim Nc$$

However, it is unrealistic to say that when there are 1000 people at a convention, each person interacts with all of them. In fact for the case of people it has been suggested that we can only have meaningful relations with about 150 other people [55], a number known as “Dunbar’s Number”. Therefore, in a big convention with N people, each person is expected

to only interact with $\sim 150/N$ of them, so that total number of interactions remains around 150. This suggests that the $\gamma_{ij} = c \sim c'/N$ and that the interactions are normalized by a factor of $1/N$ for each sum over indices j . With this argument, the general potential should have a form

$$\mathcal{V} = \int dx dt \left[\frac{1}{N} \sum_{i,j} f_{ij}^{(2)} \phi_i \phi_j + \frac{1}{N^2} \sum_{i,j,k} f_{ijk}^{(3)} \phi_i \phi_j \phi_k + \dots \right] \quad (3.4)$$

in which $\int d^d x f_{ij..k} \sim c$ with c being independent of N and generally $c \ll N$. The adjacency matrix becomes

$$\begin{aligned} A_{ij}(T) &= A(x_i, t_0, x_j, t_0; T) \\ &= \frac{1}{N} \int d^n y \int_{t_0}^T dt G(x_i, t_0, y, t) f_{ij}(y, t) \\ &\quad \times G(x_j, t_0, y, t) + O\left(\frac{1}{N^2}\right) \end{aligned} \quad (3.5)$$

where G is the propagator or Green's function of $\mathcal{L}_{x,t}$, defined by

$$\mathcal{L}_{y,t} G(x, t_0, y, t) = \delta^n(y - x) \delta(t - t_0)$$

and f_{ij} is the ensemble average of the interactions

$$f_{ij} = f_{ij}^{(2)} + \sum_k f_{ijk}^{(3)} \langle \phi_k \rangle_T + \dots \quad (3.6)$$

Recall that $\langle \phi_k \rangle_T$ represents the time average of the distribution ϕ_k , which is the ensemble average of the spatial distribution of agent k up to time T .

3.3.1 Two-point Interactions and “Rendezvous Points”

Usually in field theory a ϕ^2 term is referred to as a “mass term”. The way it contributed to the propagator $G(x; y)$ is through a geometric series which for a quadratic action basically determines the location of the poles or resonances. In the momentum space this is generally

understood as follows

$$S[\phi] \sim \int \phi^\dagger (\nabla^2 + m^2) \phi \quad \Rightarrow \quad \tilde{G}(p) \sim \frac{i}{p^2 - m^2}$$

A similar thing is, of course, still true in the case we are discussing here. However, there is an important difference with what is generally done, namely the fact that the “effective mass” term $f_{ij}(x)\phi_i(x)\phi_j(x)$ can have space and time dependent mass f_{ij} . In fact, as we will argue below, most interesting networks emerge only if we break the spatial symmetry.

The meaning of f_{ij} is how likely it is for agents i, j to interact at different points in space. In the simplest case, we can assume that f_{ij} is independent of i, j (no preference among agents) and think of it as the density of meeting places or “rendezvous points” (RP’s) in space

$$\Gamma(x, t) \equiv \frac{f_{ij}(x, t)}{N}, \quad \text{for all } i, j \quad (3.7)$$

In the context of a city, f_{ij} could be the density of work places, universities, cafes and so on. We want the distribution of these meeting places or “rendezvous points” (RP’s) $\Gamma(x, t)$ to determine the strength of their interaction, beside the probability of finding agents i and j in the same place in space. Such an interaction is of form

$$\mathcal{V}(x, t) = \frac{1}{N} \sum_{i \neq j} \Gamma(x, t) \phi_i(x, t) \phi_j(x, t) \quad (3.8)$$

The $1/N$ factor enables us to evaluate $A_{ij}(T)$ perturbatively.

$$\begin{aligned} A_{ij}(T) &= A(x_i, t_0, x_j, t_0; T) \\ &= \frac{1}{N} \int d^n y \int^T dt G(x_i, t_0, y, t) \Gamma(y, t) \\ &\quad \times G(x_j, t_0, y, t) + O\left(\frac{1}{N^2}\right), \end{aligned} \quad (3.9)$$

where G is the propagator or Green’s function of $\mathcal{L}_{x,t}$, defined by

$$\mathcal{L}_{y,t} G(x, t_0, y, t) = \delta^n(y - x) \delta(t - t_0).$$

3.4 Degree and Degree Distribution

For convenience, we define the short-hand notation

$$P_{xy}Q_{yz} \equiv \int d^n y \int^T dt_y P(x, t_x, y, t_y) Q(y, t_y, z, t_z) \quad (3.10)$$

The degree of a node, k_i , is the total number of other nodes that it connects to. Here we will abuse the notation and instead use k_i for the ensemble average of the degrees.

The initial distribution of the nodes position of nodes can be written as

$$J(x, t) = \sum_i J_i(x, t) \quad (3.11)$$

The degree k_i of node is then a function of its position and time

$$\begin{aligned} k_i(T) &= k(x_i, t_0; T) = \sum_j A_{ij}(T) \\ &= \int d^n y \int^T dt A(x_i, t_0, y, t; T) J(y, t) \end{aligned} \quad (3.12)$$

Using (3.10) we can write

$$\begin{aligned} k_i &= A_{ix} J_x = [AJ]_i, \\ A_{ij} &= G_{ix} \Gamma_{xx} G_{jx} = [G \Gamma G^T]_{ij} \end{aligned} \quad (3.13)$$

In this notation we use i, j, k, \dots for the initial coordinates and x, y, \dots for generic points.

Thus note that

$$G_{ij} = G(x_i, t_0, x_j, t_0) = \delta^n(x_i - x_j) \quad (3.14)$$

Additionally, if the systems enjoys certain spatial symmetries, such as spherical symmetry, the degree –and thus also the degree distribution– will have the same symmetry. With spherical symmetry we have

$$P(k) |dk(r, t)| = dN(r, t_0) = \int dt J(r, t) \Omega_{n-1} r^{n-1} dr$$

$$P(k(r, t)) = \Omega_{n-1} r^{n-1} \left| \frac{J_r}{\partial_r A_{rx} J_x} \right| \quad (3.15)$$

Where the number of points should be at time t_0 because that's is the initial location used in calculating the degrees k and not the location where they possibly make contact with others. Since $J(r, t) \propto \delta(t - t_0)$ its integral yields N at the correct time.

3.4.1 Note on Anlaytical Solutions

Note that since the dynamics is not unitary ($\mathcal{L} \neq \mathcal{L}^\dagger$) The propagator G of \mathcal{L} is not necessarily the propagator of \mathcal{L}^\dagger , i.e. $\mathcal{L}^\dagger G \neq I$. There exists, however, another operator such that (note the indices)

$$\mathcal{L}_{xy} G_{zy} = \overline{\mathcal{L}}_{xy} G_{yz} = \delta_{xz} \quad (3.16)$$

which we will explicitly find in the examples below. Acting with $\overline{\mathcal{L}}_{ij}$ on (3.13) we find an important relation between the Rendezvous Points $\Gamma(r, t)$ and the degrees

$$\begin{aligned} \overline{\mathcal{L}}_{ij} k_j &= \Gamma_{ii} G_{il}^T J_l = \Gamma_{ii} J_i \\ \Gamma_{xx} &= \Gamma(x, t) \theta(t) = \frac{\overline{\mathcal{L}}_{xy} k_y}{J_y} \end{aligned} \quad (3.17)$$

where we have used (3.14).

3.5 Higher-Order Moments of the Network

To characterize a network one has to explore the details of connections among nodes. The degree sequence k_i and its distribution $P(k)$ are just the first order moments, i.e. they can be extracted from first power of A_{ij} . Higher order moments generally encode more information and are crucial for understanding the network structure. The first such higher order moment that is generally considered is called the “degree-degree correlation” or degree assortativity, which compares the average degree of the first neighbors $k_i^{(1)}$ of a node i to

k_i . The m th neighbor average degree, $k_i^{(m)}$ is

$$k_i^{(m)} = \frac{1}{k_i^{(m-1)}} \sum_j A_{ij} k_j^{(m-1)} = \frac{1}{k_i^{(m-1)}} [AJk^{(m-1)}]_i \quad (3.18)$$

where $J_{xy} = \delta_{xy} J_x$. Acting with $\overline{\mathcal{L}}$ on this yields

$$\overline{\mathcal{L}}_{ii} \left(k_i^{(m)} k_i^{(m-1)} \right) = \Gamma_{ii} J_i k_i^{(m-1)} \quad (3.19)$$

3.5.1 Degree-Degree Correlation and Clustering

This is a generalization of (3.17) and allows us to in principle calculate any network moment analytically, or put bounds on them. For example, $k_i^{(1)}$ versus k_i shows the degree-degree correlation, and $k^{(2)}$ puts a bound on the local clustering c_i defined as

$$c_i \equiv \frac{2 \times \# \text{ of triangles involving } i}{k_i(k_i - 1)} = \frac{[A^3]_{ii}}{k_i(k_i - 1)} \quad (3.20)$$

Since $k_i^{(2)} = \sum_j [A^3]_{ij} / k_i^{(1)}$ we have

$$c_i \leq \frac{k_i^{(2)} k_i^{(1)}}{k_i(k_i - 1)} \quad (3.21)$$

These relations should hold for any network arising from general Fokker-Planck or continuity equation with weak interaction. Now let us turn to concrete examples.

3.6 Examples: Network of interacting random walkers

Consider a flat 2D space with area $V = L^2$. Place $N \gg 1$ random walkers in this space. For simplicity we will work in units where $\frac{N}{V} \rightarrow 1$. Let $\phi_i(x, t)$ denote the probability density of finding random walker i at point x and time t . Thus, without any interaction the Fokker-Planck equation is the sourced diffusion, or heat equation

$$(\partial_t - \nabla_x^2) \phi_i(x, t) = J_i(x, t) \quad (3.22)$$

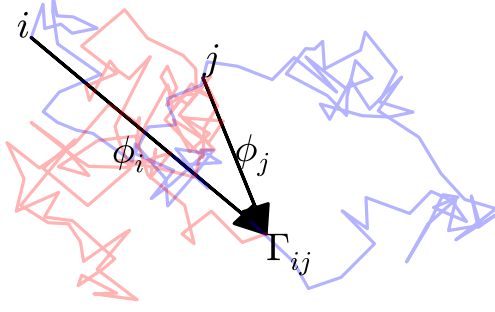


Figure 3.1: Two isotropic random walker interacting through a space and time-dependent interaction function $\Gamma(x, t)$

where we require agent i to begin its walk at time $t = t_0$ and position x_i by setting the source term to

$$J_i(x, t) \equiv \delta(t - t_0) \delta^2(x - x_i). \quad (3.23)$$

With this source, the solutions of (3.22) are in fact the retarded Green's functions $\phi_i(x, t) = G(x, t; x_i, t_0)$. In the case of 2D diffusion, this is given by

$$G(x, t_x; y, t_y) = \frac{\theta(t_x - t_y)}{4\pi(t_x - t_y)} \exp \left[-\frac{|x - y|^2}{4(t_x - t_y)} \right]. \quad (3.24)$$

Defining the operator $\mathcal{L}_{x,t} \equiv \partial_t - \nabla_x^2$ and its conjugate $\mathcal{L}_{x,t}^\dagger = -\partial_t - \nabla_x^2$ we have

$$\mathcal{L}_{x,t} G_i(x, t; y, s) = \mathcal{L}_{y,s}^\dagger G_i(x, t; y, s) \quad (3.25)$$

$$= \delta(t - s) \delta^2(x - y) \quad (3.26)$$

We assume that bonds are formed between two agents only when they meet at designated locations (coffee-shops, universities, work place, etc) in space, which we call “rendezvous points” or RP’s, characterized by a time-dependent spatial distribution $\Gamma(x, t)$. Once two agents meet at an RP, there is a small chance λ that they form a bond. Therefore, the

	$k(r, t, T)$	$\Gamma(r, t)^\dagger$	
		$k_{\max}(T-t) = 4\pi(T-t)$	$k_{\max}(T-t) = \pi c$
$\gamma = 1^*$	$\frac{\theta(T-t)}{4\pi(T-t)} e^{\frac{r^2}{4(T-t)}}$	$\delta^2(\vec{r})\delta(T-t)$	
$\gamma = 1$	$k_{\max} e^{-\frac{\pi r^2}{k_{\max}}}$	$4\pi e^{-\frac{\rho^2}{4}}$	$\frac{4(c-r^2)}{\pi c^3} e^{-\frac{r^2}{c}}$
$\gamma = 2$	$\frac{k_{\max}^2}{\pi r^2 + k_{\max}}$	$32\pi \frac{(\rho^4 + 4\rho^2 + 16)}{(\rho^2 + 4)^3}$	$4\pi \frac{c^2(c-r^2)}{(2r^2 + c)^3}$
$\gamma = 3$	$\left[\frac{k_{\max}^3}{2\pi r^2 + k_{\max}} \right]^{1/2}$	$2^{3/2}\pi \frac{(3\rho^4 + 8\rho^2 + 16)}{(\rho^2 + 2)^{5/2}}$	$4\pi \frac{c^{3/2}(c-r^2)}{(2r^2 + c)^{5/2}}$

$^\dagger(\rho \equiv \frac{r}{\sqrt{T-t}})$

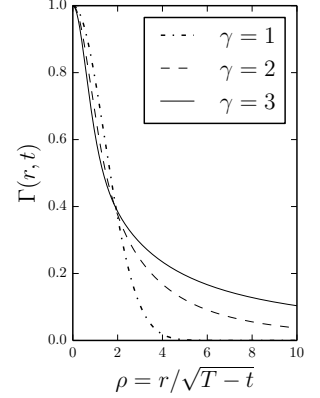


Figure 3.2: The spatial degree function $k(r, t, T)$ and RP distribution function $\Gamma(x, t)$ for various exponents in 2 spatial dimensions. The models are characterized by $k_{\max} = k_{\max}(T-t)$ taken here to be linear: $k_{\max}(s) \propto s$.

probability that agents i and j have become connected by time $T > t_0$ is given by

$$A_{ij}(t_0, T) = \lambda \int_{t_0}^T dt \int d^2x G_i(x, t; x_i, t_0) \quad (3.27)$$

$$\times \Gamma(x, t) G_j(x, t; x_j, t_0) + O(\lambda^2). \quad (3.28)$$

The A_{ij} may be interpreted either as elements of the weighted dense adjacency matrix of the network of connections, or as bond probabilities, in which case the matrix A defines an ensemble of unweighted random graphs.

3.6.1 General power-law example

We will now derive the conditions for $\Gamma(r, t)$ for which the degree distribution becomes a power-law, possibly changing over time with an overall factor $p(T-t_0)$ and with upper and lower cutoffs (which we will discuss shortly)

$$P(k; t_0, T) = p(T-t_0) k^{-\gamma}, \quad k \in [1, k_{\max}]. \quad (3.29)$$

The maximum degree k_{\max} is chosen such that the expected number of nodes of degree k_{\max} is one, i.e. $P(k_{\max}) = 1$. Therefore from (3.29)

$$k_{\max} \equiv p(T - t_0)^{1/\gamma}. \quad (3.30)$$

Now, in order to solve for $\Gamma(r, t)$, we integrate (3.55) to find $k(r, t, T)$ and plug it in (A.54). We obtain

$$\Gamma(r, t) = \mathcal{L}_{\vec{r}, t}^\dagger \left[\frac{\pi(\gamma - 1)r^2 + p(T - t)^{1/\gamma}}{p(T - t)} \right]^{\frac{1}{1-\gamma}} \quad (3.31)$$

For arbitrary $\gamma > 1$, and

$$\Gamma(r, t) = \mathcal{L}_{\vec{r}, t}^\dagger \left\{ p(T - t) \exp \left[\frac{\pi r^2}{p(T - t)} \right] \right\} \quad (3.32)$$

for $\gamma = 1$.

3.6.2 Clustering

The degree distribution is only one of many measures characterizing a graph. The simplest among higher order measures of graph connectivity is the *global clustering coefficient* C which measures the degree to which the graph is clustered [47]. Clustering may also be measured at the vertex level using the *local clustering* c_i [47] defined as the number of triangles involving node i divided by the total number of such triangles possible given the degree k_i

$$c_i \equiv \frac{\# \text{ of triangles}}{k_i(k_i - 1)} \quad (3.33)$$

By definition $c_i \leq 1$. Figure ?? (right) shows the local clustering as a function of degree for the three scale-free models we simulated.

3.6.3 Explicit Analytical Bounds for Higher Network Moments of the Interacting Random Walkers

We can use the same method we discussed before in the derivation of the recursive relation (??) and find explicit expression for the degree-degree correlation (i.e. nearestneighbor degree as a function of degree) and bounds on the clustering for the specific settings of interacting random walkers discussed above.

3.6.3.1 A^2 and degree-degree Correlation

Degree-degree correlation measures how much the degree of a node and that of its first neighbors correlate. It is intimately related to the second moment of the adjacency matrix A . Let us denote the average degree of the neighbors of node i by $\langle k_i^1 \rangle$. We have

$$\langle k_i^1 \rangle = \frac{1}{N} \sum_j A_{ij} k_j = \frac{1}{N} \sum_{jk} A_{ij} A_{jk} \quad (3.34)$$

We had defined $\mathcal{L}_{x,t} \equiv \partial_t - \nabla_x^2$ and its conjugate $\mathcal{L}_{x,t}^\dagger = -\partial_t - \nabla_x^2$. The Greens function convention was

$$\mathcal{L}_{x,t} G_i(x, t; y, s) = \mathcal{L}_{y,s}^\dagger G_i(x, t; y, s) = \delta(t - s) \delta^2(x - y) \quad (3.35)$$

For brevity let us define the infinite dimensional matrices

$$G_{xi} \equiv G(x, t_x; x_i, t_0), \quad \Gamma_{xy} \equiv \delta^n(x - y) \delta(t_x - t_y) \Gamma(x, t)$$

and their matrix products as appropriate integrals

$$O_{xy} O_{yz} \equiv \int^T dt_y \int d^n y O(x, t_x; y, t_y) O(y, t_y; z, t_z)$$

This way we can write the Adjacency matrix as

$$A_{ij}(t_0, T) = \int_{t_0}^T dt \int d^2x G_i(x, t; x_i, t_0) \quad (3.36)$$

$$\begin{aligned} & \times \Gamma(x, t) G_j(x, t; x_j, t_0) \\ & = G_{ix}^\dagger \Gamma_{xy} G_{yj} = \left[G^\dagger \Gamma G \right]_{ij} \end{aligned} \quad (3.37)$$

So in $\langle k_i^1 \rangle$ which comes from A^2 we will have a $G^\dagger G$

$$\begin{aligned} \langle k_i^1 \rangle &= \frac{1}{N} \sum_j A_{ij} k_j = \frac{1}{N} \sum_{jk} \left[G^\dagger \Gamma G \right]_{ij} \left[G^\dagger \Gamma G \right]_{jk} \\ &= \frac{1}{N} \sum_{jlyk} \left[G^\dagger \Gamma \right]_{ij} G_{jy} G_{yl}^\dagger [\Gamma G]_{lk} \end{aligned} \quad (3.38)$$

But note that in $\sum_y G_{jy} G_{yl}^\dagger$ the pint y was one of the origins of the random walkers

$$G_{jy} = G(j, t_j; y, t_0)$$

and since they all start at the same time t_0 there won't be a time integral involved in the sum over y above. This product GG^\dagger actually reduces to a single propagator (as it roughly represents two subsequent propagations). To see this explicitly note that

$$\begin{aligned} \frac{1}{t_2} (x_2 - y)^2 + \frac{1}{t_1} (x_1 - y)^2 &= \frac{1}{\tau} \left(y - \tau \left(\frac{x_2}{t_2} + \frac{x_1}{t_1} \right) \right)^2 + \frac{(x_1 - x_2)^2}{t_1 + t_2} \\ \frac{1}{\tau} &= \frac{1}{t_1} + \frac{1}{t_2}. \end{aligned} \quad (3.39)$$

Therefore

$$\begin{aligned} \sum_y G_{x_1 y} G_{y x_2}^\dagger &= \int d^n y (4\pi \Delta t_1)^{n/2} (4\pi \Delta t_1)^{n/2} \exp \left[-\frac{(x_1 - y)^2}{4\Delta t_1} - \frac{(x_2 - y)^2}{4\Delta t_2} \right] \\ &= \int d^n y (4\pi \tau)^{n/2} \exp \left[-\frac{1}{\tau} \left(y - \tau \left(\frac{x_2}{\Delta t_2} + \frac{x_1}{\Delta t_1} \right) \right)^2 \right] \\ &\quad \times (4\pi t_+)^{n/2} \exp \left[-\frac{(x_1 - x_2)^2}{t_+} \right] \end{aligned}$$

$$\begin{aligned}
&= (4\pi t_+)^{n/2} \exp \left[-\frac{(x_1 - x_2)^2}{t_+} \right] \\
&= G(x_2, t_2; x_1, 2t_0 - t_1)
\end{aligned} \tag{3.40}$$

Where $\Delta t_i = t_i - t_y$, $t_+ = \Delta t_1 + \Delta t_2$ and $\tau = (\Delta t_1^{-1} + \Delta t_2^{-1})^{-1}$. Let's call this extended propagator G_+ . Using this we can estimate $\langle k_i^1 \rangle$

$$\begin{aligned}
\langle k_i^1 \rangle &= \frac{1}{N} \sum_k \left[G^\dagger \Gamma G G^\dagger \Gamma G \right]_{ik} \\
&= \frac{1}{N} \sum_k \left[G^\dagger \Gamma G G^\dagger \Gamma \right]_{ik} \\
&= \frac{1}{N} \sum_k \left[G^\dagger \Gamma G_+ \Gamma \right]_{ik}
\end{aligned} \tag{3.41}$$

Now note that the last part on the right can be written in terms of the degree function $k(x, t; T)$. Recall that

$$k(x, t_0, T) = \lambda \int \int_{-\infty}^T dt \, d^n y G_i(y, t; x, t_0) \Gamma(y, t) \tag{3.42}$$

What we have here is

$$\begin{aligned}
\sum_y [G_+ \Gamma]_{xy} &= \int dt_y d^n y G(y, t_y; x, 2t_0 - t_x) \Gamma(y, t_y) \\
&= k(x, 2t_0 - t_x, T).
\end{aligned} \tag{3.43}$$

Putting this back into $\langle k_i^1 \rangle$

$$\begin{aligned}
\langle k_i^1 \rangle &= \frac{1}{N} \sum_k \left[G^\dagger \Gamma G_+ \Gamma \right]_{ik} \\
&= \frac{1}{N} \int^T dt \int d^n x G(x, t; x_i, t_0) \Gamma(x, t) k(x, 2t_0 - t, T) \\
&= \frac{1}{N} \int^T dt \int d^n x G(x, t; x_i, t_0)
\end{aligned}$$

$$\times k(x, 2t_0 - t, T) \mathcal{L}_{x,t}^\dagger k(x, t, T) \quad (3.44)$$

Applying $\mathcal{L}_{x,t}^\dagger$ on both sides yields $\delta(t - t_0)\delta^n(x - x_i)$ on the right and thus

$$\begin{aligned} \mathcal{L}_{x,t}^\dagger \langle k^1(x, t) \rangle &= \frac{1}{N} k(x, t, T) \mathcal{L}_{x,t}^\dagger k(x, t, T) \\ &= \frac{1}{N} \left(\mathcal{L}_{x,t}^\dagger k^2(x, t, T) + |\nabla k(x, t, T)|^2 \right) \end{aligned} \quad (3.45)$$

We can evaluate the right hand side for specific cases, such as power law

$$P[k(r)] = (k/k_{\max})^{-\gamma} = \Omega_{n-1} r^n.$$

Therefore for any γ we have

$$\nabla k = n\Omega_{n-1} r^{n-1} \left(\frac{k}{k_{\max}} \right)^\gamma \hat{r}$$

3.6.3.2 A^3 and bounds on clustering

Local clustering is usually defined as the number of triangles involving a node i , which is equal to the diagonal element $(A^3)_{ii}$, divided by total triangles that its neighbors could have formed, which is $k_i(k_i - 1)/2$. From the structure of $A = G^\dagger \Gamma G$ it is much easier to compute the total number of paths of length 3 starting from node i than just the number of such paths which close on themselves. This will yield an upper bound on the clustering because

$$\frac{k_i(k_i - 1)}{2} c(k_i) = [A^3]_{ii} \leq \sum_k [A^3]_{ik}$$

The sum $\frac{1}{N} \sum_k [A^3]_{ik}$ measures the average degree of the second neighbors of i . Therefore, we will refer to it aptly as $k_i^{(2)}$. For A^3 using the same convention as before we have

$$\begin{aligned} k_i^{(2)} &\equiv \frac{1}{N} \sum_k [A^3]_{ik} = \frac{1}{N} \sum_k [G^\dagger \Gamma G G^\dagger \Gamma G G^\dagger \Gamma G]_{ik} \\ &= \frac{1}{N} \sum_k [G^\dagger \Gamma G_+ \Gamma G_+ \Gamma]_{ik} \end{aligned} \quad (3.46)$$

We just simplified a similar expression for $k^{(1)}$. Using Eq. (3.44) we can write

$$\begin{aligned}
k_i^{(2)} &= \frac{1}{N} \left[G^\dagger \Gamma G_+ \Gamma G_+ \Gamma \right]_{ik} \\
&= \int^T dt \int d^n x G(x, t; x_i, t_0) \Gamma(x, t) k^{(1)}(x, 2t_0 - t, T) \\
&= \int^T dt \int d^n x G(x, t; x_i, t_0) k^{(1)}(x, 2t_0 - t, T) \mathcal{L}_{x,t}^\dagger k(x, t, T)
\end{aligned} \tag{3.47}$$

And similarly we have

$$\begin{aligned}
\mathcal{L}_{x,t}^\dagger k^{(2)}(x, t) &= \left[\mathcal{L}_{x,t}^\dagger \left(k^{(1)}(x, t, T) k(x, t, T) \right) \right. \\
&\quad \left. + \left(\nabla k^{(1)}(x, t, T) \right) \cdot \left(\nabla k(x, t, T) \right) \right]
\end{aligned} \tag{3.48}$$

In the same fashion we arrive at a recursive relation for average degree of m th neighbors

$$\begin{aligned}
\mathcal{L}_{x,t}^\dagger k^{(m)}(x, t, T) &= \left[\mathcal{L}_{x,t}^\dagger \left(k^{(m-1)}(x, t, T) k(x, t, T) \right) \right. \\
&\quad \left. + \left(\nabla k^{(m-1)}(x, t, T) \right) \cdot \left(\nabla k(x, t, T) \right) \right]
\end{aligned} \tag{3.49}$$

And if we define the average degree as $k^{(0)} \equiv k/N$ and $k^{(-1)} = 1$ these relations remain consistent for all non-negative powers of A .

For $\gamma = 1$ we had

$$k = k_{\max} \exp \left[-\frac{\Omega_{n-1} r^n}{k_{\max}} \right],$$

and for $\gamma > 1$

$$k = \left[\frac{(\gamma - 1) \Omega_{n-1} r^n + k_{\max}}{k_{\max}^\gamma} \right]^{\frac{1}{1-\gamma}}.$$

One can plug these into the above equation and in principle calculate the nearest neighbor degree $k^{(1)}$, or the bounds on the clustering more explicitly.

This concludes our discussion of the isotropic random walkers. In the next section we will consider a more realistic process where the stochastic agents are subject to an external potential pushing their dynamics towards its local minima.

3.7 Diffusion in Spherically Symmetric Potential with Interactions

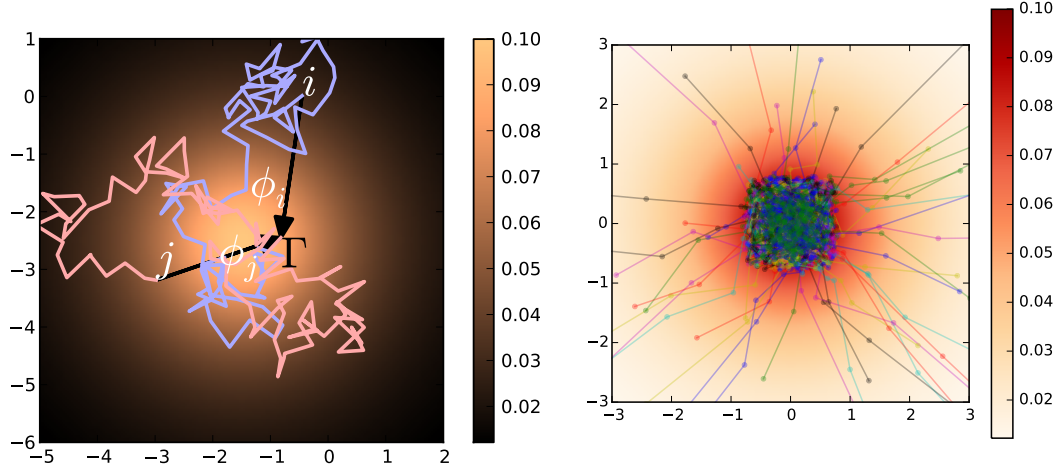


Figure 3.3: Right: Random walker in a strong harmonic potential. The walker very quickly drift toward the center of the potential. After that, since the potential is flatter there, they have a more stochastic behavior. People’s daily commute toward the center of a city may also approximately be modeled through a similar process. Left: The background potential U affects the dynamics of each random walker. But on top of this background potential, the random walker may interact with each other. As in the previous section, to lowest order this interaction will be through the “Rendezvous Point” distribution Γ similar to the distribution of businesses over the city in which people may see each other and interact.

Now we will consider dynamical agents that move in a space under the influence of a background potential $U(x)$ and a random Gaussian noise $\eta(t)$ with $\langle \eta(t)\eta(t+s) \rangle = \sigma^2 \delta(s)$ and strong friction with friction constant γ . The Langevin equation for the position of the agents is $\gamma \dot{x}(t) = -\nabla U(x) + \eta(t)$. Thus we are dealing with a Markov chain, a memory-free process. Many of the results can be extended to cases with memory and any general continuity equation, but we won’t discuss that here.

The corresponding Fokker-Planck equation can be written as (choosing units such that $\gamma/D = 1$)

$$\mathcal{L}_{x,t}\phi_i = \partial_t \phi_i - \nabla \cdot (e^{-U} \nabla (e^U \phi_i)) = J_i - \frac{\delta \mathcal{V}}{\delta \phi_i} \quad (3.50)$$

Suppose the interaction between different agents is a branching process. There are

many ways to interpret this. One is agent i split into agents j and k (like the result of gene duplication in evolution) or agent i facilitates the interaction of j and k . Such a process depends on the product of the density of all three agents, thus assuming equal chances for any interaction we get

$$\mathcal{V} \sim \sum_{ijk} \phi_i \phi_j \phi_k$$

According to (3.6) and (3.7) $\Gamma(x, t) = \sum_i \langle \phi_i(x, t) \rangle / N = \langle \phi_1 \rangle$ because to zeroth order in $1/N$ all particles have the same equilibrium distribution. $\langle \phi_i \rangle$ is like the “condensed” density of the agents and its appearance in the correlations A_{ij} is a simple case of the Higgs mechanism.

The condensed $\langle \phi_i \rangle$ has an important role in cities. Many cities that have formed around natural resources may be modeled assuming U is the attractive potential of natural resources such as rivers. The average density of the population $\langle \phi_i \rangle$ then naturally determines the density of residences and community centers over the city. Thus it is natural to assume that $\langle \phi_i \rangle$ determines the density of “rendezvous points” (RP’s) and chance of interaction.

In (3.50) the equilibrium density is easily found

$$\Gamma(x, t) \approx \langle \phi_i \rangle_T = e^{-U(x)} + O\left(\frac{1}{N}\right) \quad (3.51)$$

To use our analytical results we need to find $\overline{\mathcal{L}}$. It is easy to show that

$$\mathcal{L}^\dagger f = -\partial_t f - e^U \nabla \cdot (e^{-U} \nabla(f)) \quad (3.52)$$

Therefore we find that $\overline{\mathcal{L}}f = -e^{-U} \mathcal{L}^\dagger (e^U f)$ has the desired property of (3.16).

(3.50) has a stable equilibrium solution $\langle \phi_i \rangle = e^{-U} + O(1/N)$. Suppose that the initial distribution of locations x_i is according to this equilibrium distribution³,

$$J(r, t) = J(r) = \langle \phi_i \rangle = e^{-U}. \quad (3.53)$$

³Note that the location of an individual agent is still changing over time, but their average density is fixed.

Since $J(r)$ is fixed under the dynamics we have $\mathcal{L}J = 0$.

3.7.1 Degree Distribution in Radially Symmetric Cases

If there exists a particular spatial symmetry, like radial symmetry we have $k_i(T) = k(r_i; T)$. With this symmetry the degree distribution $P(k)$ is an implicit function of r . For $P(k)$ monotonic (possibly with cutoffs near $k = 0$ and k_{\max}), we have

$$P[k(r)]|dk(r)| = |dN(r)| \quad (3.54)$$

$$P[k(r, T)] = \left| \frac{dN}{dk} \right| = \frac{dN}{dr} \left| \frac{dk}{dr} \right|^{-1} \quad (3.55)$$

where $dN(r) = J(r)\sqrt{g}\Omega_{n-1}dr$ is the number of nodes in the annulus $[r, r+dr]$. The absolute value is necessary since dk/dr may be negative. This simple equation combined with (A.54) allows us to explicitly calculate the degree distribution given $\Gamma(x, t)$ or conversely, to solve for $\Gamma(x, t)$ given a desired degree distribution. As a simple example, with $t_0 = 0$ and a single rendezvous point activated at a single time, $\Gamma(r, t) = \delta(r)\delta(t - t_e)$, equations (3.12) and (3.55) yield

$$P[k(r)] = 4\pi t_e \theta(T - t_e) k^{-1} \quad (3.56)$$

which is a power law distribution $P(k) \propto k^{-\gamma}$ with exponent $\gamma = 1$.

counting the number of agents at radius r will yield

$$P(k)dk(r) = dN(r), \quad P(k) = \frac{dN(r)}{dk(r)}$$

This equation can be used to find the degree distribution. $dN(r) = J(r)dV(r)$, V being the volume, and so

$$P(k(r)) = \left(\frac{J(r)dV(r)/dr}{\int dy J(y) \partial_r A(r, y)} \right)$$

Let's find the degree distribution for a specific setting. Assume that the initial distri-

bution of the agents is the equilibrium distribution described above in (3.53). We have

$$k_i = G_{iy}\Gamma_{yy}G_{yx}J_x = G_{iy}\Gamma_{yy}J_y. \quad (3.57)$$

After long times agents lose any reference to the initial locations and the Green's function relaxes to the equilibrium solution

$$\text{if: } t_x \gg t_y \quad \Rightarrow \quad G_{xy} \approx \exp[-U(y)] \quad (3.58)$$

Suppose there was no space-dependence in the probability of interaction of agents i, j , meaning that $\Gamma(x, t) = 1$. Then

$$k_i = G_{iy}J_y = J_i = e^{-U(x_i)}$$

Using (3.15), the degree distribution becomes

$$P(k(r, T)) = \Omega_{n-1}r^{n-1} \left| \frac{J_r}{\partial_r J_r} \right| = \frac{\Omega_{n-1}r^{n-1}}{|\partial_r U(r)|} \quad (3.59)$$

If $U \sim r^\alpha$ we get

$$P(k) = cr^{n-\alpha} = c(-\ln k)^{\frac{n}{\alpha}-1} \quad (3.60)$$

In 2D (n=2) a hyperbolic potential $U = c\sqrt{1+r^2}$ will yield

$$\begin{aligned} \partial_r U &= \frac{cr}{U} = \frac{cr}{-\ln k} \\ P(k(r, T)) &= \frac{\pi}{c} |\ln k| \end{aligned} \quad (3.61)$$

3.7.2 Establishments and Three-Point Interactions

The density of businesses in many cities correlates with what used to be population density $J = \langle \phi_i \rangle$. Later, when a metropolitan area emerges from a city, the actual density of people

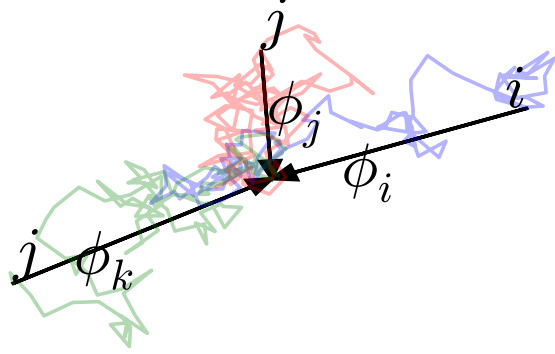


Figure 3.4: Three-point interaction of stochastic agents. If one of the agents is condensed to $\langle\phi\rangle$ this interaction will define a natural background, space-dependent interaction $\Gamma \propto \langle\phi\rangle$

at day and night varies greatly and will no longer be the old $\langle\phi\rangle$. However, a business established by i may facilitate establishing a link between j and k . This is a three point interaction $\mathcal{V} \sim \phi_i \phi_j \phi_k$. The correlation of ϕ_j and ϕ_k will then depend on $f_{ijk}^{(3)} \langle\phi_i\rangle_T$ as in (3.6). In this sense $\langle\phi_i\rangle$ represents the density of established businesses, institutions, and so on. Similarly, in the context of scientific collaboration, $\langle\phi_i\rangle$ may represent the existing body of work around a topic, which may become the source of future collaboration of j and k . Density ϕ_i represents the the spread of interest of scientist i in the spectrum of interests parametrized by \vec{x} . Thus this time

$$\Gamma(x, t) = \langle\phi_i\rangle = e^{-U}$$

According to (3.17)

$$\begin{aligned} \overline{\mathcal{L}}_{xx} k_x &= \Gamma_{xx} J_x \\ \partial_t k + \nabla \cdot (e^{-U} \nabla (e^U k)) &= e^{-U} J \end{aligned} \tag{3.62}$$

Solving this for generic J may not be easy, but if J is uniform over space and all agents start at the same time we have

$$J = \frac{N}{V} \delta(t - t_0)$$

In this case using the ansatz $k = f(t)e^{-U}$ we get

$$\overline{\mathcal{L}}k = e^{-U} \partial_t f = \frac{N}{V} \delta(t - t_0) e^{-U}$$

Thus we get

$$k(x, t) = \frac{N}{V} \theta(t - t_0) \exp[-U(x)] \quad (3.63)$$

Thus using (3.15) the degree distribution for $t > t_0$ is

$$P(k) = \frac{N\Omega_{n-1}}{V} \frac{r^{n-1}}{k \partial_r U} \quad (3.64)$$

When $U = cr^\alpha$ we get

$$P(k) \propto \frac{r^{n-\alpha}}{k} \propto \frac{(\ln k)^{\frac{n}{\alpha}-1}}{k} \quad (3.65)$$

Another example which is relevant for cities is a hyperbolic potential $U \propto \sqrt{1+r^2}$. It has the property that the force, and thus the speed of the over-damped agents approaches a constant at large distances –thus the agents have a maximum speed limit– instead of blowing up, as it does for the quadratic $U = r^2$. It also has the benefit that it becomes quadratic near the origin. For this U we have

$$P(k) \propto \frac{r^{n-2} \ln k}{k} \quad (3.66)$$

Which in 2D is a power law with a log cutoff at low degrees. The distribution of agents over this space of interest may be much more spread out than this. If the agents were spread uniformly over space and $U \sim r^\alpha$ then we'll have

$$k(r) = e^{-U}$$

$$P(k) \propto \frac{r^{n-\alpha}}{k} = \frac{(\ln k)^{\frac{n}{\alpha}-1}}{k} \quad (3.67)$$

For a hyperbolic potential $U = c\sqrt{1+r^2}$ we get

$$\begin{aligned} \partial_r U &= \frac{cr}{U} = \frac{cr}{-\ln k} \\ P(k) &\propto \frac{\pi r}{crk/U} = \frac{\pi \ln k}{c k} \end{aligned} \quad (3.68)$$

3.7.2.1 Exact Results from a Generic Case

To lowest order, a generic potential U expanded around a saddle point will be quadratic⁴ $U \sim \sum_m c_m (x - x_m)^2$ where x_m are its various local extrema. If these local minima are far enough apart, i.e. if the average densities localized at each quadratic well does not have much overlap with others, so that $\langle \phi_i \rangle \approx \sum_m \exp[-(x - x_m)^2/\sigma_m^2]$. In such generic cases and assuming $J(r) = 1$ is uniform we have

$$P(k) \propto \frac{(\ln k)^{\frac{n}{2}-1}}{k} \quad (3.69)$$

For small n such degree distributions look like a $P(k) \propto k^{-1}$ with a lower cut-off. Let us examine the higher network moments.

3.8 Real Data Analysis

We show that many networks that seem to form from local interactions indeed fit well with our model, while others, such as online networks where any person can follow anyone, have different characteristics, better described by random network models such as the Barabasi-Albert (“rich gets richer” or preferential attachment) model.

3.8.1 Co-authorship on arXiv.org: HEP Theory vs HEP Phenomenology

Structurally, the collaboration networks in High Energy Physics Theory (HET) and High Energy Physics Phenomenology (HEPPh) can be very different. In HET there are usually a few hot topics and central and seminal papers about them. Everyone checks arXiv every night and most research will be focused around big problems such as AdS/CFT or black hole mechanics or M Theory. Every researchers often switch topics, as they require similar skill sets, and it is easy to collaborate on a new topic. In HEPPh, however, people are more specialized. They generally focus on the phenomenology of a specific class of particles. A neutrino researcher, for example, may rarely collaborate with someone working with Kaon experiments. The important experiments are also clustered in the same way. Therefore it is harder for researchers to collaborate with someone in a different part of the map of research in particle physics. This makes the HEPPh co-authorship a better candidate for a network forming out of local interactions inside the abstract space of research interests in particle physics than the HET network. Below we first show that the HEPPh network can indeed be very well fitted with simulations from our model. After that we also show in Fig. 3.6 that HET has in fact a different behavior and deviates significantly from our model. HET seems more consistent with the preferential attachment model of Barabasi and Albert (BA). In the BA model all agents have global knowledge of who is more famous than others and preferentially attach to those who have more connections. This is similar to what we would expect of HET based on the fact that its researchers have a broad spectrum of skills that allows them to collaborate with whoever has written important papers, more easily than in the more localized space HEPPh.

3.8.2 Gowalla Geotagging Social Network

Gowalla was an online service where people could put pictures tagged with the geographical location it was taken. People would have a network of friends based on the places they liked,

⁴unless, of course, it is in a critical phase, where the quadratic term vanishes and higher order terms kick in.

and thus people whose posts they would like to follow. Such a network does not necessarily have local interactions, since people can follow anyone from anywhere around the world. The question that arises is if our model which is based on locality of interactions will have properties that are not consistent with the network from Gowalla. The data we have used is from Stanford’s SNAP institute. As can be seen in Fig. 3.7 these online social networks have properties different than our model. This is most visible in their higher order network moments, the degree-degree correlation and local clustering. The degree correlations show a descending trend, a property sometimes referred to as “disassortativity”. This is in stark contrast to our model’s behavior and more consistent with random network model like the preferential attachment model of Barabasi and Albert (BA) shown by green in the plots. A similar inconsistency between our model and the data is seen in the local clusterings. For comparison, the bottom row of the figure shows the C. Elegans Protein-protein Interaction network (CE), which we will briefly reexamine below. The CE network has a different behavior compared to Gowalla and is more similar to our model’s simulations.

3.8.3 Protein-Protein interactions

The results for $\gamma = 1, 2, 3$ and two different $p(t)$ are given in Fig. 3.2. Using these results, we can simulate the model by placing agents and RP’s on a finite area of the 2D space with appropriate distributions, and computing the A_{ij} . To avoid boundary effects, the characteristic range of the random walkers $\sigma = \sqrt{4T}$ must be much smaller than the system size L . For the continuum approximation to hold, σ must be much larger than the inter-agent distance L/\sqrt{N} . With proper normalization, A_{ij} may be interpreted as the probability that the unweighted edge (i, j) exists, and different realizations of the network can be constructed accordingly. Figure 3.2 summarizes the results of simulations for scale-free distributions with $\gamma = 1, 2, 3$. In each case, one realization of the unweighted random graph ensemble is generated and the degree distribution computed.

Here we compare two protein-protein interaction (PPI) networks against our model: the human PPI (HS PPI) and the C. Elegans (CE), a nematode. Protein-protein interaction

data is notoriously noisy. The systematics of the way the experiments are conducted play an important role in the results. The data we have used here comes from freely available datasets compiled by the Dana Farber Institute at Harvard Medical School. We do not wish to make any general statement about these networks and just state our observations from the analysis. The particular datasets we analyzed showed a high degree of clustering and “degree assortativity”, which is the property of high degree nodes being mostly connected to other high-degree nodes (i.e. average nearest neighbor degree $\langle k_1 \rangle$ is an ascending function of degree k). Our model shows the same properties, although it is not a perfect match for either the human PPI (HS PPI) Simulations from our model show

3.9 Discussion

Our main result is that given any (monotonic) degree distribution, we can analytically compute the RP distribution (or weight) resulting in a network with that degree distribution.

While we demonstrated the derivations in the case of power-law distributions, other monotonic distributions can also be handled similarly. Furthermore, our model is generalizable to agent dynamics other than isotropic random walks. In principle, one can solve the model for any agent dynamics with a linear Fokker-Planck equation of the form

$$\mathcal{L}_{x,t}\phi(x,t) = J(x,t) \tag{3.70}$$

where the linear operator $\mathcal{L}_{x,t}$ admits a well-defined Green’s function. Finally, the model can be solved in higher spatial dimensions as well, with similar results.

One of the major shortcomings of many scale-free network models such as Barabási-Albert (BA) is the fact that they possess a very small degree of clustering. In some real world networks, especially biological networks such as Brain and gene interaction networks, $C > 20\%$. For a BA network of 10^4 nodes C is well below 1%. There have been many attempts to remedy this by modifying the BA model (see for example [51]). Others propose models where both clustering and degree distribution are tunable [54, 56].

Our model, interestingly, has a naturally high degree of clustering because agents close to the RP's are all likely to connect and form close-knit subgraphs. Figure 3.8 illustrates how our model compares to a particular real world network, namely the network of human protein-protein interactions (PPI) compiled from the human interactome database [57], as well as a BA network of the same size as the real data. The PPI network has a power-law degree distribution with power $P(k) \approx k^{-2}$. We therefore compare it with a $\gamma = 2$ from our model. The PPI network has an average clustering of $C = 0.29$ versus our model's $C = 0.15$. For the BA network on the other hand, $C = 0.006$. The shaded area is one standard deviation and the thick curves are the means. Our model, though having on average a smaller degree of clustering than the PPI data, follows the PPI data closely and stays within one standard deviation. The BA (with the same number of nodes as PPI and with $m = 9$ to produce similar density) on the other hand, deviates significantly from the PPI data. To draw an analogy with our model, one can conceive of evolving proteins as random walkers inside a parameter space, diverging as a result of mutations from common ancestors distributed according to $\Gamma(r, t)$. The analogy is completed if one can assume that having originated from similar ancestors renders proteins more likely to interfere with one another's functions and thus to be linked in the PPI network. Establishing the viability of this analogy requires further investigation.

3.10 Cities: Businesses as “Rendezvous Point” for Interactions over Cities

Using interacting stochastic fields inside a background landscape we present a model of city formation and subsequent interactions of people through the established businesses in the city.

The process inside a background potential described in the sections before is a good candidate for modeling dynamics and interaction of people over cities. Cities usually form around resources such as water. The water source would act like an attractive potential. The movements of people could then be modeled through diffusion with a drift. They then establish residences around base of the potential well where the most resources are. This

establishment forms the city. The distribution of businesses in the city must have evolved from these initial residences that represented the equilibrium distribution of the drifting random walkers inside the potential well of resources such as water.

After the city forms, the businesses can play the role of our “Rendezvous points” Γ . People generally talk to and interact with people they meet inside businesses where they spend most of their time in. This could be the workplace, school, or cafes and bars. Figure 3.9 shows the radial distribution of businesses extracted from satellite images of night lights for Paris and Shanghai. Our model predicts that this distribution, which can be taken to be the interaction potential Γ of our model, determines the network structure. The network here would be the friendship network of people living over the city. We make a simplistic assumption and assume that population density is roughly uniform over the city. With this somewhat unrealistic assumption we can find the analytical form of Γ which would result in different degree distributions. In Fig. 3.9 we fit two different Γ 's to the city light distribution. The light distribution in Paris seems more consistent with a Γ from our model that would result in $P(k) \sim k^{-1}$ while for Shanghai there is no conclusive result. The model predicts the friendship network to have a degree distribution that may not be a power-law or one that has exponent between 1 and 2.

3.10.1 Cellphone data from Shanghai

We have data from cellphone calls that happened over Shanghai from 2010 to 2012 through our collaborators. The first three network moments are shown in Fig. 3.10. The degree distribution fits more with a log-normal distribution than a power-law. The lower degree part of it, though, can be partially fitted with a $\gamma = 1$ power-law and the upper half can be covered with a BA model. This does not mean that this is the structure of the network, but based on the observation we made in the co-authorship network we guess that there may be a preferential attachment process describing the higher degree end of the network and wish to check this. Interestingly, even this poorly fitted simulation in 2D with $\gamma = 1$ describes the degree-degree correlation and local clustering of the cellphone network very

well. These two network moments also reveal a rather abrupt shift in the properties of the network at higher degrees which make it resemble more a BA model. Thus, maybe our guess about high degree nodes having different network formation strategies than the rest of the network may be justified.

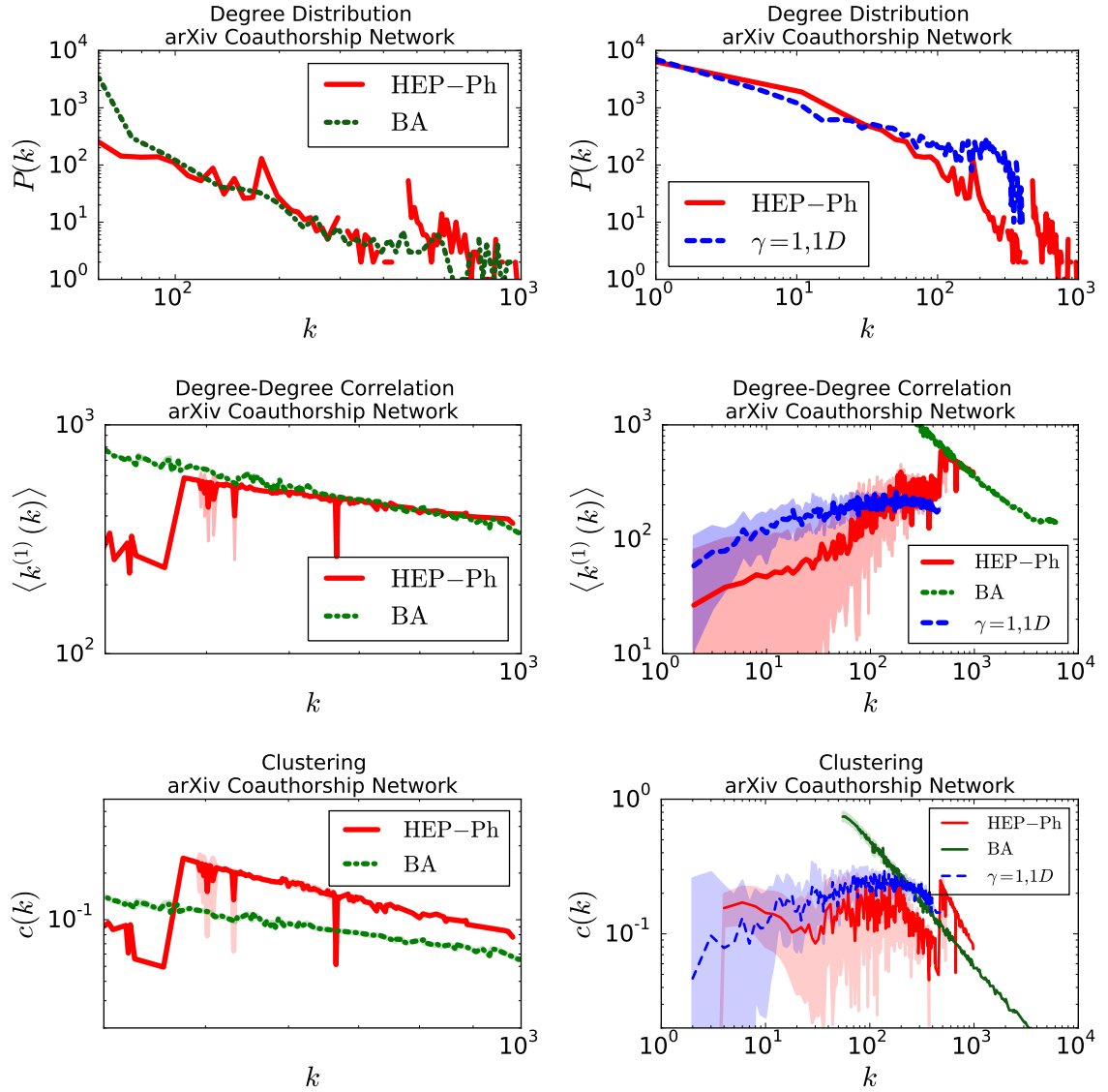


Figure 3.5: Co-authorship network of High Energy Phenomenology. The left column zooms into the high degree tail. BA denotes a Barabasi-Albert simulations. As we see the high degree tail fits very well with the BA. Right shows the full network's moments. As we see the lower degree part of the network fits very well with simulations from our model.

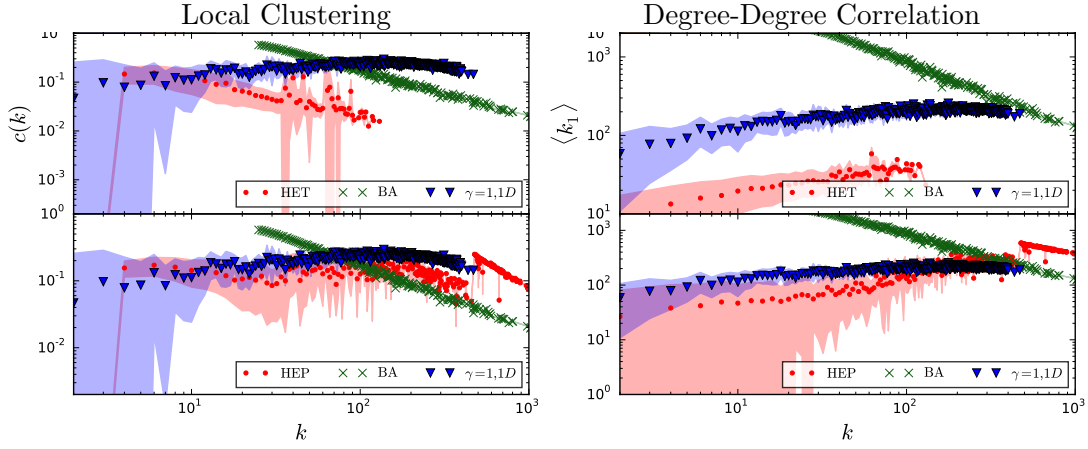


Figure 3.6: Co-authorship network of High Energy Phenomenology vs High Energy Theory. As we see they have different patterns of local clustering and degree-degree correlation. HEPPh is consistent with our model while HET is not.

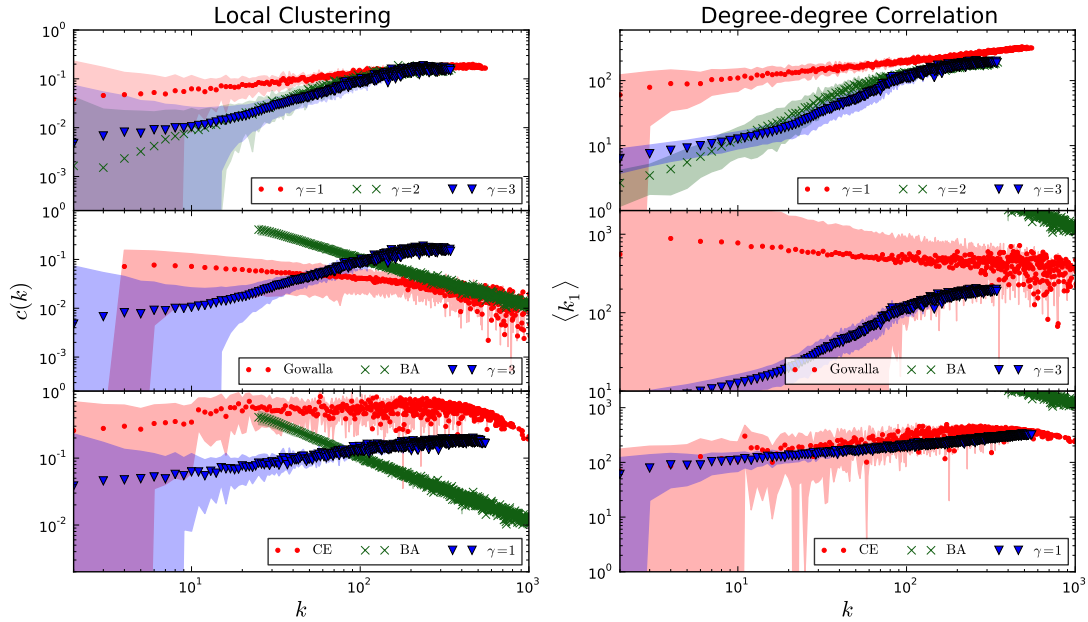


Figure 3.7: Gowalla vs C. Elegans PPI and simulations from our model. The online platform Gowalla, which is *not* formed from local interactions and is highly non-local due to the fact that anyone can find anyone else in the online system, behaves very differently from the rest. Note the descending trend in the local clustering and degree-degree correlation.

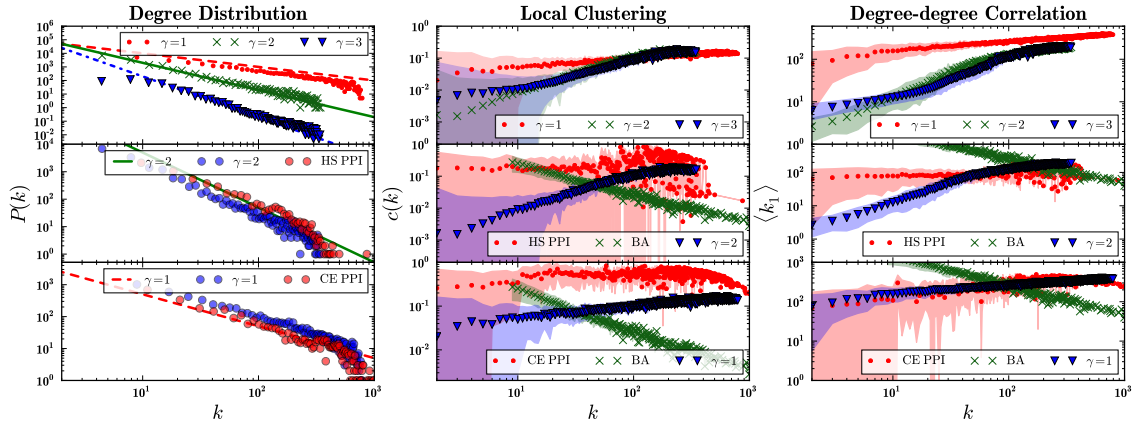


Figure 3.8: Top row: Simulations with power-law degree distributions using our model in 2D space. Degree distributions of graphs generated for power-law distributions with $\gamma = 1, 2, 3$. In the left column the dashed lines represent $k^{-\gamma}$ for $\gamma = 1, 2, 3$. Second row: Human Protein-Protein Interaction (HS PPI) network compared to a simulation with power-law $P(k) \sim k^{-\gamma}$ with $\gamma = 2$ and Barabasi-Albert (BA) model with minimum degree $m = 9$ chosen to endow it with a density similar to the PPI network, and which gives it non-zero clustering. The very high degree part of the HS PPI behaves similar to the BA model in the clustering, but for most of the network the local clustering and the degree-degree distribution is closer to a $\gamma = 1$ simulation of our model. Bottom row: PPI of the worm *C. Elegans*. It's degree-degree correlation fits very well with a $\gamma = 1$ simulation of our model, but it has higher clustering than our model.

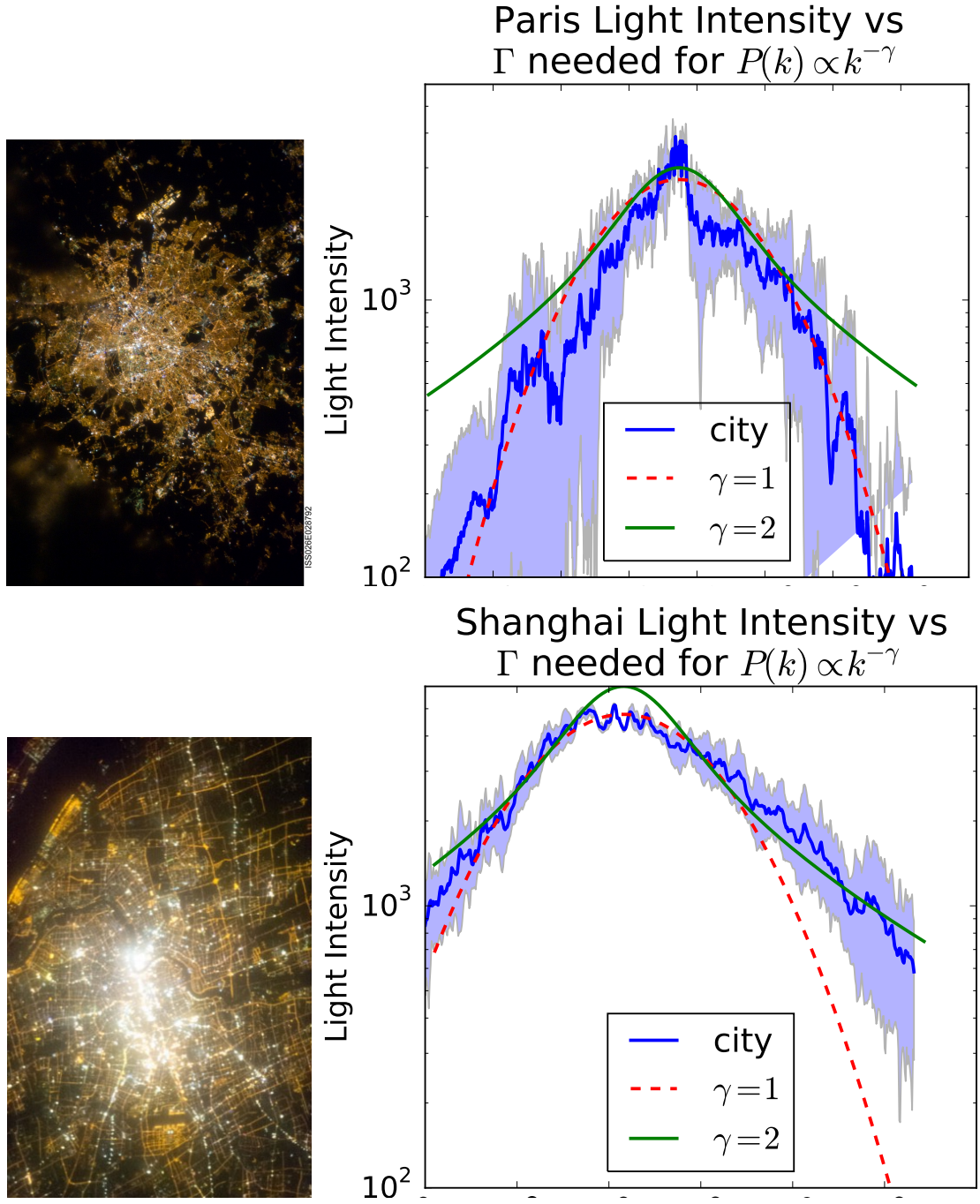


Figure 3.9: Paris and Shanghai night light satellite pictures (left) and radial distributions (right). The dashed lines in the plots on the right are “Rendezvous Point” distributions Γ which our model would predict would result in power-law degree distributions with exponents $\gamma = 1$ and 2.

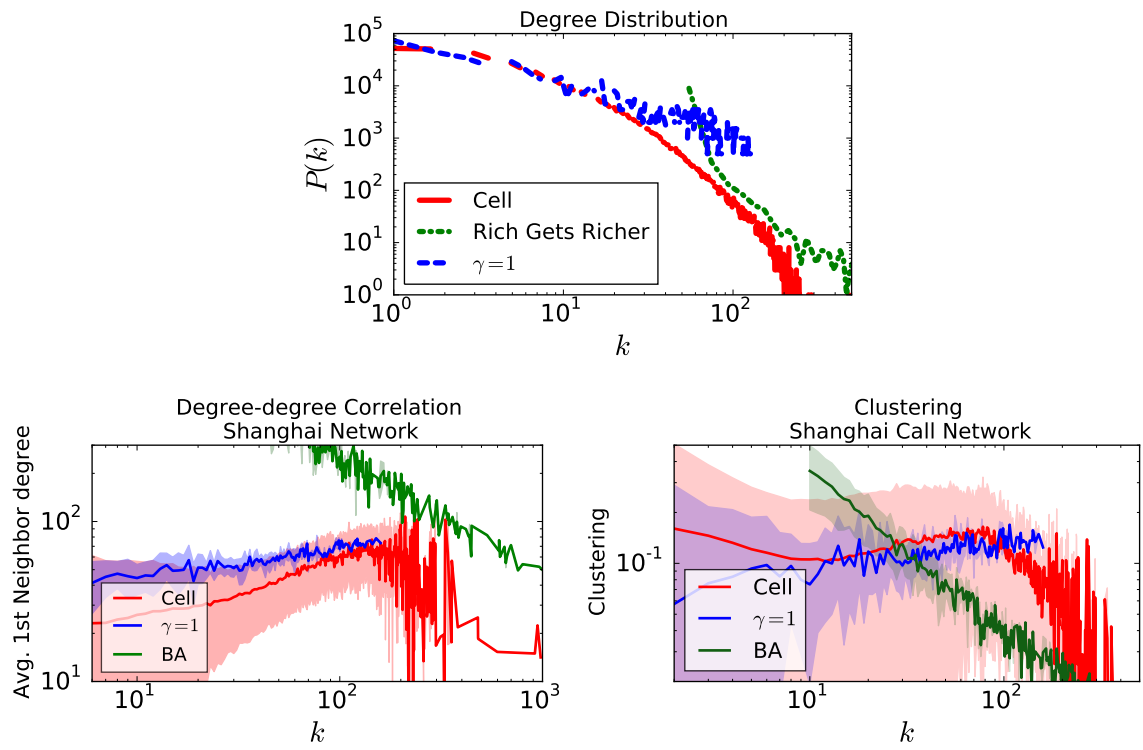


Figure 3.10: Shanghai cell phone call network against the BA model and our model's simulations.

Chapter 4

Concluding Remarks

In thesis I examined the utility of using some familiar concepts from theoretical physics in modeling the dynamics and formation of complex networks. The idea of using Lagrangians in networked systems is not new. In fact, it is a popular method in linear control theory. However, using it from a model building perspective and constructing effective linear response models for networks, to my knowledge, has not been widely studied before. This type of analysis provides a powerful method for building models for response of highly dynamical networks which also have flow redistribution taking place on them. An example would be financial networks and I demonstrated the use of this type of modeling for these systems, which yields concrete results about stability of the financial network.

In the latter half of my dissertation I described a model of network formation. The definition of the network as a correlation-based network is not a new idea. Also, networks embedded in a metric space do exist in the context of random geometric graphs. My contribution to this field was building a general framework that allows us to answer general questions such as: ‘does a network that forms out of local interactions have properties that distinguish it from non-local networks?’ as well as specific, concrete questions like: ‘if we model people over cities as stochastic agents inside a potential well and the businesses they frequent as the source of a space-dependent interaction between them, what will be the most probable friendship network that emerges among them?’. I showed that, indeed, there are analytical relations that one can derive for weakly interacting agents forming a network out of local interactions in a metric space. I also compared simulations using this framework with some networks that are mostly forming out of local interactions, either in real space,

as in friendship networks, or in an abstract space, such as spectrum of interests in different research topics. I showed that such networks are consistent with our model, while networks that may form from non-local processes show characteristics very different from our model's simulations.

Appendices

Appendix A

Lagrangian and Hamiltonian in Response Dynamics of Networks

A.0.2 Equations of motion

The Lagrangian introduced for the response of networks is complicated and has many terms. But not all of those terms play independent roles in the equation of motion. Let us simplify this Lagrangian. We start by using partial integration of the action to change the form of the a_2 and the b terms. For the b_+ term we have:

$$\begin{aligned} \int dt \Phi^T A_+ \partial_t \Phi &= \Phi^T A_+ \Phi \Big|_{t_i}^{t_f} - \int dt \Phi^T \partial_t A_+ \Phi - \int dt \partial_t \Phi^T A_+ \Phi \\ \Rightarrow 2 \int dt \Phi^T A_+ \partial_t \Phi &= \Phi^T A_+ \Phi \Big|_{t_i}^{t_f} - \int dt \Phi^T \partial_t A_+ \Phi \end{aligned} \quad (\text{A.1})$$

The first term is a boundary term and doesn't affect the equations of motion. But the other term is effectively a new time-dependent harmonic potential term for Φ . So we could successfully get rid of the single derivative A_+ term. For A_- , however, this trick will be different. Note that:

$$\int dt \partial_t \Phi^T A_- \Phi = - \int dt \Phi^T A_- \partial_t \Phi$$

Therefore the same partial integration for this term yields:

$$0 = \Phi^T A_- \Phi \Big|_{t_i}^{t_f} - \int dt \Phi^T \partial_t A_- \Phi$$

Which is trivial because both terms are automatically zero from anti-symmetry of A_- . In addition it doesn't say anything about the value of the Lagrangian term we started from.

Thus the b_- term cannot be simplified this way. The q_+ term admits the exact same procedure and the resulting Lagrangian looks like:

$$\begin{aligned}\mathcal{L} = & a \partial_t \Phi^T A_+ \partial_t \Phi + \Phi^T \left[\left(-\frac{q_+}{2} \partial_t^2 - \frac{b_+}{2} \partial_t + c \right) A_+ \right] \Phi \\ & + \Phi^T [(q_- \partial_t + b_-) A_-] \partial_t \Phi\end{aligned}\tag{A.2}$$

A.1 Hamiltonian and Stability Analysis

We wish to find out under what conditions the above theory would admit stable solutions, i.e. minimum of potential, and under which it would develop instabilities. We have too many free coefficients that may be adjusted.

A.1.1 Scaling and Simplifications

Let's first get rid of some by scaling different variables. We will absorb $|a|$ in A_+ and will assume $|A_+| \geq 0$. This way a reduces to:

$$a = \pm 1, 0$$

After this scaling, $q_{\pm}/|a|$ has dimensions t^2 . We absorb $|q_+|$ into the time scaling and thus we are left with q_-/a which we will rename to:

$$\tau^2 \equiv \frac{|q_-|}{|a|}$$

And we absorb the sign of q_-/a into $|A_-|$. The sign of q_+/a still remains, but that basically becomes the relative sign of the kinetic $\partial_t \Phi^2$ term and the $\Phi^T(\dots)A_+\Phi$ term. Thus without loss of generality we can take $a = 1, 0$ and just allow $q_+/a = \pm 1, 0$, because we don't care about the overall sign of \mathcal{L} which has to be such that it admits a minimum. If $a \neq 0$ we can take the first kinetic term to be positive. And finally, for $b_{\pm} = (b_1 \pm b_2)/2$ we can rescale $b_1 \rightarrow 2$ by absorbing it into Φ and then repeating the procedure above to get rid of the

a, q_{\pm} that seem to appear from the scaling. This way:

$$b_{\pm} = 1 \pm b$$

Thus, in the end we are left with three free parameters τ, b and c and a relative sign for the first and second term, if $q_+ \neq 0$:

$$\begin{aligned} \mathcal{L} = & \partial_t \Phi^T A_+ \partial_t \Phi + \Phi^T \left[\left(\pm \partial_t^2 - \frac{1+b}{2} \partial_t + c \right) A_+ \right] \Phi \\ & + \Phi^T \left[(\mp \tau^2 \partial_t + 1 - b) A_- \right] \partial_t \Phi \end{aligned} \quad (\text{A.3})$$

Let us also for brevity define:

$$\begin{aligned} B_+ &= \left(\pm \partial_t^2 - \frac{1+b}{2} \partial_t \right) A_+ \\ B_- &= (\mp \tau^2 \partial_t + 1 - b) A_- \\ \mathcal{L} &= \partial_t \Phi^T A_+ \partial_t \Phi + \Phi^T B_+ \Phi + \Phi^T B_- \partial_t \Phi + c \Phi^T A_+ \Phi \end{aligned} \quad (\text{A.4})$$

A.1.2 Hamiltonian

In order to analyze stability, we will need to separate the true kinetic terms (constructed from conjugate momenta) from the potential terms. Both Φ and A are dynamic variables. But they are coupled in a nonlinear fashion and rewriting the Lagrangian in terms of the conjugate momenta is a bit more complicated than quadratic theories. Let's first start from conjugate momenta:

$$\begin{aligned} \pi_{\Phi} &= \frac{\partial \mathcal{L}}{\partial \partial_t \Phi^T} = 2A_+ \partial_t \Phi + B_-^T \Phi \\ \pi_{A_+} &= \frac{\partial \mathcal{L}}{\partial \partial_t A_+} = -\frac{1+b}{2} \Phi \Phi^T \mp \Phi \partial_t \Phi^T \\ \pi_{A_-} &= \frac{\partial \mathcal{L}}{\partial \partial_t A_-} = \mp \tau^2 \Phi \partial_t \Phi^T \end{aligned} \quad (\text{A.5})$$

Let us first assume that A_+ is positive-definite, i.e. $|A_+| > 0$ instead of $|A_+| \geq 0$ (if not, we will have to work with the largest positive-definite minor of A_+) to make sure A_+^{-1} exists.

The Hamiltonian is:

$$\begin{aligned}
\mathcal{H} &= \partial_t \Phi^T \pi_\Phi + \text{Tr}[\partial_t A_+ \pi_{A_+} + \partial_t A_- \pi_{A_-}] - \mathcal{L} \\
&= \frac{1}{2}(\pi_\Phi^T - \Phi^T B_-) A_+^{-1} \pi_\Phi + \Phi^T B_+ \Phi \\
&\quad + \frac{1}{2} \Phi^T B_- A_+^{-1} (\pi_\Phi + B_- \Phi) - \mathcal{L} \\
&= \frac{1}{2} \pi_\Phi^T A_+^{-1} \pi_\Phi + \Phi^T B_+ \Phi + \frac{1}{2} \Phi^T B_- A_+^{-1} B_- \Phi - \mathcal{L}
\end{aligned} \tag{A.6}$$

We will first have to rewrite \mathcal{L} in terms of the π_i by replacing the $\partial_t \Phi$ and $\partial_t A$ terms, but since $\partial_t A$ does not appear in any of the π_i we don't need to rewrite the $\partial_t A$ terms.

$$\begin{aligned}
\mathcal{L} &= \frac{1}{4}(\pi_\Phi^T - \Phi^T B_-) A_+^{-1} (\pi_\Phi + B_- \Phi) + \Phi^T B_+ \Phi + \frac{1}{2} \Phi^T B_- A_+^{-1} (\pi_\Phi + B_- \Phi) \\
&= \frac{1}{4} \pi_\Phi^T A_+^{-1} \pi_\Phi + \Phi^T B_+ \Phi + \frac{1}{4} \Phi^T B_- A_+^{-1} B_- \Phi
\end{aligned} \tag{A.7}$$

Where we used $B_-^T = -B_-$. Putting the two together, the Hamiltonian becomes:

$$\mathcal{H} = \frac{1}{4} \pi_\Phi^T A_+^{-1} \pi_\Phi + \Phi^T \left[\frac{1}{4} B_- A_+^{-1} B_- - c A_+ \right] \Phi \tag{A.8}$$

Now we can finally see the “potential energy” terms and analyze the stability of solutions.

A.1.3 Potential and Its Minima

In general A_- (hence also B_-) and A_+ need not be related to each other at all. Moreover, B_- may not be invertible either. Even when $|B_-| \neq 0$ the potential energy is given by:

$$\begin{aligned}
\mathcal{V} &= \frac{1}{4} \Phi^T [B_- A_+^{-1} B_- - 4c A_+] \Phi = \Phi^T V \Phi \\
&= \frac{1}{4} \Phi^T B_- [C + 4c C^{-1}] \Phi \\
C &\equiv A_+^{-1} B_-
\end{aligned} \tag{A.9}$$

$V = V^T$ and invertible if $|A_+| \neq 0$ and $|B_-| \neq 0$. Where C is a general matrix has no special symmetries, unless A_+^{-1} and B_- either commute or anti-commute. So in order to understand the behavior of this potential, let us start from some special cases.

A.2 Equations of Motion

Because A only appears to first power in the Lagrangian, the variations with respect to A yield equations involving only Φ and no A 's. These equations are:

$$\begin{aligned}\frac{\delta\mathcal{L}}{\delta A_+} &= \frac{\partial\mathcal{L}}{\partial A_+} - \partial_t\pi_{A_+} = \frac{\partial\mathcal{L}}{\partial\partial_t A_+} \\ &= \partial_t\Phi\partial_t\Phi^T + c\Phi\Phi^T + \frac{1+b}{2}\Phi\Phi^T \pm \Phi\partial_t\Phi^T \\ \frac{\delta\mathcal{L}}{\delta A_-} &= \frac{\partial\mathcal{L}}{\partial A_-} - \partial_t\pi_{A_-} = (1-b)\Phi\Phi^T \pm \tau^2\Phi\partial_t\Phi^T\end{aligned}\tag{A.10}$$

A.2.1 Implications and conservation laws of the variational method for financial networks

First note that the Lagrangian $L = L_2 + L_\gamma + L_C$ for the financial network is not dissipative, i.e. the “energy” (Hamiltonian) associated with it is conserved. If L_γ was the whole Lagrangian, its Hamiltonian would have been:

$$H_\gamma = \sum_{q=E,p,A} \partial_t q \frac{\partial L_\gamma}{\partial(\partial_t q)} - L_\gamma = 0$$

Which doesn't seem to tell us anything at first. But when we include the kinetic terms L_2 and assume that there exists a potential term and use the full action:

$$S \equiv S_2 + S_\gamma + S_C - \int dt V(x, A, p; t)$$

we find that the energy gets non-zero contributions:

$$H = H_K + V$$

Where H_K is the kinetic energy found in the canonical way from the Lagrangian terms with time derivatives through first defining the conjugate momenta to each of the variables E, A, p as:

$$\pi_E \equiv \frac{\partial L}{\partial\partial_t E}, \quad \pi_A \equiv \frac{\partial L}{\partial\partial_t A}, \quad \pi_p \equiv \frac{\partial L}{\partial\partial_t p},$$

and this Hamiltonian is conserved if V is not explicitly time dependent.

A.3 Generalized Langevin and logistic equations

A.3.1 Friction terms and variation

It is well known that for Langevin equations of the form $\ddot{x} + \gamma\dot{x} = F(x)$ it is not possible to write an action whose variational minima give the Langevin equation. The point is that the Euler-Lagrange procedure keeps the number of time derivatives constant. This means that to get $\gamma\partial_t x$ term we needed to have a term like $\gamma x\partial_t x$. This term however yields:

$$L_\gamma \equiv \gamma x \partial_t x$$

$$\partial_t \frac{\partial L}{\partial(\partial_t x)} - \frac{\partial L}{\partial x} = \gamma \partial_t x - \gamma \partial_t x = 0 \quad (\text{A.11})$$

Basically there is no way to have first derivative terms like $\partial_t x$ in the equation of motion if there is only one variable. However this problem goes away if there are more than one variables and a certain group of Langevin equations with multiple variables can be obtained by the variational procedure from an action functional. For example consider the Lagrangian:

$$L(x, y) = \gamma x \partial_t y + V(x, y)$$

$$\partial_t \frac{\partial L}{\partial(\partial_t y)} - \frac{\partial L}{\partial y} = \gamma \partial_t x - \partial_y V(x, y) = 0$$

$$\partial_t \frac{\partial L}{\partial(\partial_t x)} - \frac{\partial L}{\partial x} = -\gamma \partial_t y - \partial_x V(x, y) = 0 \quad (\text{A.12})$$

So it is in fact possible to derive a Langevin-type equation for some systems of multiple variables using the Euler-Lagrange procedure. Notice, however, that γ does not mean “dissipation” or friction for the whole system here. The total energy is conserved in this system¹. To get energy loss the system must be open and one way of writing a Lagrangian

¹since there is no explicit time dependence and the Noether procedure shows that the Hamiltonian is a constant of motion. Nevertheless one of the variables could be losing energy and the other one gaining such that total energy remains fixed.

for such cases is through explicit time dependent terms. for instance:

$$\begin{aligned}
L_\lambda &\equiv e^{-\lambda t} \left\{ (\partial_t x)^2 + V(x) \right\} \\
\partial_t \frac{\partial L_\lambda}{\partial (\partial_t x)} - \frac{\partial L_\lambda}{\partial x} &= e^{-\lambda t} \left\{ \partial_t^2 x - \lambda \partial_t x + \partial_x V(x) \right\} = 0
\end{aligned}
\tag{A.13}$$

Which is a familiar 1D Langevin equation. For multiple variables, we may have a combination of L_γ (which is not “dissipative” for the whole system, just taking energy from one mode to the other) and L_λ which represents an open system. For instance:

$$\begin{aligned}
L(x, y) &= e^{-\lambda t} \left\{ \partial_t y \partial_t x + \gamma x \partial_t y + V(x, y) \right\} \\
\frac{\delta L}{\delta y} &\equiv \partial_t \frac{\partial L}{\partial (\partial_t y)} - \frac{\partial L}{\partial y} \\
\frac{\delta L}{\delta y} &= e^{-\lambda t} \left\{ \partial_t^2 x - (\lambda + \gamma) \partial_t x - \lambda \gamma x - \partial_y V \right\} = 0 \\
\frac{\delta L}{\delta x} &= e^{-\lambda t} \left\{ \partial_t^2 y - (\lambda - \gamma) \partial_t y - \partial_x V \right\} = 0
\end{aligned}
\tag{A.14}$$

This is however a very special case and most of the times it is not possible to write a simple time-dependent Lagrangian for a dissipative system².

A.4 Dynamics

We will start by motivating our system of equations by comparing it to perturbing a dynamical system that has damping (friction terms) around its equilibrium. Here we will use our assumptions about the GIIPS problem as guidelines.

First let's denote all three variable types collectively as $\Phi_I \equiv (E_i, A_{i\mu}, p_\mu)$. If the number of banks (i indices) is N_b and number of GIIPS assets (μ) is N_a , the number of ϕ_I 's is:

$$N \equiv N_b + N_b N_a + N_a = (N_a + 1)(N_b + 1) - 1$$

²Even when it is possible to do so, it generally does not add much toward understanding the problem more than the Langevin equations do. The only thing evident here is that the volume of a distribution on the classical phase space of such a system shrinks with time.

and in order to fully define the dynamics we will need N equations (one for each degree of freedom).

A.4.1 General non-linear Langevin-type action

Generalizing the argument above, for multiple variables Φ_I we may start with a term in the action which looks like:

$$L_\gamma \equiv \Phi_I \gamma^{IJ} \partial_t \Phi_J$$

The equations of motion would then be:

$$\begin{aligned} \partial_t \frac{\partial L_\gamma}{\partial(\partial_t \Phi_I)} - \frac{\partial L_\gamma}{\partial \Phi_I} &= \partial_t(\Phi_J \gamma^{JI}) - \gamma^{IJ} \partial_t \Phi_J \\ &= \gamma^{[JI]} \partial_t \Phi_J + \Phi_J \partial_t \gamma^{JI} \end{aligned} \quad (\text{A.15})$$

Where $\gamma^{[JI]} = \gamma^{JI} - \gamma^{IJ}$. In our bipartite network, assuming that there are no predefined time dependent coefficients, the term $\partial_t \gamma^{IJ}$ is nonzero only if it contains the variables E, A, p . The lowest order possible terms we can then have in the Lagrangian are then³:

$$E^T A \partial_t p, \quad (\partial_t E^T) A p, \quad E^T (\partial_t A) p$$

But since adding the total derivative term $\lambda \partial_t (E^T A p)$ doesn't change the equations of motion we can always absorb the last term into the other two terms. Thus the most general action to lowest order for this system can be written as:

$$L_\gamma = \gamma_1 \partial_t E^T A p + \gamma_2 E^T A \partial_t p$$

Where one of the two constants γ_1, γ_2 , if nonzero, can be absorbed by rescaling one of the variables E, A, p . Thus, assuming $\gamma_2 \neq 0$, and defining $\gamma \equiv -\gamma_1/\gamma_2$ the Lagrangian is just:

$$L_\gamma = \gamma \partial_t E^T A p - E^T A \partial_t p \quad (\text{A.16})$$

³Notice that we could not have terms like $E^T \partial_t E$, $\text{Tr}[A^T \partial_t A]$, $p^T \partial_t p$ because they are also total derivatives and don't appear in the equations of motion. Such terms belong to the symmetric part of γ^{IJ} .

A.5 Initial conditions for simulations

We show later below that the choice of $\tau_{A,B}$ does not affect the stability of the system and that the stability only depends on α , β and the shock. The $f_i(t)$, which are changes in the equity from what banks own outside of this network, can be thought of as external noise or driving force. We use $f_i(t)$ to shock the banks and make them go bankrupt. We shock a single bank, say bank j , at a time by reducing its equity 10% by putting $f_i(t) = -0.1E_j\delta_{ij}\delta(t)$.⁴ ⁵ Starting with $\partial_t p_\mu(-\varepsilon) = \partial_t A_{i\mu}(-\varepsilon) = 0$, plugging $\partial_t E_i$ into (2.15) and integrating over a small interval $t \in [-\varepsilon, +\varepsilon]$ yields

$$\partial_t A_{i\mu}(+\varepsilon) \approx \beta A_{i\mu}(0) \ln(1 + f_i(0)/E_i(0)) \quad (\text{A.17})$$

This and $E_i(\varepsilon) = 0.9E_i(0)$ are the initial conditions we start with. In addition, we require $E, A, p \geq 0$ during the simulations.

A.6 Initial conditions after the shock

The $f_i(t)$, which are changes in the equity from what banks own outside of this network, can be thought of as external noise or driving force. We use $f_i(t)$ to shock the banks and make them go bankrupt. We shock a single bank, say bank j , at a time by reducing its equity 10% by putting $f_i(t) = -0.1E_j\delta_{ij}\delta(t)$ (δ_{ij} is the Kronecker delta, or the identity matrix elements, and $\delta(t)$ is the Dirac distribution or impulse function). Note that the magnitude of the shock only rescales time, according to eq. (2.17) because $f_i \rightarrow \lambda f_i$ is the same as $\partial_t \rightarrow \lambda^{-1}\partial_t$ and thus $\tau_{A,B} \rightarrow \lambda\tau_{A,B}$. In short, as we show below, starting with $\partial_t p_\mu(-\varepsilon) = \partial_t A_{i\mu}(-\varepsilon) = 0$, plugging $\partial_t E_i$ into (2.15) and integrating over a small interval $t \in [-\varepsilon, +\varepsilon]$ yields:

$$\partial_t A_{i\mu}(+\varepsilon) \approx \beta A_{i\mu}(0) \ln(1 + f_i(0)/E_i(0)) \quad (\text{A.18})$$

⁴Note that the magnitude of the shock only rescales time, according to Eq. (2.17) because $f_i \rightarrow \lambda f_i$ is the same as $\partial_t \rightarrow \lambda^{-1}\partial_t$ and thus $\tau_{A,B} \rightarrow \lambda\tau_{A,B}$

⁵ δ_{ij} is the Kronecker delta, or the identity matrix elements, and $\delta(t)$ is the Dirac distribution or impulse function.

This and $E_i(\varepsilon) = 0.9E_i(0)$ are the initial conditions we start with. In addition, we require $E, A, p \geq 0$ during the simulations.

With more details, for the numerical solutions we shock one bank, say i , by imposing a 10% loss on their equity

$$\delta E_j(t=0) = f_j(0) = \tilde{f}\delta_{ij}E_j(0) = -0.1\delta_{ij}E_i(0)$$

We integrate equations (2.15)-(2.17) from shortly before the shock $t = -\epsilon$ to shortly after it, $t = +\epsilon$ and find that, if values of E, A, p are finite, then A, p will remain continuous⁶. Then, integrating (2.15) with this assumption yields

⁶In (2.17), A cannot jump to infinity, because that would make (2.16) wrong. Also, if $\partial_t p$ absorbs the $\delta(t)$, integrating (2.16) would require $A \propto \delta(t)$ again. Thus the only solution is to have E absorb the $f\delta(t)$, which means $\partial_t A, \partial_t p < \infty$ and thus A, p both remain continuous.

$$\begin{aligned}
\int_{-\epsilon}^{\epsilon} dt (\tau_B \partial_t^2 A_{i\mu} + \partial_t A_{i\mu}) &= \beta \int_{-\epsilon}^{\epsilon} dt A_{i\mu} \partial_t \ln E_i \\
\tau_B \partial_t A_{i\mu}(t) + A_{i\mu}(t) \Big|_{-\epsilon}^{\epsilon} &= \beta A_{i\mu}(0) \ln(1 + \tilde{f}) + O(\epsilon) \\
\partial_t A_{i\mu}(+\epsilon) - \partial_t A_{i\mu}(-\epsilon) &\approx \beta A_{i\mu}(0) \ln(1 + \tilde{f})
\end{aligned} \tag{A.19}$$

Which means that if we had started with $\partial_t A_{i\mu}(0) = 0$ the initial conditions can be changed to:

$$E_i(0) \rightarrow \tilde{f} E_i(0) \qquad \partial_t A_{i\mu}(0) \rightarrow \beta A_{i\mu}(0) \frac{\ln(1 + \tilde{f}_i)}{\tau_B} \tag{A.20}$$

A.7 Estimating $\gamma = \alpha\beta$

From examining the behavior of the model for different values of α and β we found that the phases are roughly a function of the product $\gamma = \alpha\beta$ and for $\alpha, \beta > 0$, the curve $\gamma = 1$ seems to be approximately where the phase transition happens. The $\gamma < 1$ phase is the one where the system reaches a new equilibrium without any of the prices collapsing to zero.

We now wish to know in which of the two phases the real GIIPS system is. We will try to estimate the value of $\gamma = \alpha\beta$ using a simplified version of the equations.

First we start by noting that the distribution of the holdings for each country is roughly log-normal, or close to a power law, which means that a handful of the institutions hold most of the debt. If we denote the top holders holding by A_μ^* for each country we may approximate:

$$A_\mu \approx c \times A_\mu^*, \quad c \sim O(1)$$

Where the constant c to correct for the contribution of other banks. For each country we will only look at this dominant bank. The first approximation is to assume:

$$\delta p_\mu(t + \tau_A) \approx \delta p_\mu(t), \quad \delta A_{i\mu}(t + \tau_B) \approx \delta A_{i\mu}(t)$$

We guess that the response time for both banks and the market are at most of the order

of a few days. For this approximation to be valid, we examine changes over the course of several months.

This allows us to write:

$$\delta A_\mu \approx \beta \sum_i \frac{\delta E_i}{E_i} A_{i\mu} \approx \beta \frac{\delta E_{(\mu)}^*}{E_{(\mu)}^*} A_\mu^*$$

Where $E_{(\mu)}^*$ denotes the equity of the dominant bank for asset μ . With this approximation, we can relate the first two equations in the following way:

$$\frac{\delta p_\mu}{p_\mu} \approx \alpha \frac{\delta A_\mu^*}{A_\mu^*} \approx \alpha \beta \frac{\delta E_{(\mu)}^*}{E_{(\mu)}^*}$$

Thus, we may be able to approximate γ with:

$$\gamma \approx \frac{\delta p_\mu / p_\mu}{\delta E_{(\mu)}^* / E_{(\mu)}^*}. \quad (\text{A.21})$$

The equity of the banks is mostly comprised of the shareholders' equity, or common stocks. These banks usually have multiple stock tickers, but there is generally one or two main stock tickers where most of the equity is. We can use the movements in these main stocks to estimate $\delta E_{(\mu)}^* / E_{(\mu)}^*$.

For this approximation we use the following formula:

$$\frac{\delta E_{(\mu)}^*}{E_{(\mu)}^*} = \frac{E_f - E_i}{(E_f + E_i)/2}$$

where E_i is the stock price at the beginning of the period and E_f is at the end of it.

A.8 Continuous Time Dynamics

Equations (2.14)–(2.12) were phenomenological and based on intuition. Here we review how transition to continuous time and derive the differential equations (2.15)–(2.17) for the model. To motivate, note that our equations are in fact not first order finite difference equations, but rather higher order. To see this note the following. We used $\delta f(t) =$

$f(t) - f(t - 1)$. If the time steps would be ε instead of 1 we would have used a finite difference derivative:

$$\delta_\varepsilon f(t) = \frac{f(t) - f(t - \varepsilon)}{\varepsilon} \quad (\text{A.22})$$

In our equations (2.14)–(2.12) the time lag is due to some natural time lag in the response of banks and market to changes that happen. Therefore, in an expression like $\delta A_{i\mu}(t + 1)$ the $t + 1$ really means $t + \tau$ where τ is some natural lag in the response of the banks to a change. The value of τ obviously depends on the unit we choose for time and data from real markets seem to suggest that, for example, the lag in response in stock markets is milliseconds. It will surely be different for a bond market or other markets where decisions would be done in meetings etc. We will assume that τ is small in the units we work with and only keep the leading orders in τ . Thus we will interpret such terms as:

$$\delta_\varepsilon f(t + \tau) \approx \tau \delta_\varepsilon^2 f(t) + \delta_\varepsilon f(t)$$

Where $\delta_\varepsilon^2 f(t)$ is a finite difference second order derivative.

A.8.1 Derivation in continuous time limit for the phenomenological model

We start by modifying equation (2.13). We first introduce an explicit time lag τ by changing $t + 1 \rightarrow t + \tau$. We then promote (2.13) to the more constrained equation below:

$$\delta p_\mu(t + 1) = \alpha \frac{\delta A_{i\mu}(t)}{A_{i\mu}(t)} p_\mu(t) \quad (\text{A.23})$$

where each bank i now satisfies this equation, instead of the sum of all banks. One equation which is derived from (A.23) but which contains less information is found by multiplying both sides by $A_{i\mu}(t)$ and summing over μ

$$A_{i\mu}(t) \delta p_\mu(t + 1) = \alpha \sum_\mu \delta A_{i\mu}(t) p_\mu(t) \quad (\text{A.24})$$

From this point on we will use a matrix notation where E and p will be columnar vectors with entries E_i and p_μ respectively, and A will be an $N_b \times N_a$ matrix with entries $A_{i\mu}$. In this notation, for example $E^T A p$ is a scalar (E^T denotes E transpose, i.e. a horizontal vector) because:

$$E^T A p = \sum_{i,\mu} E_i A_{i\mu} p_\mu$$

So (A.24) can be written as:

$$A(t) \delta p(t + \tau) = \alpha \delta A(t) p(t) \quad (\text{A.25})$$

Doing similar modifications to (2.14) and (2.12) yields:

$$E^T(t) \delta A(t + \tau) = \beta \delta E^T(t) A(t) \quad (\text{A.26})$$

$$\delta E(t) = A(t) \delta p(t) \quad (\text{A.27})$$

Note that here we have chosen the same time lag in both (A.25), which is about the market's response to trading, and (A.26) which is about how banks react. In principle these two timescales are different and we will see below how that may naturally arise. If we only keep the leading order of τ , the equations above become:

$$A (\tau \partial_t^2 p + \partial_t p) = \alpha \partial_t A p \quad (\text{A.28})$$

$$E^T (\tau \partial_t^2 A + \partial_t A) = \beta \partial_t E^T A \quad (\text{A.29})$$

$$\partial_t E = A \partial_t p \quad (\text{A.30})$$

Where now everything is at time t and there are no time terms with explicit time lags. We will see how generic these equations are in the next section.

A.9 Time-dependent Mass

When we fit a damped oscillator curve to the auto-correlation of the returns, $\partial_t P$, the fit is generally good, but there is a significant variation in the frequency of the oscillator, while

the damping life-time τ is more or less constant at about $\tau \approx 0.4$ days. We wish to extract the mass m from the Green's function. To extract the mass, according to the fitting to the damped oscillator, we have:

$$\begin{aligned} G(\Delta t) &\sim \exp[-\Delta t/(2\tau)] \cos(\omega \Delta t) \\ \omega &= \frac{1}{\Delta t} \cos^{-1} [\exp[\Delta t/(2\tau)] G(\Delta t)] \\ m &= \frac{(2\tau\omega)^2 + 1}{4\tau} \end{aligned} \quad (\text{A.31})$$

If we look at the drop after one day ($\Delta t = 1$), it should have the value:

$$\omega = \cos^{-1} [\exp[1/(2 \times 0.4)] G(1)]$$

A.10 Green's Function

Given a linear equation of the form:

$$\tau \partial_t^2 P + \partial_t P \approx F$$

We can solve for $\partial_t P$ using the Green's function:

$$\partial_t P(t) = \int dy G(t-y) F(y)$$

The Green's function can be found from inverting the operator in the equation.

$$G(t) = \int \frac{dk}{2\pi} \frac{e^{ikt}}{i\tau k + 1} = \frac{1}{\tau} \exp[-t/\tau] \approx \int dy \langle \partial_t P(t-y) \partial_t P(y) \rangle \approx \exp[-|t|/\tau] \quad (\text{A.32})$$

If we want to check if only the past values of $F(t)$ affect $\partial_t P(t)$, we need to use the “retarded Green's function” G_R . This means that if $t - y < 0$, $G_R(t - y) = 0$. Therefore, we need to include a step function into $G(t)$:

$$G_R(t) = \theta(t) G(t)$$

Using this, the lagged inner product of the prices becomes:

$$\begin{aligned}
& \int dt \partial_t P(t) \partial_t P(t + \Delta t) \\
&= \int dt dy dy' G_R(t - y) F(y) G_R(t + \Delta t - y') F(y') \\
&= \frac{1}{\tau^2} \int dt dy dy' F(y) F(y') \exp[-(2t + \Delta t - y' - y)/\tau] \theta(t - y) \theta(t + \Delta t - y') \quad (\text{A.33})
\end{aligned}$$

This integral can be broken down to two pieces: one where $y > y' - \Delta t$ and one for $y < y' - \Delta t$. redefining $t - y \rightarrow y$ we get:

$$\int dy F(y) G_R(t - y) = \int_0^\infty dy G(y) F(t - y)$$

and similarly for $t + \Delta t - y' \rightarrow y'$. Thus we have:

$$\begin{aligned}
& \int dt \partial_t P(t) \partial_t P(t + \Delta t) \\
&= \frac{1}{\tau^2} \int dt \int_0^\infty dy dy' F(t - y) F(t + \Delta t - y') e^{-(y+y')/\tau} \\
&= \frac{1}{\tau^2} \int dt \int_0^\infty dy dy' \exp[-(y + y')/\tau] F(t) F(t + \Delta t + y - y') \\
&= \frac{1}{\tau^2} \int dt \int_{-\infty}^\infty dx \int_0^\infty dy \exp[-(2y + \Delta t - x)/\tau] F(t) F(t + x) \\
&= \frac{e^{-\Delta t/\tau}}{2\tau} \int_{-\infty}^\infty dx e^{x/\tau} \int_{-\infty}^\infty dt F(t) F(t + x) \\
&= C \frac{e^{-\Delta t/\tau}}{2\tau} \quad (\text{A.34})
\end{aligned}$$

Where we defined $x = \Delta t + y - y'$ which gives $y + y' = y' - y + 2y = 2y - x + \Delta t$. The constant C is the result of the remaining integrations, but as long as it is finite and nonzero the above is suggesting that the convolution of price returns with itself should fall as an exponential. If we also normalize the convolution by dividing out $\int P^2(t) dt$ the constants $C/2\tau$ go away and only the exponential part remains.

A.11 More General Field-theory Networks

A.11.1 Solution for Harmonic Potential with Strong Friction

In the case of strong friction where $m/\gamma \rightarrow 0$ we get essentially the Smoluchowski equation

$$\partial_t \rho - D \nabla^2 \rho - \frac{1}{\gamma} \nabla \cdot (\rho \nabla V) = 0.$$

For $V = kx^2/2$ we get and inside a harmonic potential $V = kx^2/2$ we have

$$\partial_t \rho - D \nabla^2 \rho - \frac{k}{\gamma} \nabla \cdot (\vec{r} \rho) = 0 \quad (\text{A.35})$$

Since this potential has spherical symmetry we can express everything in terms of r and the $d-1$ angular coordinates θ_i . The line element has the form

$$dx^2 = dx^i dx^j g_{ij} = dr^2 + r^2 d\Omega_{d-1}^2$$

We have

$$\begin{aligned} \nabla \cdot (\nabla V \rho) &= \frac{1}{\sqrt{|g|}} \partial_i \left(\sqrt{|g|} g^{ij} \rho \partial_j V \right) \\ &= \rho r^{1-d} \partial_r \left(r^{d-1} \partial_r V \right) + \partial_r V \partial_r \rho \end{aligned} \quad (\text{A.36})$$

and there are no angular parts because $\nabla V = \partial_r V$.

A.11.2 Mapping to Curved Space

We can absorb D and γ into x, t by putting $Dt \rightarrow t$ and $\sqrt{D\gamma}x \rightarrow x$

$$\partial_t \rho - \nabla^2 \rho - \nabla \cdot (\rho \nabla V) = 0,$$

which using the usual trick

$$\rho = \exp[V] \hat{\rho}$$

becomes

$$\partial_t \rho - \nabla \cdot (e^{-V} \nabla (e^V \rho)) = 0. \quad (\text{A.37})$$

Writing this in terms of the spatial metric and the rescaled density $\hat{\rho}$ we get

$$\partial_t \hat{\rho} + \frac{1}{e^{-V} \sqrt{|g|}} \partial_i (e^{-V} \sqrt{|g|} g^{ij} \partial_j \hat{\rho}) = 0. \quad (\text{A.38})$$

In the general case, this may be a complicated equation. But in cases with spherical symmetry we have $V = V(r)$ and

$$\partial_t \hat{\rho} + e^V r^{1-d} \partial_r (e^{-V} r^{d-1} \partial_r \hat{\rho}) + r^2 g^{\theta\theta'} \partial_\theta \partial_{\theta'} \hat{\rho} = 0 \quad (\text{A.39})$$

where $g^{\theta\theta'}$ is the angular part of the metric. We can try to redefine r and absorb V into a “warping factor” for the angular part. For example, if we want a metric of the form

$$dx^2 = dz^2 + e^{2z} d\Omega_{d-1}^2 \quad (\text{A.40})$$

we have to have

$$e^{-V} r^{d-1} \partial_r = \sqrt{g} \partial_z = e^{(d-1)z} \partial_z$$

!!!! See what happens with the sign of $V \rightarrow -V$ flipped now!! Thus for $d > 1$ and positive potentials $V > 0$ with $\partial_r V \geq 0$ we get

$$\frac{\exp[(1-d)z(r)]}{d-1} = \int_r^\infty e^{-V(y)} y^{1-d} dy. \quad (\text{A.41})$$

For the harmonic potential $V = kx^2/2$ this yields

$$\begin{aligned} \frac{\exp[(1-d)z(r)]}{d-1} &= \int_r^\infty e^{-ky^2/2} y^{1-d} dy \\ &= \left(\frac{k}{2}\right)^{d/2-1} \int_{kr^2/2}^\infty e^{-x} x^{-d/2} dx \\ &= \left(\frac{k}{2}\right)^{d/2-1} \Gamma\left(1 - \frac{d}{2}, \frac{kr^2}{2}\right). \end{aligned} \quad (\text{A.42})$$

Here $\Gamma(s, x)$ denotes the incomplete gamma function which at $x \rightarrow 0$ reduces to the regular gamma function. Thus the transformation that puts the metric in the form of (A.40) is

$$z(r) = \frac{1}{1-d} \ln \left[\left(\frac{k}{2} \right)^{d/2-1} \Gamma \left(1 - \frac{d}{2}, \frac{kr^2}{2} \right) \right] \quad (\text{A.43})$$

the line element in (A.40) is the metric of the d dimensional Euclidean de Sitter space EdS_d . This shows that, save for the $\partial_t \hat{\rho}$ term, the diffusion equation in strong friction inside a harmonic potential is the equation of motion of field $\hat{\rho}$ in a Euclidean de Sitter space.

A.12 Analytical results

With this simple linear equation many network characteristics can be computed analytically. In what follows we will first prove an important relation between degrees and the RP distribution $\Gamma(x, t)$. Then we will outline the procedure which allows one to 1) Derive the degree distribution when $\Gamma(x, t)$ is given, and more importantly 2) Find $\Gamma(x, t)$ such that a desired degree distribution such as a power-law is obtained.

A.12.0.1 Degree-Degree Correlation

The sum of the degrees of the first neighbors is given by:

$$\sum_j k_i^{1j} = \sum_{l,j} A_{ij} A_{jl}$$

The average first neighbor degree is this divided by k_i .

A.12.1 Adjacency Matrix and Partition Function

The time-ordered 2-point function $\langle \phi_i^\dagger(x, 0) \phi_i(y, t) \rangle$ is the usual propagator, or Green's function for ϕ_i which yields the probability of a particle moving from point x to point y in the time interval 0 to t . But now consider $\langle \phi_i(x, t_x) \phi_j(y, t_y) \rangle$. For regular diffusion in absence of interactions this function is zero, even for $i = j$, just as it is in the case of

Schrödinger's equation. Intuitively, it measures the total joint probability of agents i, j interacting somewhere in space any time after $\max\{t_x, t_y\}$. Since in cases such as regular diffusion any i, j will eventually meet after long enough time, it is useful to evaluate such two point functions up to a time T . We will denote this by $\langle \phi_i \phi_j \rangle_T$. Based on this, it is natural to try to form a network based on these two point correlation functions. In such networks, the ensemble average of the adjacency matrix entries A_{ij} would be simply (for brevity, we will use A_{ij} for the ensemble average of the adjacency matrix entries)

$$A_{ij}(T) = A(x_i, t_i; x_j, t_j; T) \equiv \langle \phi_i \phi_j \rangle_T \quad (\text{A.44})$$

The weak interaction $\mathcal{V}(\vec{\phi}, \vec{\phi}^\dagger)$ –meaning that agents rarely interact– is what allows ϕ_i, ϕ_j to interact. Since ϕ_i are probability densities and since interaction between i, j only happens if they are both present in a neighborhood, we expect \mathcal{V} to have at least a term proportional to the product⁷ $\phi_i \phi_j$.

As an example, if the agents are subject to strong friction with negligible mass and are diffusing under the action of a random Gaussian noise $\sigma\eta(t)$ with variance σ^2 and inside a potential $U(x)$ the Langevin equation for the positions is $\gamma\dot{x}(t) = \sigma\eta(t) - \nabla U(x)$ where γ is the friction constant. The Fokker-Planck equation arising from this is

$$\partial_t \hat{\phi}_i - D \nabla^2 \hat{\phi}_i - \frac{1}{\gamma} \nabla \cdot (\hat{\phi}_i \nabla U) = 0 \quad (\text{A.45})$$

with $D = \sigma^2/\gamma$. The potential U can be absorbed into the spatial metric of the space $\hat{g}_{\mu\nu}$ to yield a new metric $g_{\mu\nu}$ such that, as shown in the appendix A.11.2,

$$\phi_i \equiv e^{\frac{U}{\gamma D}} \hat{\phi}_i, \quad \sqrt{g} \equiv e^{-\frac{U}{\gamma D}} \sqrt{\hat{g}} \quad (\text{A.46})$$

The example above does not include any interaction among different agents $i \neq j$. In order for a network to form we must have some type of interaction between agents. To discuss

⁷Weakness of interaction then also means that to first order these ϕ_i, ϕ_j are independent and thus the interaction only depends on the product of the probabilities.

interactions, it is easier to start with a Lagrangian with the Fokker-Planck equation being its classical equation of motion. For example, the equation above can be derived from the non-unitary Euclidean action⁸ of complex fields ϕ and ϕ^\dagger

$$\begin{aligned}
I = & V \int dt \sqrt{g} d^n x \left[\frac{1}{2} \left(\vec{\phi}^\dagger \partial_t \vec{\phi} - \vec{\phi} \partial_t \vec{\phi}^\dagger \right) - D \partial_\mu \vec{\phi}^\dagger \partial^\mu \vec{\phi} \right. \\
& \left. + \mathcal{V}(\vec{\phi}, \vec{\phi}^\dagger) \right] + \int dt \sqrt{g} d^n x \left(\vec{\phi} \cdot \vec{J}^\dagger + \vec{\phi}^\dagger \cdot \vec{J} \right) \\
= & \frac{V}{2} \int dt \sqrt{g} d^n x \left[\vec{\phi}^\dagger \mathcal{L}_{x,t} \vec{\phi} + \vec{\phi} \cdot \vec{J}^\dagger + \mathcal{V}(\vec{\phi}, \vec{\phi}^\dagger) \right] + h.c. \tag{A.47}
\end{aligned}$$

where μ signifies the spatial coordinates, n the number of spatial dimensions, g the determinant of the spatial metric $g_{\mu\nu}$, and $h.c.$ is the Hermitian conjugate. The factor V , the volume of the space, makes the action dimensionless. The source currents J_i, J_i^\dagger will be used to impose initial conditions for the distribution of the agents. $\mathcal{L}_{x,t}$ is the operator producing the dynamics in absence of \mathcal{V} and may in principle be more involved than the expression in the action above. We will not restrict ourselves to the one given above and work with a general $\mathcal{L}_{x,t}$. The ϕ_i will satisfy the familiar Fokker-Planck equations, while ϕ_i^\dagger satisfy the time-reversed equations⁹. The partition function is given by the Euclidean path integral

$$Z[J, J^\dagger] = \int [d\vec{\phi}] [d\vec{\phi}^\dagger] \exp [-I] \tag{A.48}$$

Note that, just like any $O(N)$ field theory, the sum over ϕ_i inside the action means that the non-interacting part of the action is N times the action of a single ϕ . So like all $O(N)$ models $1/N$ acts as \hbar and the semi-classical limit is where $N \gg 1$. Thus all of the machinery of field theory can be used for calculating n -point correlation functions. In particular we can calculate transition probabilities of various ϕ_i or ϕ_i^\dagger into each other.

⁸This action is for the strong friction limit. A generalized action may also be found for other regimes, though the form may be more involved.

⁹This is evident from the fact that $t \rightarrow -t, \vec{\phi}^\dagger \leftrightarrow \vec{\phi}$ is a symmetry of the action.

A.13 Analytical Results

The correlation function used as A_{ij} is special. As noted above, it vanishes when $\mathcal{V}(\vec{\phi}, \vec{\phi}^\dagger) = 0$. From perturbative field theory and since the regular propagators are time ordered $\langle \phi_i \phi_j^\dagger \rangle$ we see that to have nonzero probability of two agents colliding somewhere in space we will need an interaction proportional to $\phi_i^\dagger \phi_j^\dagger$. Consider the case where $(\phi_i = \phi_i(x, t))$

$$\mathcal{V}(\vec{\phi}, \vec{\phi}^\dagger) = \frac{\Gamma(x, t)}{N} \sum_{i \neq j} \left(\phi_i \phi_j + \phi_i^\dagger \phi_j^\dagger \right). \quad (\text{A.49})$$

For this interaction we can find an exact expression for A_{ij}

$$\begin{aligned} A_{ij}(T) &= \langle \phi_i \phi_j \rangle_T = \frac{\delta^2 \ln Z}{\delta J_i^\dagger \delta J_j^\dagger} \Big|_{J^\dagger \rightarrow 0} \\ &= \left(\mathcal{L}_{x,t} + \frac{\Gamma(x, t)}{N} \right)^{-1} (x_i, t_i; x_j, t_j; T) \\ &= \int dy \int^T dt \mathcal{L}^{-1}(x_i, t_i; y, t) \frac{\Gamma(y, t)}{N} \\ &\quad \times \mathcal{L}^{-1}(x_j, t_j; y, t) + O\left(\frac{1}{N^2}\right). \end{aligned} \quad (\text{A.50})$$

$\mathcal{L}^{-1}(x, t_x; y, t_y)$ is the propagator, or the Green's function of the operator $\mathcal{L}_{x,t}$

$$\mathcal{L}_{x,t} \mathcal{L}^{-1}(x, t_x; y, t_y) = \delta^n(y - x) \delta(t_y - t_x).$$

The full expansion of A_{ij} can be found in the supporting information.

The interaction (A.49) is the simplest interaction leading to nonzero A_{ij} . It is also the only possible such interaction at tree level. If we include loops, and fluctuations around a ground state, e.g. Higgs mechanism, we can have contributions from other interaction terms. We will use a cubic interaction with condensation in an example below.

The case where $\Gamma(x, t) = 1$ in (A.49) is what is known in the literature as vicious random walks [58]. They have the property that any two agents i, j annihilate each other upon meeting. The case of such random walks inside harmonic potentials has also been studied [59].

A.13.1 Degree Function

\vec{J} and \vec{J}^\dagger are the source current for the nodes and can spawn the nodes from desired locations and at desired times.

$$J_i(x, t) = \delta(x - x_i)\delta(t - t_i)$$

With slight abuse of notation, let $J(x, t) \equiv \sum_i J_i$ be the density distribution of the points x_i over space and time. The degree k_i is then a function of position and time

$$\begin{aligned} k_i(T) &= k(x_i, t_i; T) = \sum_j A_{ij}(T) \\ &= \int \sqrt{\hat{g}} d^n x dt A(x_i, t_i, x, t) J(x, t). \end{aligned} \quad (\text{A.51})$$

Note that this is a normal integral over space and time and therefore involves the normal spatial metric $\hat{g}_{\mu\nu}$ and *not* the modified $g_{\mu\nu}$. If we assume that the x_i are distributed according to the equilibrium solution of (A.45), which is $J(x, t) = \exp[-U/\gamma D]$, we retrieve the determinant of the rescaled metric $g_{\mu\nu}$ and

$$k(x_i, t_i; T) = \int \sqrt{g} d^n x dt A(x_i, t_i, x, t). \quad (\text{A.52})$$

Using $\int \sqrt{g} d^n x_j \mathcal{L}^{-1}(x, t; x_j, t_j) = 1$ for diffusion we obtain

$$\begin{aligned} k(x_i, t_i, T) &= \frac{1}{N} \int \sqrt{g} d^n x \int_{-\infty}^T dt \mathcal{L}^{-1}(x_i, t_i; x, t) \Gamma(x, t) \\ &\quad + O\left(\frac{1}{N^2}\right) \end{aligned} \quad (\text{A.53})$$

where $k(x_i, t_i, T)$ is the degree, measured at time T , of an agent starting at position x_i at time t_i . Applying $\mathcal{L}_{x_i, t_0}^\dagger$ on both sides of (A.53) thus yields the first important result

$$\mathcal{L}_{x, t}^\dagger k(x, t, T) = \lambda \theta(T - t) \Gamma(x, t) \quad (\text{A.54})$$

where $\theta(x)$ is the Heaviside step function. The significance of Eq. (A.54) is in that it relates the node degrees to the RP distribution. This allows us for instance to solve for the RP

distribution required for an arbitrary degree distribution as we now proceed to do.

Let us now focus on rotationally symmetric RP distributions $\Gamma(r, t)$.

A.14 Eurocrisis exposure data

The listed banks, insurance companies, and funds in the order of largest holders of the GIIPS holdings is given in table A.1.

	Name	Code Name	Holdings	Equity	Greece	Italy	Portugal	Spain	Ireland
0	GESPASTOR	Gespastor	3.5e+02	1.6e+03	0	0	0	3.5e+02	0
1	M&G	M&G	37	1.1e+04	0	0	37	0	0
2	UNION INVESTMENT	Union Inv.	3.4e+03	7e+02	1.6e+02	2e+03	77	1e+03	1.5e+02
3	ATTICA BANK	Attica	1.8e+02	1.5e+04	1.8e+02	0	0	0	0
4	MILANO ASSICURAZIONI	Milano Assic.	74	9.3e+02	23	0	0.71	49	2.1
5	GROUPAMA	Groupama	4.4e+02	4.3e+03	0	4.2e+02	19	0	0
6	AEGON NV	Aegon	1.1e+03	2.6e+04	2	65	9	9.8e+02	26
7	RIVERSOURCE	River Source	48	7.4e+03	48	0	0	0	0
8	AVIVA PLC	Aviva	1.1e+04	1.8e+04	1.5e+02	8.4e+03	2.3e+02	1.4e+03	7.2e+02
9	EMPORIKI BANK	Emporiki	2.9e+02	1.2e+03	2.9e+02	0	0	0	0
10	MELLON GLOBAL	Mellon	16	2.8e+04	0	0	0	0	16
11	DAIWA	Daiwa	7.1e+02	7.3e+03	0	5e+02	0	2e+02	0
12	FIDEURAM	Fideuram	2e+03	5.5e+02	0	2e+03	0	0	0
13	UNIPOL	Unipol	1.3e+04	2.5e+03	26	1.2e+04	1.5e+02	1.1e+03	2.4e+02
14	WGZ BANK AG WESTDT. GENO.	DE029	3.6e+03	1.9e+03	3.2e+02	1.4e+03	4.6e+02	1.2e+03	2.2e+02
15	JYSKE BANK	DK009	1.2e+02	1.4e+04	64	0	19	15	22
16	OESTERREICHISCHE VOLKSBANK AG	AT003	3.7e+02	4.8e+02	1.1e+02	1.5e+02	29	66	13
17	CAIXA PORTUGAL	Caixa (PT)	8.1e+03	2.4e+04	35	4.6e+02	30	7.5e+03	44
18	BLACKROCK	Blackrock	2e+03	2e+04	1.2e+02	1.1e+03	29	7.1e+02	30
19	BANK OF AMERICA	BofA	3.8e+02	1.8e+05	13	2.5e+02	5.4	83	29
20	NORDEA BANK AB (PUBL)	SE084	1.6e+02	2.6e+04	0	97	0	64	1.4
21	CAJA DE AHORROS Y M.P.	ES077	1.5e+03	-	0	0	0	1.5e+03	0
22	SELLA GESTION	Sella	6.6e+02	1.3e+02	0	6.6e+02	0	0	0
23	MITSUBISHI UFJ	Mitsubishi	1.6e+03	8.1e+04	0	9.2e+02	71	5.2e+02	62
24	UBS	UBS	1.3e+03	4.8e+04	53	6.8e+02	55	4.4e+02	42
25	OPPENHEIMER	Oppenheimer	2.4e+02	3.8e+02	15	0	0	2.2e+02	0
26	VONTOBEL	Vontobel	18	1.2e+03	18	0	0	0	0

Continued on next page

	Name	Code Name	Holdings	Equity	Greece	Italy	Portugal	Spain	Ireland
27	NOMURA		39	1.8e+04	0	0	20	0	19
28	MACKENZIE		15	3.4e+03	15	0	0	0	0
29	AGEAS		5.3e+03	7.8e+03	6.4e+02	2e+03	1e+03	1.1e+03	5.1e+02
30	DEUTSCHE POSTBANK		9.2e+02	5.7e+03	9.2e+02	0	0	0	0
31	MORGAN STANLEY		4.6e+02	5e+04	0	4.6e+02	0	0	0
32	HELVETIA HOLDING		1e+03	3.6e+03	7.6	7.2e+02	18	2.4e+02	15
33	HWANG-DBS		23	8.7e+02	23	0	0	0	0
34	ASSICURAZIONI GENERALI		1.7e+04	1.8e+04	1.3e+03	5.4e+03	3.1e+03	5.7e+03	1.7e+03
35	AMLIN PLC		15	1.6e+03	0	0	0	15	0
36	SWISS LIFE HOLDING		5.9e+02	7.5e+03	30	1.7e+02	77	1.8e+02	1.3e+02
37	PHOENIX GROUP		3.2e+02	2.8e+03	0	2.3e+02	11	76	2.2
38	PRICE T ROWE		15	2.6e+03	0	0	0	0	15
39	AXA		2.9e+04	4.9e+04	7.6e+02	1.7e+04	1.5e+03	9.4e+03	7.5e+02
40	TOKIO MARINE		56	1e+04	0	0	30	0	26
41	ROTHSCHILD		1.1e+02	6e+02	61	0	52	0	0
42	TT ELTA AEDAK		27	9.3e+02	27	0	0	0	0
43	BALOISE		7.9e+02	3.2e+03	84	2.7e+02	98	2.3e+02	1.1e+02
44	NATIXIS		3.3e+03	2.1e+04	4.3e+02	1.3e+03	3.9e+02	8.6e+02	3.9e+02
45	CREDIT AGRICOLE		1.7e+04	4.9e+04	6.6e+02	1.1e+04	1.2e+03	3.9e+03	1.6e+02
46	JULIUS BAER		1.2e+02	3.5e+03	68	0	0	0	57
47	FRANKLIN TEMPLETON		5.1e+03	9.7e+03	0	0	0	0	5.1e+03
48	NOVA LJUBLJANSKA BANKA		1.7e+02	-	20	96	15	26	15
49	STATE STREET		51	1.6e+04	0	0	27	0	24
50	ALLIANZ		3.8e+04	1e+05	6.2e+02	2.9e+04	7.5e+02	7.1e+03	4.9e+02
51	VIENNA INSURANCE		93	5e+03	21	13	0	7	52
52	BANCO POPOLARE - S.C.		1.2e+04	33	87	1.2e+04	0	2e+02	0
53	COMMERZBANK AG		2e+04	2.5e+04	3.1e+03	1.2e+04	9.9e+02	4e+03	32
54	LEGAL & GENERAL		3.8e+02	6.3e+03	1.1	3.3e+02	6.6	35	4.4
55	EFFIBANK		3e+03	2.7e+03	37	0	16	2.9e+03	0
56	INTESA SANPAOLO S.P.A		6.2e+04	6.4e+05	6.2e+02	6e+04	73	8.1e+02	1.1e+02
57	IRISH LIFE AND PERMANENT		1.9e+03	3.5e+03	0	0	0	0	1.9e+03

Continued on next page

	Name	Code Name	Holdings	Equity	Greece	Italy	Portugal	Spain	Ireland
58	HSBC HOLDINGS PLC	GB089	1.5e+04	1.3e+05	1.3e+03	9.9e+03	1e+03	2e+03	2.9e+02
59	DANSKE BANK	DK008	1.2e+03	1.3e+05	1	5.8e+02	1.1e+02	1.2e+02	4.1e+02
60	ROYAL BANK OF SCOTLAND	GB088	1e+04	9.6e+04	1.2e+03	7e+03	2.9e+02	1.5e+03	4.5e+02
61	BNP PARIBAS	FR013	4.1e+04	8.6e+04	5.2e+03	2.8e+04	2.3e+03	5e+03	6.3e+02
62	BARCLAYS PLC	GB090	2e+04	8e+04	1.9e+02	9.4e+03	1.4e+03	8.8e+03	5.3e+02
63	LLOYDS BANKING GROUP PLC	GB091	94	5.8e+04	0	32	0	62	0
64	DEUTSCHE BANK AG	DE017	1.3e+04	5.5e+04	1.8e+03	7.7e+03	1.8e+02	2.6e+03	5.3e+02
65	SOCIETE GENERALE	FR016	1.8e+04	5.1e+04	2.8e+03	8.8e+03	9e+02	4.8e+03	9.8e+02
66	BPCE	FR015	8.5e+03	4.1e+04	1.3e+03	5.4e+03	3.5e+02	1e+03	3.4e+02
67	BBVA	ES060	6.1e+04	4e+04	1.3e+02	4.2e+03	6.6e+02	5.6e+04	0
68	BANK OF VALLETTA (BOV)	MT046	24	-	10	3.9	2.8	0	7
69	BANCO BPI, SA	PT056	5.5e+03	8.2e+02	3.2e+02	9.7e+02	3.9e+03	0	2.8e+02
70	BANCO SANTANDER S.A.	ES059	5.1e+04	2.6e+04	1.8e+02	7.2e+02	3.7e+03	4.6e+04	0
71	CAIXA DE AFORROS DE GALICIA,	ES067	4.7e+03	2.3e+04	0.0022	1.6e+02	1.3e+02	4.4e+03	0
72	CAIXA D'ESTALVIS DE CATALUNYA	ES066	2.8e+03	2.3e+04	0	0	0	2.8e+03	0
73	CAJA DE AHORROS Y PENSIONES	ES062	3.7e+04	2.2e+04	0	1.3e+03	26	3.5e+04	0
74	KBC BANK	BE005	7.9e+03	1.7e+04	4.4e+02	5.6e+03	1.6e+02	1.4e+03	2.7e+02
75	ERSTE BANK GROUP (EBG)	AT001	1.2e+03	1.5e+04	3.5e+02	6e+02	1e+02	1.4e+02	40
76	JP MORGAN	JPM	17	1.5e+05	0	0	17	0	0
77	BAYERISCHE LANDESBANK	DE021	1.3e+03	1.4e+04	1.5e+02	5.1e+02	1.1e-05	6.6e+02	20
78	BFA-BANKIA	ES061	2.5e+04	1.2e+04	55	0	0	2.5e+04	0
79	SNS BANK NV	NL050	1e+03	5.4e+03	47	7.6e+02	0	57	1.6e+02
80	RAIFFEISEN BANK (RBI)	AT002	4.6e+02	1.1e+04	1.7	4.5e+02	2.1	3.5	0.00016
81	DZ BANK AG DT.	DE020	8.7e+03	1.1e+04	7.3e+02	2.7e+03	1e+03	4.2e+03	51
82	F VAN LANSCHOT	Lanschot	18	7.4e+02	0	0	0	0	18
83	ALLIED IRISH BANKS PLC	IE037	6.5e+03	1.4e+04	40	8.2e+02	2.4e+02	3.3e+02	5e+03
84	SKANDINAVISKA ENSKILDA BANKEN	SE085	6.3e+02	1.2e+04	1.2e+02	2.9e+02	1.3e+02	86	0
85	IBERCAJA	Ibercaja	9.6e+02	2.7e+03	0	0	0	9.6e+02	0
86	LANDESBANK BADEN-WURT...	DE019	2.8e+03	9.5e+03	7.8e+02	1.4e+03	95	5.4e+02	0
87	BANCO POPULAR ESPANOL, S.A.	ES064	9.7e+03	9.1e+03	0	2.1e+02	6.4e+02	8.9e+03	0
88	CAJA ESP. DE INVER. SALAMANCA	ES070	7.6e+03	-	0	0	27	7.6e+03	0

Continued on next page

Name	Code Name	Holdings	Equity	Greece	Italy	Portugal	Spain	Ireland
89 NORDDEUTSCHE LANDESBANK	DE022	2.8e+03	6.5e+03	1.5e+02	1.9e+03	2.6e+02	5e+02	41
90 BANCA MARCH, S.A.	ES079	1.5e+02	6.5e+03	0	0	0	1.5e+02	0
91 OP-POHJOLA GROUP	FI012	43	6.2e+03	3.1	0.36	0.00093	0.07	40
92 BANCO COMERCIAL PORTUGUES,	PT054	7.4e+03	4.4e+03	7.3e+02	50	6.5e+03	0	2.1e+02
93 BANCO DE SABADELL, S.A.	ES065	7.4e+03	5.9e+03	0	0	91	7.3e+03	38
94 HYPO REAL ESTATE HOLDING AG,	DE023	1.1e+04	-	0	7.1e+03	4.9e+02	3.4e+03	44
95 FRANKLIN ADVISERS INC	Franklin Adv.	3.6e+02	4.7e+02	0	0	0	0	3.6e+02
96 ABN AMRO BANK NV	NL049	1.5e+03	2.8e+02	0	1.3e+03	0	1.1e+02	1.3e+02
97 MUENCHENER RV	Munich RV	8.2e+03	2.3e+04	5.8e+02	3.6e+03	4.2e+02	1.9e+03	1.8e+03
98 HSH NORDBANK AG, HAMBURG	DE025	1e+03	4.8e+03	1e+02	6.6e+02	62	1.8e+02	0
99 GRUPO BANCA CIVICA	ES071	4.8e+03	-	5.4	0	0	4.7e+03	0
100 CAIXA GERAL DE DEPOSITOS, SA	PT053	6.8e+03	5.3e+03	51	0	6.5e+03	2e+02	23
101 CAJA DE AHORROS DEL MEDITER...	ES083	5.6e+03	3.8e+03	0	20	4.8	5.6e+03	15
102 GRUPO BMN	ES068	3.7e+03	-	0	0	88	3.6e+03	0
103 BANK OF IRELAND	IE038	5.6e+03	1e+04	0	30	0	0	5.6e+03
104 DEKABANK	DE028	6e+02	3.3e+03	87	2.7e+02	32	1.8e+02	30
105 DEXIA	BE004	2.3e+04	3.3e+03	3.5e+03	1.6e+04	1.9e+03	1.5e+03	0.34
106 GRUPO BBK	ES075	3.1e+03	-	0	0	3	3.1e+03	4
107 BANKINTER, S.A.	ES069	3.6e+03	3.1e+03	0	1.2	0	3.6e+03	0
108 WESTLB AG, DUSSELDORF	DE024	2.2e+03	3e+03	3.4e+02	1.1e+03	0	7.5e+02	35
109 UNIONE DI BANCHE ITALIANE SCPA	IT044	1.1e+04	1.1e+04	25	1.1e+04	0	0	0
110 CAJA DE AHORROS Y M.P.	ES072	3.3e+03	2.7e+03	0	3.8e+02	0	2.9e+03	0
111 CAIXA D'ESTALVIS UNIO DE CAIXES	ES076	2.6e+03	-	0	11	0	2.6e+03	13
112 BANK OF CYPRUS PUBLIC CO	CY007	2.8e+03	2.4e+03	2.4e+03	36	0	58	3.2e+02
113 LANDESBANK BERLIN AG	DE027	1.1e+03	2.3e+03	4.5e+02	3.3e+02	0	3.7e+02	0.075
114 ALPHA BANK	GR032	5.5e+03	2e+03	5.5e+03	0	0	0	0
115 UNICREDIT S.P.A	IT041	5.2e+04	9.3e+05	6.7e+02	4.9e+04	94	1.9e+03	58
116 MARFIN POPULAR BANK PUBLIC CO	CY006	3.4e+03	1.7e+03	3.4e+03	0	0	0	39
117 BANCO PASTOR, S.A.	ES074	2.6e+03	1.6e+03	41	1e+02	1.2e+02	2.3e+03	0
118 GRUPO CAJAS	ES078	1.5e+03	-	0	0	0	1.5e+03	8.4
119 TT HELLENIC POSTBANK S.A.	GR035	5.3e+03	9.3e+02	5.3e+03	0	0	0	0

Continued on next page

	Name	Code Name	Holdings	Equity	Greece	Italy	Portugal	Spain	Ireland
120	EFG EUROBANK ERGASIAS S.A.	GR030	8.9e+03	8.8e+02	8.8e+03	1e+02	0	0	0
121	ESPIRITO SANTO GROUP,	PT055	3.1e+03	6.2e+03	3.1e+02	0	2.7e+03	55	0
122	AGRICULTURAL BANK OF GREECE	GR034	7.9e+03	7.5e+02	7.9e+03	0	0	0	0
123	CAJA DE AHORROS DE VITORIA	ES080	6e+02	-	0	0	0	6e+02	0
124	ING BANK NV	NL047	1.1e+04	3.5e+04	7.5e+02	7.7e+03	7.6e+02	1.9e+03	92
125	RABOBANK NEDERLAND	NL048	1.1e+03	-	3.8e+02	4.4e+02	82	1.6e+02	60
126	WUERTTTEMBERGISCHE LV	Wuertter. LV	7.7e+02	1.2e+02	85	4.5e+02	52	1.8e+02	8
127	NYKREDIT	DK011	1.1e+02	-	22	88	0	0	0
128	MONTE DE PIEDAD Y CAJA	ES073	3.3e+03	58	6	3.1e+02	0	2.9e+03	0
129	CAJA DE AHORROS Y M.P.	ES081	6	58	0	0	0	6	0
130	BANCA MONTE DEI PASCHI DI	IT042	3.3e+04	1.9e+03	8.1	3.2e+04	2e+02	2.8e+02	0
131	COLONYA - CAIXA D'ESTALVIS DE	ES082	26	-	0	0	0	26	0
132	BANQUE ET CAISSE D'EPARGNE DE	LU045	2.8e+03	2.9e+03	85	2.4e+03	1.8e+02	1.7e+02	0
133	PIRAEUS BANK GROUP	GR033	8.2e+03	-1.9e+03	8.2e+03	0	0	0	0
134	NATIONAL BANK OF GREECE	GR031	1.9e+04	-4.3e+03	1.9e+04	0	0	0	18
135	ZURICH FINANCIAL	Zurich	8.7e+03	2.5e+04	0	4.2e+03	3.7e+02	3.7e+03	3.7e+02
136	MITSUI	Mitsui	6.4e+02	6.9e+04	0	3.7e+02	25	1.7e+02	76

Table A.1: GIIPS debt data used in the analysis. All numbers are in million Euros. Our data is based on two sources: 1) The EBA 2011 stress test data, which only includes exposure of European banks and funds (these are the ones where the “Code Name” is of the form CC123); 2) A list of top 50 global banks, insurance companies and funds with largest exposures to GIIPS debt by end of 2011 provided by S. Battiston et al. (These have a name as their “Code Name”), which was consolidated by us.

Bibliography

- [1] Mark Newman. *Networks: an introduction*. Oxford University Press, 2010.
- [2] Caroline H Ko and Joseph S Takahashi. Molecular components of the mammalian circadian clock. *Human molecular genetics*, 15(suppl 2):R271–R277, 2006.
- [3] Mark EJ Newman. Detecting community structure in networks. *The European Physical Journal B-Condensed Matter and Complex Systems*, 38(2):321–330, 2004.
- [4] Raj Rao Nadakuditi and Mark EJ Newman. Graph spectra and the detectability of community structure in networks. *Physical review letters*, 108(18):188701, 2012.
- [5] Mark EJ Newman. Modularity and community structure in networks. *Proceedings of the National Academy of Sciences*, 103(23):8577–8582, 2006.
- [6] Florent Krzakala, Cristopher Moore, Elchanan Mossel, Joe Neeman, Allan Sly, Lenka Zdeborová, and Pan Zhang. Spectral redemption in clustering sparse networks. *Proceedings of the National Academy of Sciences*, 110(52):20935–20940, 2013.
- [7] Sary Levy Carciente, Dror Y Kenett, Adam Avakian, H Eugene Stanley, and Shlomo Havlin. Dynamical macro-prudential stress testing using network theory. *Available at SSRN 2482742*, 2014.
- [8] Petter Holme. Modern temporal network theory: a colloquium. *The European Physical Journal B*, 88(9):1–30, 2015.
- [9] Petter Holme and Jari Saramäki. Temporal networks. *Physics reports*, 519(3):97–125, 2012.
- [10] Petter Holme and Jari Saramäki. *Temporal networks*. Springer, 2013.

- [11] Ricardo Riaza. Some qualitative problems in network dynamics. *arXiv preprint arXiv:1501.01904*, 2015.
- [12] Soon-Jo Chung and Jean-Jacques E Slotine. Cooperative robot control and concurrent synchronization of lagrangian systems. *Robotics, IEEE Transactions on*, 25(3):686–700, 2009.
- [13] Gregory C Chow. Dynamic economics: optimization by the lagrange method. *OUP Catalogue*, 1997.
- [14] Jonathan E Ingersoll. *Theory of financial decision making*, volume 3. Rowman & Littlefield, 1987.
- [15] F. Allen, , and D. (2000). Gale. Financial contagion. *Journal of political economy*, 108(1), 1-33.
- [16] F. Allen, , and D. (2007). Gale. Systemic risk and regulation. in the risks of financial institutions. (pp. 341-376). *University of Chicago Press*.
- [17] C. H. Furfine. Interbank exposures: quantifying the risk of contagion. *Journal of Money, Credit and Banking* 35, 111-128 (2003).
- [18] S. Wells. Uk interbank exposures: systemic risk implications. *Bank of England Financial Stability Review December*, 175-182 (2002).
- [19] C. Upper and A. Worms. Estimating bilateral exposures in the german interbank market: is there a danger of contagion? *European Economic Review* 48, 827-49 (2004).
- [20] H. Elsinger, A. Lehar, and M. Summer. Risk assessment for banking systems. *Management Science* 52, 1301 (2006).
- [21] E. Nier, J. Yang, T. Yorulmazer, and A. Alentorn. Network models and financial stability. *J. Econ. Dyn. Control* 31, 2033 (2007).

- [22] R. Cifuentes, G. Ferrucci, and H. S. Shin. Liquidity risk and contagion. *Journal of the European Economic Association* 3, 556 (2005).
- [23] A. G. Haldane and R. M. May. Systemic risk in banking ecosystems. *Nature* 469, 351-355 (2011).
- [24] Rodríguez-Moreno M., Peña J. I., Journal of Banking Systemic risk measures: The simpler the better?, and Issue 6 June 2013 Pages 1817-1831 Finance, Volume 37.
- [25] N. Johnson and T. Lux. Financial systems: Ecology and economics. *Nature* 469, 302-303 (2011).
- [26] F. et al. Schweitzer. Economic networks: the new challenges. *Science* 325, 422-425 (2012).
- [27] Watts D. A simple model of global cascades on random networks. *PNAS*, no. 99, pp. 5766-5771, 2002.
- [28] S. V. Buldyrev, R. Parshani, G. Paul, H. E. Stanley, , and S. (2010). Havlin. Catastrophic cascade of failures in interdependent networks. *Nature*, 464(7291), 1025-1028.
- [29] S. Levy Carciente, D. Y. Kenett, A. Avakian, H. E. Stanley, and S. and Havlin. Dynamical macro-prudential stress testing using network theory. (August 18, 2014). Available at SSRN: <http://ssrn.com/abstract=2482742>.
- [30] Ranking the Economic Importance of Countries, W. Industries Li, D. Y. Kenett, K. Yamasaki, Stanley H. E., and S. and Havlin. Ranking the economic importance of countries and industries. <http://arxiv.org/abs/1408.0443>.
- [31] Puliga M. Kaushik R. Tasca P. Battiston, S., , and G. Caldarelli. Debt-rank: Too central to fail? financial networks, the fed and systemic risk. , *Nature, Scientific Reports*, Published 02 August 2012.
- [32] P.R. Lane. The european sovereign debt crisis. *The Journal of Economic Perspectives*, Vol. 26, No. 3, Pages: 49-67 Published: Summer 2012.

- [33] Fujiwara Y. Aoyama H., Battiston S. Debt-rank analysis of the Japanese credit network. *RIETI Discussion Paper Series 13-E-087, October 2013*.
- [34] Vodenska I. Havlin S. Stanley H.E. Huang, X. Cascading failures in bi-partite graphs: Model for systemic risk propagation. , *Nature, Scientific Reports, Published 05 February 2013*.
- [35] Shrestha M. Caccioli, F., C. Moore, , and J. D. Farmer. Stability analysis of financial contagion due to overlapping portfolios.
- [36] I. Tsatskis. Systemic losses in banking networks: indirect interaction of nodes via asset prices. *arXiv, 1203.6778v1 (2012)*.
- [37] G. Halaaj, , and C. Kok. Assessing interbank contagion using simulated networks. *Computational Management Science (2013): 1-30*.
- [38] S. Battiston, D. Delli Gatti, M. Gallegati, B. Greenwald, , and J. E. (2012). Liasons dangereuses: Stiglitz. Increasing connectivity, risk sharing, and systemic risk. *Journal of Economic Dynamics and Control 36(8) (2012): 1121-1141*.
- [39] G. Halaaj, , and C. (2013). Kok. Modeling emergence of the interbank networks. *ECB Working Paper, forthcoming*.
- [40] M. Montagna, , and C. (2013) Kok. Multi-layered interbank model for assessing systemic risk. *No. 1873. Kiel Working Paper*.
- [41] S. Battiston, D. D. Gatti, M. Gallegati, B. Greenwald, , and J. E. (2012). Stiglitz. Default cascades: When does risk diversification increase stability? *Journal of Financial Stability, 8(3), 138-149*.
- [42] Andrew W Lo and A Craig MacKinlay. An econometric analysis of nonsynchronous trading. *Journal of Econometrics, 45(1):181–211, 1990*.
- [43] Duncan J Watts and Steven H Strogatz. Collective dynamics of 'small-world' networks. *Nature, 393:440–442, 1998*.

- [44] Albert-László Barabási and Réka Albert. Emergence of scaling in random networks. *science*, 286(5439):509–512, 1999.
- [45] Gautier Krings, Francesco Calabrese, Carlo Ratti, and Vincent D Blondel. Urban gravity: a model for inter-city telecommunication flows. *Journal of Statistical Mechanics: Theory and Experiment*, 2009(07):L07003, 2009.
- [46] J Sylvan Katz. Geographical proximity and scientific collaboration. *Scientometrics*, 31(1):31–43, 1994.
- [47] Mark EJ Newman. The structure and function of complex networks. *SIAM review*, 45(2):167–256, 2003.
- [48] Reuven Cohen and Shlomo Havlin. Scale-free networks are ultrasmall. *Physical Review Letters*, 90:058701, Feb 2003.
- [49] Victor M Eguiluz, Dante R Chialvo, Guillermo A Cecchi, Marwan Baliki, and A Vania Apkarian. Scale-free brain functional networks. *Physical review letters*, 94(1):018102, 2005.
- [50] P. L. Krapivsky and S. Redner. Organization of growing random networks. *Physical Review E*, 63(6):066123, May 2001.
- [51] Petter Holme and Beom Jun Kim. Growing scale-free networks with tunable clustering. *Physical review E*, 65(2):026107, 2002.
- [52] S. N. Dorogovtsev and J. F. F. Mendes. Evolution of networks with aging of sites. *Physical Review E*, 62(2):1842–1845, August 2000.
- [53] Konstantin Klemm and Víctor M. Eguíluz. Highly clustered scale-free networks. *Physical Review E*, 65(3):036123, February 2002.
- [54] Erik Volz. Random networks with tunable degree distribution and clustering. *Physical Review E*, 70(5):056115, 2004.

- [55] Robin IM Dunbar. Neocortex size as a constraint on group size in primates. *Journal of Human Evolution*, 22(6):469–493, 1992.
- [56] M Angeles Serrano and Marián Boguná. Tuning clustering in random networks with arbitrary degree distributions. *Physical Review E*, 72(3):036133, 2005.
- [57] Barabasi, A.L. Ghiassian, S., Menche, J. A disease module detection (diamond) algorithm derived from a systematic analysis of connectivity patterns of disease proteins in the human interactome, 2014.
- [58] Michael E Fisher. Walks, walls, wetting, and melting. *Journal of Statistical Physics*, 34(5-6):667–729, 1984.
- [59] Karen Winkler and Supervisor Bray (Prof). *Vicious walkers in one-body potentials*. University of Manchester, 2004.

Curriculum Vitae

NIMA DEHMAMY

Room 255, 590 Commonwealth Ave. Boston, MA 02215

+1 (617) 353-8051

nimadt@bu.edu

EDUCATION

PHD STUDENT IN PHYSICS

Boston University,

advisor: H. Eugene Stanley (01/2013–) GPA: 3.75/4 JAN 2009 – SEP 2015

MASTERS IN PHYSICS

Sharif University of Technology,

advisor: Shahin Rohani GPA: 17/20 AUG 2008

Bachelor in Physics Sharif University

of Technology GPA: 18/20 AUG 2006

HONORS AND AWARDS

- “Extraordinary Achievement in Teaching” award BU Physics 2011
- As “Exceptional Talent” admitted to Masters program in physics at Sharif University of Technology FALL 2006
- Ranked top 1% among over 30,000 in the national Physics, Mathematics 2000 AND 2001
and Computer Science Olympiads in Iran

PUBLICATIONS

1. *Arbitrary degree distribution and high clustering from a local geometric network growth model* 2015

Nima Dehmamy, Navid Dianati (equal contribution) arXiv:1501.03543 (under review at PRL)

2. *Classical mechanics of economic networks* 2014

Nima Dehmamy, Sergey Buldyrev, Shlomo Havlin, H. Eugene Stanley and Irena Vodenska.

arXiv:1410.0104 (under review PNAS)

3. *On the universality of inner black hole mechanics and higher curvature gravity* 2013

Alejandra Castro, Nima Dehmami, Gaston Giribet, David Kastor. JHEP 1307 2013 164

arXiv:1304.1696 [hep-th]

4. *Symmetries and Index theorems on Graphene*, Master's thesis. 2008

5. *From Quantum Commutators to Poisson Brackets* 2006

Published in the physics department journal, Tekaaneh and refereed by Dr. M. Sa'adat.

6. *From quantum to semiclassical Hamilton-Jacobi perturbation theory* 2006

MANUSCRIPTS IN PREPARATION

1. *City Structure Affects Friendship Networks*

Nima Dehmamy, Navid Dianati, Asher Mullokandov, Zhi-Qiang Jiang, H Eugene Stanley, Shlomo Havlin

2. *Modeling Networks of Local Interaction through Field Theory*

Nima Dehmamy, Navid Dianati, Asher Mullokandov

3. *Stock Market and News Linear Response*

Nima Dehmamy, Asher Mullokandov, Irena Vodenska, Sergey Buldyrev, Igor Mozetic, Petra Kralj

4. *Landau-Ginzburg Model of Network Response and Phase Transitions*

Nima Dehmamy

CONFERENCES, PRESENTATIONS, POSTERS AND SUMMER SCHOOLS

PRESENTATIONS

- *Properties of Networks of Local Interaction*

CCS2015

SEP 2015
- *Empirically validated model of stock return dynamics*

CCS2015

SEP 2015
- *A Systemic Stress Test Model in Bank-Asset Networks*

CCS2015

SEP 2015
- *Cities as attractive potential: Networks over cities from physical interactions*

MIT Senseable City Lab

JUN 2015
- *Properties of Networks of Interacting Stochastic Agents*

BU Departmental Seminar

MAY 2015
- *Landau-Ginzburg-type Effective Lagrangians for Dynamical Networks*

2015

Condensed Matter Theory Group Meeting

JAN
- *From Classical Fields to Networks of Arbitrary Degree Distribution and High Clustering*

Condensed Matter Theory Seminar

JAN 2015
- *Cities as Attractive Potentials: Modeling City Social Networks as Physical Interactions*

MIT HumNet Group seminar

FEB 2015
- *A Systemic Stress Test Model in Bank-Asset Networks*

MIT Media Labs, The Consortium for Systemic Risk Analytics and SYRTO,

DEC 2014
- *Structure of News Sentiment Time Series*

JUN 2014

NetSci, Presentation in the Net-O-Nets Satellite,

POSTERS

- *Arbitrary degree distribution and high clustering from a local geometric network growth model* JUN 2015
NetSci, Zaragoza, Spain, Nima Dehmamy, Navid Dianati.
- *Landau-Ginzburg Network Dynamics and Stability Analysis* JAN 2015
Dynamics Days XXIV, Poster, Nima Dehmamy.
- *Analytically Solvable Network Growth Model* JAN 2015
Dynamics Days XXIV, Poster, Navid Dianati, Nima Dehmamy.
- *A Dynamical Model of Systemic Risk in Bank-Asset Networks* JUN 2014
NetSci, Poster, Nima Dehmamy, Sergey Buldyrev, Shlomo Havlin, H. Eugene Stanley and Irena Vodenska.
- *Communal Peer Selection and Scale-free Networks* JUN 2014
NetSci, Poster, Navid Dianati, Nima Dehmamy.

LECTURES

- MATHEMATICAL PHYSICS, 4 lectures at IPM, Tehran, Iran FALL 2007
on Gauge theory, Path integrals, Moyal Deformation General Relativity and Supersymmetry
- CLASSICAL PERTURBATION THEORY SPRING 2006
invited lecturer for Intermediate Classical Mechanics class
- INTRODUCTORY LECTURE ON STRING THEORY AUG 2006
at High School for Exceptional Talents in Shahr-e-Rey
- RENORMALIZATION AND EFFECTIVE LAGRANGIAN BY J. POLCHINSKI SPRING 2006
for Quantum Field Theory II

SUMMER SCHOOLS AND CONFERENCES

- CCS2015 (CONFERENCE ON COMPLEX SYSTEMS) Tempe, AZ, USA SEP 2015
- DYNAMICS DAYS XXIV Houston, TX, USA JAN 2015
- NETSCI Berkeley, CA, USA JUN 2014

- SIMONS WORKSHOP IN MATHEMATICS AND PHYSICS AUG 2010
- EMERGENT GRAVITY, SISSA, Trieste, Italy MAR 2007
- NEUROSCIENCE, IPM, Tehran, Iran JUN 2005

SKILLS

PROGRAMMING • **Python** (expert, sympy, scipy, numpy, pandas, igraph) • **C/C++** (numerical, object-oriented) • **Mathematica** (expert, symbolic) • **Matlab** (Image Processing, DAQ) • **Unix-based shell scripting** • **HTML5/CSS3, Javascript, JQuery and experience with Amazon Web Services** • **L^AT_EX** (expert) Wrote a style file (.sty) for Sharif University Thesis format. • **Assembly** Programming 8051 series microcontrollers.

PHYSICS AND MATH SKILLS • Network Science • Quantum Field Theory in curved space • General Relativity • Differential Geometry • String Theory • Many-particle physics

ROBOTICS AND ELECTRONICS

1. **“Internet of Things” projects with Raspberry Pi** (2015) temperature sensing with ADC of ATTiny45 and reporting with I²C to Raspberry Pi; 2 day project with friend.
2. **Halloween robotic doll “Overly-attached Cyborg”** (2014) with sonic ranging, scouts different angles by turning neck, warns proximal subjects by making eyes glow red and waves arm at them.
3. **LED star with touch control** (2014) ATTiny45 and custom built and coded capacitive touch sensor and wireless charging; with a friend.
4. **Transformer Biped** (2012) car and biped hybrid with 15 micro-servos and driven by Arduino Micro and Adafruit I²C motor servo shield.
5. **Humanoid Arm** (2003) with 8051 microcontroller with serial interface to Matlab
6. **Object Gatherer** (2003) college team, Amir Kabir University
7. **Fire-fighting pathfinder robot** (2003) Amir Kabir University (no microcontrollers,

just TTL logical gates, OP-Amps, FET H-bridges and basic electronics.)

LANGUAGES • **German** fluent • **English** fluent • **Farsi** fluent • **Arabic, French, Italian**
basic

PROFESSIONAL EXPERIENCE

RESEARCH ASSISTANT, GROUP OF PROF. H.E. STANLEY	JAN 2013-PRESENT
ANALYTIC RESEARCH INTERN, QUANTLAB LLC. BOSTON	JUN–AUG 1015
GK-12 FELLOW	JUN–DEC 2012
TEACHING FELLOWSHIP	2007–2013

- **Boston University** Intermediate Mechanics lab, Elementary Physics for engineers, and non-math majors,
- **Sharif University** Quantum Mechanics II, Electro-acoustics Lab

PEER REVIEW FOR JOURNALS

• Physica A	2014
-------------	------

WEB

PERSONAL WEB-PAGE

nimadehmamy.com

LINKEDIN

<http://www.linkedin.com/pub/nima-dehmamy/4a/70a/577>

GOOGLE SCHOLAR

<http://scholar.google.com/citations?user=gVHpUtgAAAAJ&hl=en>

RESEARCHGATE

http://www.researchgate.net/profile/Nima_Dehmamy

REFERENCES

PROFESSOR H EUGENE STANLEY

Director, Center for Polymer Studies

Department of Physics, Boston University, 590 Commonwealth Avenue,

Boston, MA 02215 USA

E-MAIL: hes@bu.edu

FAX: +1 617 353-9393

TEL: Preferred +1 857 891-1941 (mobile). +1 617 353-2617 (office)

WEB: <http://polymer.bu.edu/hes>

PROFESSOR SERGEY BULDYREV

Department of Physics

Yeshiva University, 500 West 185th Street Room 1112, Belfer Hall

New York, NY, 10033,

E-MAIL: buldyrev@verizon.net, or buldyrev@yu.edu

FAX: +1 212 960 0035

TEL: +1 212 960 5430

PROFESSOR SHLOMO HAVLIN

Department of Physics

Bar-Ilan University

Ramat-Gan 52900 Israel

FAX: +972-3-5317884,+972-3-5353298

TEL: +972-3-5318436

EMAIL: havlin@ophir.ph.biu.ac.il

PROFESSOR IRENA VODENSKA

Center for Polymer Studies and Administrative Sciences Department,

Metropolitan College, Boston University,

Boston, MA 02215

E-MAIL: vodenska@bu.edu

FAX: +1 617 353-9393

TEL: +1 617 353-2617 WEB: <http://havlin.biu.ac.il/>